LUND UNIVERSITY

Models and biomarkers of motor and neuropsychiatric complications in Parkinson's disease

Skovgård, Katrine

2023

Link to publication

Citation for published version (APA):
Skovgård, K. (2023). *Models and biomarkers of motor and neuropsychiatric complications in Parkinson's disease*. [Doctoral Thesis (compilation), Department of Experimental Medical Science]. Lund University, Faculty of Medicine.

Total number of authors:
1

General rights
Unless other specific re-use rights are stated the following general rights apply:
Copyright and moral rights for the publications made accessible in the public portal are retained by the authors and/or other copyright owners and it is a condition of accessing publications that users recognise and abide by the legal requirements associated with these rights.
• Users may download and print one copy of any publication from the public portal for the purpose of private study or research.
• You may not further distribute the material or use it for any profit-making activity or commercial gain
• You may freely distribute the URL identifying the publication in the public portal

Read more about Creative commons licenses: https://creativecommons.org/licenses/

Take down policy
If you believe that this document breaches copyright please contact us providing details, and we will remove access to the work immediately and investigate your claim.

LUND UNIVERSITY

PO Box 117
221 00 Lund
+46 46-222 00 00

Download date: 12. Oct. 2024

Models and biomarkers of motor and neuropsychiatric complications in Parkinson's disease

KATRINE SKOVGÅRD | FACULTY OF MEDICINE | LUND UNIVERSITY

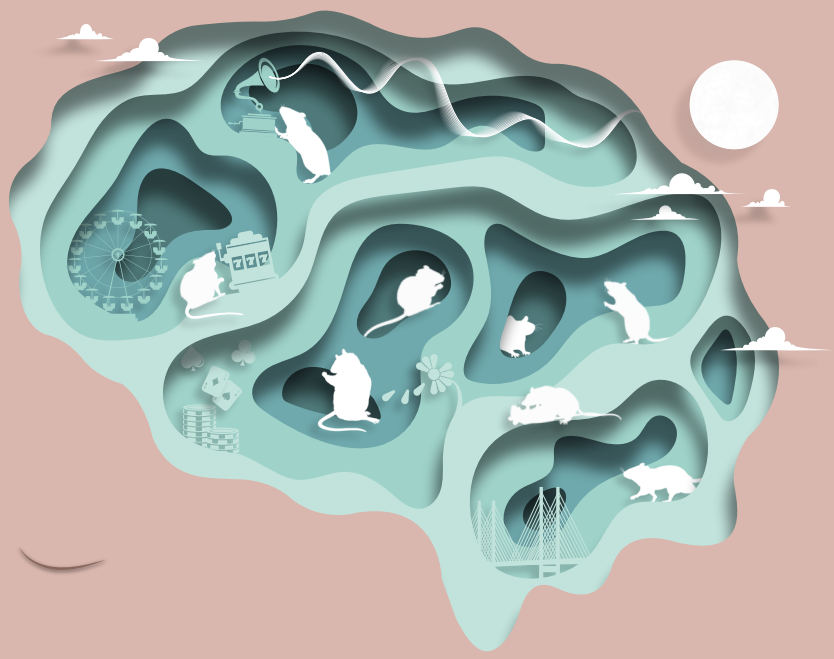

Models and biomarkers of motor and neuropsychiatric complications in Parkinson's disease

Katrine Skovgård

LUND UNIVERSITY

DOCTORAL DISSERTATION

Doctoral dissertation for the degree of Doctor of Philosophy (PhD) at the Faculty of Medicine, Lund University, Sweden.

To be publicly defended on January 19th 2023 at 13:00 in Segerfalksalen, Wallenberg Neuroscience Center, Lund University, Lund, Sweden.

Faculty opponent
Dr. María Cruz Rodríguez-Oroz
Clínica Universidad de Navarra and Centro de Investigación Médica Aplicada
University of Navarre, Pamplona, Spain

Models and biomarkers of motor and neuropsychiatric complications in Parkinson's disease

Katrine Skovgård

LUND
UNIVERSITY

Cover by Katrine Skovgård (artwork inspired by Eiko Ojala, created with Biorender.com)

Copyright pp 1-118 Katrine Skovgård and respective publishers

Paper 1 © Frontiers in Systems Neuroscience

Paper 2 © Neurotherapeutics

Paper 3 © Movement Disorders

Paper 4 © by the Authors (Manuscript unpublished)

Faculty of Medicine
Department of Experimental Medical Science

ISBN 978-91-8021-342-4
ISSN 1652-8220

Printed in Sweden by Media-Tryck, Lund University
Lund 2022

Media-Tryck is a Nordic Swan Ecolabel certified provider of printed material. Read more about our environmental work at www.mediatryck.lu.se

MADE IN SWEDEN

Til min mor

"Allt stort som skedde i världen
skedde först i någon människas fantasi"
Astrid Lindgren

Table of Contents

Papers and Manuscript **9**

Published papers outside the thesis **10**

Summary **11**

Sammenfattning **13**

Resumé **15**

List of abbreviations **17**

Introduction **21**
- Parkinson's disease 21
- The basal ganglia circuitry 22
- Dopamine and its modulatory role in the basal ganglia 25
- Pharmacological treatments for PD motor symptoms 27
- Treatment-related complications in PD 28
- Toxin-based rodent models of PD and LID 30
- Mechanisms of LID 31
- Mechanisms of drug-induced ICBs 37
- Oscillations in cortico-basal ganglia circuits 39

Aims of this thesis **47**

Materials and Methods **51**
- Animals 51
- Surgical procedures 51
- Drugs 52
- Behavioural testing 53
- Electrophysiological recordings 57
- Ex-vivo experiments 59
- Statistical analysis 61

Results **65**
- Paper I 65
- Paper II 69
- Paper III 74
- Paper IV 79

Discussion 87
Acknowledgements 97
References 101
Appendix (Papers I-IV) 119

Papers and Manuscript

This thesis is based on the following papers:

I. Cortico-striatal oscillations are correlated to motor activity levels in both physiological and parkinsonian conditions

Moënne-Loccoz C*, Astudillo-Valenzuela C*, Skovgård K, Salazar-Reyes CA, Barrientos SA, García-Núñez XP, Cenci MA, Petersson P, Fuentes-Flores RA

Front Syst Neurosci 2020; 14:56. DOI: 10.3389/fnsys.2020.00056

II. Distinctive effects of D1 and D2 receptor agonists on cortico-basal ganglia oscillations in a rodent model of L-DOPA-induced dyskinesia

Skovgård K, Barrientos SA, Petersson P, Halje P[§], Cenci MA[§]

Neurotherapeutics 2022. DOI: 10.1007/s13311-022-01309-5

III. Dopamine agonist cotreatment alters neuroplasticity and pharmacology of L-DOPA-induced dyskinesia

Espa E*, Song L*, Skovgård K, Fanni S, Cenci MA

Mov Disord (accepted)

IV. Dopamine agonist drives impulsive-compulsive behaviours in rats independent of L-DOPA cotreatment and early parkinsonism

Skovgård K, Espa E, Wolfschlag M, Cenci MA

Manuscript in preparation

*/[§]Equal contribution

Published papers outside the thesis

Verification of multi-structure targeting in chronic microelectrode brain recordings from CT scans

Censoni L, Halje P, Axelsson J, Skovgård K, Ramezani A, Malinina E, Petersson P

J Neurosci Methods 2022; 382:109719. DOI: 10.1016/j.jneumeth.2022.109719

Non-dopaminergic approaches to the treatment of motor complications in Parkinson's disease

Cenci MA, Skovgård K, Odin P

Neuropharmacology 2022; 210:109027. DOI: 10.1016/j.neuropharm.2022.109027

Summary

Parkinson's disease (PD) is a neurodegenerative disorder characterised by typical motor symptoms that are caused by severe dopamine depletion in the cortico-basal ganglia network. Parkinsonian motor symptoms are improved by dopaminergic medications, the most effective being the dopamine precursor L-DOPA. This compound exerts its motor effects by stimulating dopamine D1 and D2 receptors, whose expression are segregated between the movement-promoting and movement-suppressing pathways of the basal ganglia circuitry. As the disease progresses, treatment with L-DOPA give rise to involuntary movements (dyskinesia), which limits its utility. Drugs that directly stimulate dopamine receptors, referred to as dopamine agonists, are commonly used to delay the use of L-DOPA or reduce its dosage. Although less prone to induce dyskinesia, dopamine agonists have a high liability to induce neuropsychiatric side effects, in particular, impulsive-compulsive behaviours. However, it remains to be established whether pharmacotherapies combining L-DOPA and dopamine agonists give rise to specific profiles of motor and non-motor complications.

The overarching aim of this thesis is to develop improved experimental models to advance translational research on the motor and neuropsychiatric complications of PD therapy. Both well-established and new experimental models are used to define correlations and causal links between regimens of dopaminergic treatment, behavioural changes, and biomarkers of network and cellular dysfunction in the cortico-basal ganglia system.

Using in vivo local field potential recordings to study biomarkers of network dysfunctions, we show that changes in broad-band oscillatory activities of cortico-striatal circuits are correlated to ongoing motions and do not reflect parkinsonian-specific states. Moreover, we demonstrate that dyskinesias induced by D1 receptor stimulation are associated with prominent narrowband cortico-striatal oscillations in the high gamma range (70-110 Hz). Following treatment with a D2 agonist, these narrowband gamma oscillations are less pronounced, whereas this treatment induces prominent theta oscillations (5-10 Hz) in the deep basal ganglia nuclei. Thus, the composition of the dopaminergic therapies might affect these neurophysiological biomarkers and should be considered in future investigations.

Next, using a set of pharmacological tools and markers of cellular dysfunctions, we show that adjuvant treatment with D2/3 agonists alters the pattern of dopamine-related neuroplasticity in the basal ganglia compared to L-DOPA monotherapy, despite similar dyskinetic behaviours. The antidyskinetic effects of compounds

modulating D1 receptor signalling were stronger in L-DOPA-treated animals, while NMDA receptor antagonists produced markedly larger effects in the combined treatment group. Thus, adjuvant dopamine agonist treatment has a significant impact on the neuroplasticity and pharmacological response profiles of L-DOPA-induced dyskinesia. In a last study, we show that treatment with a D2/3 agonist induces compulsive behaviours and impulsive decision-making in both intact and partially dopamine-depleted rats regardless of L-DOPA coadministration.

Taken together, the findings of this thesis shed new light on the maladaptive cellular changes and network dynamics through which dopaminergic pharmacotherapies for PD affects motor behaviours. Moreover, this thesis work reveals the importance of including realistic models of combined therapies in future translational research on L-DOPA-induced dyskinesia.

Sammenfattning

Parkinsons sjukdom är en kronisk neurodegenerativ sjukdom karaktäriserad av typiska motoriska symtom i form av långsamma rörelser, muskelstelhet och vilotremor. Dessa symtom orsakas av en brist på signalsubstansen dopamin i de områden av hjärnan som kontrollerar rörelser (hjärnbarken, basala ganglierna och thalamus). Parkinsonmedicin, varav det mest effektiva är levodopa, mildrar symtomen genom att öka mängden dopamin i hjärncellerna. Levodopa stimulerar dopaminreceptorer i hjärnan, mer specifikt D1- och D2-receptorer, som uttrycks i rörelsefrämjande respektive rörelsehämmande signalvägar i basala ganglierna. Med tiden kan behandling med levodopa ge upphov till ofrivilliga rörelser (dyskinesier), vilket begränsar nyttan av behandlingen. Dopaminagonister, som verkar direkt på nervcellernas dopaminreceptorer, används ofta för att försena eller minska bruket av levodopa. Risken att utveckla dyskinesier är lägre med dopaminagonister, men å andra sidan för de med sig en större risk att utveckla neuropsykiatriska biverkningar, i synnerhet impulskontrollsstörningar. Det är fortfarande oklart om läkemedelsbehandlingar som kombinerar levodopa och dopaminagonister ger upphov till specifika profiler av motoriska och neuropsykiatriska symtom.

Det överordnade syftet med denna avhandling är att utveckla förbättrade experimentella modeller för att främja translationell forskning om de motoriska och neuropsykiatriska komplikationer som uppstår som en följd av behandling av Parkinsons sjukdom. Både väletablerade och nya experimentella modeller användes till att definiera korrelationer och orsakssamband mellan olika typer av dopaminerga behandlingar, beteendeförändringar och biomarkörer för dysfunktion på nätverksnivå och cellulär nivå i hjärnkretsar involverade i Parkinsons sjukdom.

Genom att mäta rytmiska mönster i hjärnaktiviteten (neuronala oscillationer) i basala ganglie-kretsar i en djurmodell av Parkinsons sjukdom, visar vi att ändringar i hjärnaktiviteten i breda frekvensband korrelerar med pågående rörelser och inte specifikt med det parkinsonistiska tillståndet. Dessutom visar vi att dyskinesier inducerade av behandling med en D1-receptoragonist är förbundna med framträdande gammaoscillationer i ett smalt frekvensband (70-110 Hz) i motorkortex och striatum. Efter behandling med en D2-receptoragonist är dessa gammaoscillationer inte lika framträdande. Istället induceras framträdande thetaoscillationer (5-10 Hz) i de djupa kärnorna av basala ganglierna (globus pallidus och substantia nigra). Olika kombinationer av dopaminerga läkemedel kan således ha olika påverkan på dessa neurofysiologiska biomarkörer, vilket bör beaktas i framtida vetenskapliga undersökningar.

Vidare visar vi med hjälp av farmakologiska verktyg och markörer för cellulära dysfunktioner att tilläggsbehandling med D2/3-receptoragonister ändrar den dopaminrelaterade neuroplasticiteten i basala ganglierna jämfört med monobehandling med levodopa, trots att båda behandlingarna inducerar liknande dyskinesier. De antidyskinetiska effekterna av substanser som påverkar D1-receptorsignalering har dessutom störst effekt i djur behandlade med levodopa, medan glutamatreceptor-antagonister (NMDA-antagonister) har en markant större effekt i djur behandlade med en kombination av levodopa och en D2/3-receptoragonist. Tilläggsbehandling med dopaminagonister har således en signifikant påverkan på levodopa-inducerad neuroplasticitet och på effekten av farmakologiska behandlingar mot dyskinesi. I en sista undersökning visar vi att behandling med D2/3-receptoragonister inducerar tvångsmässiga beteenden och impulsivitet under normala och sänkta dopaminnivåer i striatum, oavsett om behandlingen ges ensamt eller tillsammans med levodopa.

Sammantaget kastar resultaten i denna avhandling nytt ljus över de dysfunktionella förändringar på cellulär- och nätverksnivå genom vilka olika typer av dopaminerg behandling påverkar motoriska beteenden i Parkinsons sjukdom. Dessutom visar resultaten på vikten av att inkludera realistiska modeller av kombinationsterapier i framtida translationell forskning på levodopa-inducerade dyskinesier.

Resumé

Parkinsons sygdom er en kronisk neurodegenerativ sygdom som er karakteriseret ved typiske motoriske symptomer i form af langsomme bevægelser, muskelstivhed, og hvilerysten Disse symptomer er forårsaget af alvorlig mangel på signalstoffet dopamin i de områder af hjernen, der kontrollerer vores bevægelser (hjernebarken, basalganglierne og thalamus). Parkinsonmedicin, hvoraf den mest effektive er levodopa, forbedrer symptomerne ved at øge mængden af dopamin i hjernen. Levodopa stimulerer dopaminreceptorer i hjernen, mere specifik D1 og D2 receptorer, som udtrykkes af henholdsvis bevægelsesfremmende og bevægelseshæmmende signalveje i basalganglierne. Med tiden kan behandling med levodopa imidlertid give anledning til ufrivillige bevægelser (dyskinesier), hvilket begrænser lægemidlets anvendelighed. Dopaminagonister, der virker direkte på nervecellernes dopaminreceptorer, anvendes ofte til at forsinke eller mindske brugen af levodopa. Risikoen for at udvikle dyskinesier er lavere med dopaminagonister, men til gengæld medfører de en højere risiko for at udvikle neuropsykiatriske bivirkninger, især manglende impulskontrol. Det er stadig uvist om lægemiddelbehandlinger, der kombinerer levodopa og dopaminagonister, giver anledning til specifikke profiler af motoriske og neuropsykiatriske symptomer.

Det overordnede formål med denne afhandling er at udvikle forbedrede eksperimentelle modeller for at fremme translationel forskning i de motoriske og neuropsykiatriske komplikationer som opstår som følge af behandling af Parkinsons sygdom. Både veletablerede og nye eksperimentelle modeller anvendes til at definere korrelationer og årsagssammenhænge mellem forskellige slags dopaminerge lægemiddelbehandlinger, adfærdsændringer og biomarkører for dysfunktioner på netværks- og cellulært niveau i hjernekredsløb involveret i Parkinsons sygdom.

Ved at måle rytmiske mønstre af hjerneaktivitet (neuronale oscillationer) lokalt i basalgangliernes kredsløb i en dyremodel af Parkinsons sygdom, viser vi at ændringer i hjerneaktiviteten i brede frekvensbånd ikke er specifik for Parkinson's sygdom, men generelt korrelerer med igangværende bevægelser. Desuden demonstrerer vi, at dyskinesier induceret af D1 receptor stimulering er forbundet med fremtrædende gammabølger i et smalt frekvensbånd (70-110 Hz) i motor cortex og striatum, hvorimod denne gamma-aktivitet er mindre udtalt efter D2 receptor stimulering. Til gengæld inducerer behandling med D2 receptor dopaminagonister fremtrædende thetabølger (5-10 Hz) i de dybe kerner af basalganglierne (globus pallidus og substantia nigra). Forskellige kombinationer af dopaminerge lægemidler

kan således påvirke disse neurofysiologiske biomarkører, hvilket bør tages i betragtning i fremtidige videnskabelige undersøgelser.

Dernæst viser vi ved hjælp af farmakologiske værktøjer og markører for cellulære dysfunktioner, at den dopaminrelaterede neuroplasticitet i basalganglierne ændres når behandling med levodopa kombineres med D2/3 dopaminagonister, til trods for at de to behandlinger fremkalder lignende dyskinesier. Desuden demonstrerer vi, at effekten af potentielle lægemidler mod dyskinesi, der påvirker D1 receptorsignalering, har størst effekt i dyr behandlet med levodopa, mens glutamat NMDA-receptorantagonister har en markant større virkning i dyr behandlet med kombinationen af levodopa og D2/3 dopaminagonisten. Tillægsbehandling med dopaminagonister har således en signifikant indvirkning på levodopa-induceret neuroplasticitet og på effekten af farmakologiske behandlinger mod dyskinesi. I en sidste undersøgelse viser vi, at behandling med D2/3 dopaminagonister forårsager tvangsmæssig adfærd og impulsivitet under normale og reducerede dopaminniveauer i striatum, uanset om behandlingen gives alene eller kombineres med levodopa.

Samlet set kaster resultaterne af denne afhandling nyt lys over de dysfunktionelle forandringer på cellulært- og netværksniveau, hvorigennem forskellige typer af dopaminerge behandlinger påvirker motorisk adfærd i Parkinsons sygdom. Desuden fremhæver resultaterne vigtigheden af at inkludere realistiske modeller af kombinationsterapier i fremtidig translationel forskning af levodopa-inducerede dyskinesier.

List of abbreviations

5-HT	Serotonin
6-OHDA	6-hydroxydopamine
ACC	Anterior cingulate cortex
AIMs	Abnormal involuntary movements
AMPA	α-amino-3-hydroxy-5-methyl-4-isoxazolepropionic
AP	Anterior-posterior
BBB	Blood brain barrier
cAMP	Cyclic adenosine monophosphate
ChIN	Cholinergic interneuron
COMT	Catechol-O-methyltransferase
CPA	Conditioned place aversion
CPP	Conditioned place preference
CT	Computed tomography
DA	Dopamine
DARPP-32	DA- and cAMP-regulated phosphoprotein
DAT	Dopamine transporters
DBS	Deep brain stimulation
DLS	Dorsolateral striatum
DMS	Dorsomedial striatum
DMSO	Dimethyl sulfoxide
dSPN	Direct pathway spiny projection neuron
DV	Dorsal-ventral
EPM	Elevated plus maze
ERK1/2	Extracellular signal-regulated protein kinase 1 and 2
GABA	Gamma-aminobutyric acid
GPe	Globus pallidus pars externa
GPi	Globus pallidus pars interna
ICB	Impulsive-compulsive behaviour
iGluR	Ionotropic glutamate receptor
i.p.	Intraperitoneal
IRASA	Irregular-resampling auto-spectral analysis
iSPN	Indirect pathway spiny projection neuron
LD3	L-DOPA 3 mg/kg
LD6	L-DOPA 6 mg/kg
LD24	L-DOPA 24 mg/kg

L-DOPA	L-3,4-dihydroxyphenylalanine
LFP	Local field potentials
LID	L-DOPA-induced dyskinesia
M1FL	Forelimb are of the primary motor cortex
M1Tr	Trunk area of the primary motor cortex
mAChR	Muscarinic acetylcholine receptor
MAO-B	Monoamine oxidase
MFB	Medial forebrain bundle
mGluR	Metabotropic glutamate receptor
mGluR5	Metabotropic receptor type 5
ML	Medial-lateral
MOR	μ Opioid receptor
NAM	Negative allosteric modulator
NBG	Narrowband gamma
NMDA	N-methyl-d-aspartate
OFC	Orbitofrontal cortex
PAM	Positive allosteric modulator
PD	Parkinson's disease
PFC	Prefrontal cortex
PKA	Protein kinase A
PSD	Power spectral density
R0.5	Ropinirole 0.5 mg/kg
R1.5	Ropinirole 1.5 mg/kg
R2.5	Ropinirole 2.5 mg/kg
Reca-1	Rat endothelial cell antigen 1
RFA	Rostral forelimb area
rIGT	Rat Iowa Gambling Task
s.c.	Subcutaneous
SNc	Substantia nigra pars compacta
SNr	Substantia nigra pars
SPN	Spiny projection neuron
STN	Subthalamic nucleus
TH	Tyrosine hydroxylase
VCNDD	Vanderbilt Center for Neuroscience
VTA	Ventral tegmental area

Introduction

Introduction

Parkinson's disease

In 1817, James Parkinson described six aged men who suffered from unusual motor symptoms in *An Essay on the Shaking Palsy* (Parkinson, 2002). His findings formed the foundation for the diagnosis of what would later be known as Parkinson's disease (PD), the second most common neurodegenerative disorder worldwide.

PD is a complex disorder with diverse clinical features that include both motor and non-motor symptoms. Nevertheless, the cardinal signs of PD are slowness of movements (bradykinesia), shaking at rest (tremor), and increased muscle tone (rigidity), with postural instability occurring at a later stage (Postuma et al., 2015). These motor symptoms emerge as the result of a progressive loss of dopaminergic neurons in the substantia nigra pars compacta (SNc), with the histopathological hallmark being the formation of intraneuronal alpha-synuclein inclusions in the form of Lewy bodies or Lewy neurites (Kouli et al., 2018). At motor symptom onset, approximately 30% of the dopaminergic neurons in the SNc are degenerated, reaching more than 60% as the disease progresses (Fearnley and Lees, 1991; Kordower et al., 2013; Ma et al., 1997; Rudow et al., 2008). This denervation of the nigrostriatal pathway leads to diminished dopamine (DA) levels in the striatum, that are responsible for the appearance of the cardinal motor symptoms in PD. Many of the non-motor symptoms in PD, however, do not require that level of dopaminergic denervation and also depend on pathological changes in various non-dopaminergic neurotransmitter systems, namely the serotonergic, noradrenergic, and cholinergic systems (Fox et al., 2008). These neurotransmitter systems might be affected before the onset of the cardinal motor symptoms, which may explain why non-motor symptoms such as constipation, rapid-eye movement sleep behaviour disorder, olfactory deficit, and depression often precede the expression of motor symptoms (Chaudhuri and Naidu, 2008). Thus, non-motor features have a potential utility for early diagnosis, although the clinicopathological correlation remains uncertain. With continuing disease progression, the motor disabilities are often accompanied by additional non-motor symptoms, including neuropsychiatric symptoms, autonomic dysfunction, sleep disturbances, and pain or sensory problems (Chaudhuri et al., 2006).

Due to the complex nature of PD, the etiology and pathogenic mechanisms remain incompletely understood. While a minor proportion of PD patients have a genetic cause for their disease, the majority of PD cases are idiopathic. Thus, the

PD-related degeneration of dopaminergic neurons in SNc is likely influenced by a combination of genetic, molecular, and environmental factors that can cause cell death over time (Kouli et al., 2018).

The basal ganglia circuitry

The generation of naturalistic behaviours adapted to the environment is highly dependent on a complex network of interconnected nuclei referred to as the basal ganglia. Anatomically, the basal ganglia refer to five subcortical structures: the striatum (caudate and putamen in primates), the globus pallidus (pars interna, GPi, and externa, GPe), the subthalamic nucleus (STN), and the substantia nigra pars reticulata, SNr). The striatum constitutes the main input structure of the basal ganglia and integrates information about planned movements from frontal, sensory, and motor cortices, and related thalamic areas. Indeed, the striatum receives excitatory glutamatergic input from the entire cerebral cortex (Redgrave et al., 2010), the thalamus (the centromedian and parafascicular nuclei in particular) (Smith et al., 2004), and the amygdala (Kelley et al., 1982), as well as a serotonergic input from the raphe nucleus (Jacobs and Fornal, 1997). In addition, the dorsal striatum is densely innervated by dopaminergic projections from the SNc, while the ventral tegmental area (VTA) primarily targets the ventral striatum (Smith and Kieval, 2000). Interestingly, movement initiation is associated with premovement activity in motor cortex and other motor-related brain circuits. To prevent the ongoing activity in those regions from leading to unwanted or wrongly timed movements, the output nuclei (GPi and SNr) of the basal ganglia keep their downstream thalamocortical target cells under tonic inhibitory control via gamma-aminobutyric acid (GABA)-ergic projections (Hikosaka et al., 2000). Thus, the dorsal striatum constitutes a crucial component in integrating relevant information about planned movements and translate it into specific changes in this widespread tonic inhibition, to support the initiation of the desired voluntary movement.

Classic and novel views on the basal ganglia circuitry

Classically, the striatum is thought to convey information to the output nuclei of the basal ganglia via two distinct pathways. Approximately half of the GABAergic neurons in the striatum, identified as spiny projection neurons (SPNs), project directly to the basal ganglia output nuclei (direct pathway; dSPNs), while the remaining SPNs influence the output nuclei indirectly via intermediate connections to the GPe and STN (indirect pathway; iSPNs) (Gerfen and Surmeier, 2011). In turn, the GPe provides inhibitory inputs to the output nuclei and STN, whereas the STN provide excitatory inputs to the output nuclei. In the classical model, the direct and indirect pathways are proposed to exert opposite effects on motor control, activating or inhibiting cortically-initiated movements, respectively (Albin et al., 1989; Kravitz et al., 2010). According to this model, activation of dSPNs will inhibit the

output nuclei, which leads to a disinhibition of the motor thalamus, thus facilitating movement. Conversely, activation of the iSPNs will inhibit the GABAergic neurons in the GPe leading to a disinhibition of the STN, which altogether increase the inhibition of the output nuclei on their target cells and consequently supress movement (see Figure 1).

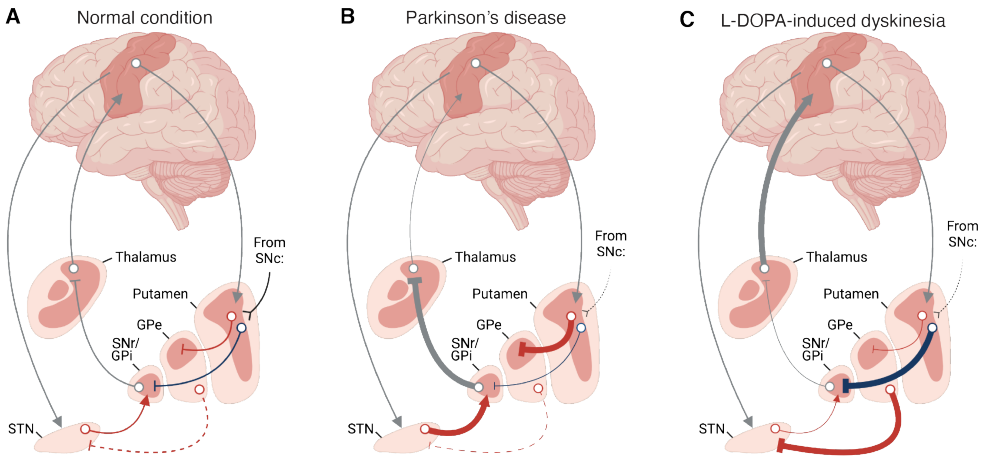

Figure 1. Simplified representation of the basal ganglia circuitry in physiological, parkinsonian, and dyskinetic conditions. The striatum (putamen) receives excitatory glutamatergic inputs from the cortex and thalamus as well as dopaminergic inputs from the SNc. These inputs converge onto inhibitory GABAergic SPNs, which give rise to the direct and indirect pathway. Direct pathway SPNs project directly to the output nuclei of the basal ganglia, namely GPi/SNr (blue), whereas neurons of the indirect pathway influence these output nuclei indirectly via intermediate projections to the GPe and STN (red). The output nuclei keep their excitatory thalamic target cells under tonic inhibition via GABAergic projections. **A.** In physiological conditions, a balance between the pathways is maintained by DA. **B.** In PD, the DA denervation of the striatum results in hyperactivity of the indirect pathway and reduced activity of the direct pathway, altogether increasing the tonic inhibition of the output nuclei on downstream motor targets. **C.** LID is associated with hyperactivity of the direct pathway and a decreased activity of the indirect pathway, which results in overactivation of the thalamus. For abbreviations, see main text. *(Created with BioRender.com)*

This classical view is however being challenged by several recent studies adding new insights to the functional organisation of the basal ganglia circuitry. Importantly, the Costa laboratory showed concurrent increases in the neuronal activity of both dSPNs and iSPNs during the initiation and execution of actions, with low activity in both populations during immobility (Cui et al., 2013; Tecuapetla et al., 2016). Corroborated by others, this led to a model suggesting that coordinated activation of the direct and indirect pathway will affect different output neurons of the basal ganglia, with the direct pathway inhibiting specific neurons to facilitate the desired movements, while the indirect pathway disinhibits other neurons to supress competing actions (Cui et al., 2013; Klaus et al., 2017; Markowitz et al., 2018; Parker et al., 2018; Tecuapetla et al., 2016). In this view, the coordinated spatial and temporal activation of specific SPNs of the two pathways is crucial for the proper selection and initiation of actions.

Although current models provide a better understanding of how basal ganglia circuits and their inputs influence movement selection and initiation, they are based on a rather simplistic organisation of the basal ganglia circuitry. Indeed, new findings on anatomical and functional connectivity reveal a much more complex circuitry, involving substantially more projections, feedback loops, and collateralisations. For instance, striatal SPNs are known to exhibit lateral inhibition on other proximal SPNs through axon collaterals (Dobbs et al., 2016). Moreover, the control of action is managed by the matrix compartment of the striatum, whereas the striosomes project directly to SNc and VTA to regulate the activity of dopaminergic neurons (Gerfen, 1984, 1985; Grillner et al., 2020). The projections that are less often considered in these models extend to other structures of the basal ganglia network. One important example is the collateral projections from the direct pathway neurons to the GPe (Wu et al., 2000), proclaiming that the GPe is not an exclusive target of the indirect pathway neurons as originally suggested. In addition to the projection from the GPe to the STN considered by current models, the prototypic and arkypallidal neurons of the GPe also form distinct projections directly to the striatum, cortex, and thalamus (Mallet et al., 2012; Mallet et al., 2016; Saunders et al., 2015). These are just some of the projections that may add valuable information on the connectivity in the cortico-basal ganglia-thalamic circuitry in future models.

Functional organisation of the basal ganglia circuitry

The flow of information is suggested to be transmitted through the basal ganglia via parallel cortico-subcortical circuits that are compartmentalised in an orderly fashion (Alexander and Crutcher, 1990; Alexander et al., 1986; Haber, 2003). In addition to the basal ganglia motor circuits involved in sensorimotor control that has already been introduced, these circuits are commonly separated into an associative circuit, involved in the control of executive function, and a limbic circuit associated with emotional processing (Alexander et al., 1986). Since the projections within the basal ganglia show a high degree of spatial topography (Foster et al., 2021), these functional differences rely on the contribution of separate subregions of the various basal ganglia nuclei involved in each circuit (see Figure 2). As an example, the dorsal part of the striatum is subdivided into a dorsolateral (DLS) and dorsomedial part (DMS), that receives input from sensorimotor and prefrontal- and parietal cortices, respectively. Thus, the DLS has been linked to the control of innate and learnt motor patterns or habit formation, while the DMS is involved in the control of goal-directed movements adapted to the current environmental situation. Instead, the ventral striatum (nucleus accumbens) receive input from prefrontal and anterior cingulate cortices (PFC and ACC, respectively) as well as from limbic structures such as amygdala and hippocampus, with downstream processing by the ventral pallidum and the SNr. Accordingly, the ventral striatum has been implicated in the control of reinforcement learning and motivation (Macpherson and Hikida, 2019; Redgrave et al., 2010). The topographic organisation of these functionally distinct

cortico-subcortical circuits provides the potential for limbic information to affect motor circuits and vice versa (Aoki et al., 2019). Furthermore, alterations in the cortico-striatal connectivity in the limbic basal ganglia circuits have been found to contribute to the pathogenesis of neuropsychiatric disorders such as obsessive compulsive disorder (Macpherson and Hikida, 2019). The contributions and interactions of these subregions are therefore important to consider in addition to alterations in cortical and limbic regions, in order to gain a complete picture of the mechanisms underlying both the motor and neuropsychiatric features of PD.

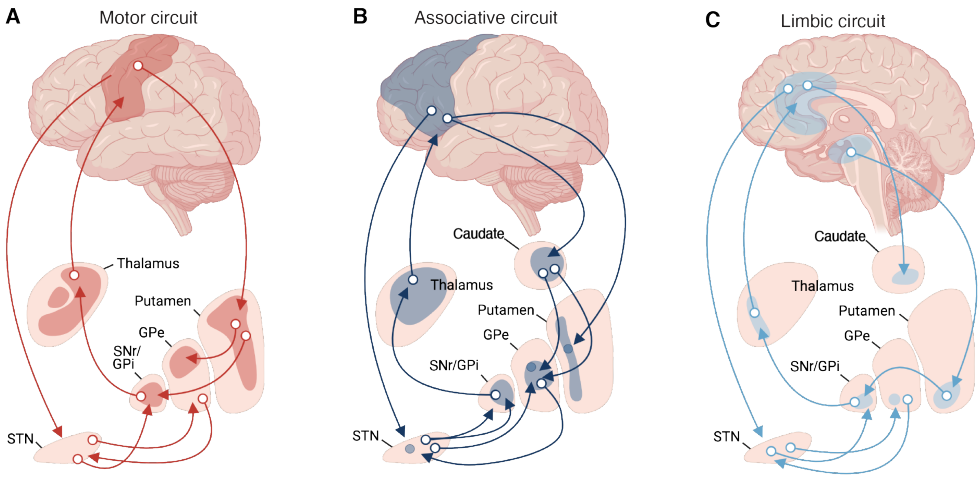

Figure 2. Functional organisation of the basal ganglia. The basal ganglia circuitry is divided into topographically segregated subregions transmitting motor (**A**), associative (**B**), and limbic (**C**) information. (Created with BioRender.com)

Dopamine and its modulatory role in the basal ganglia

DA is an essential neurotransmitter of the central nervous system involved in almost all aspects of behaviour, including movement control, motivation, reward, cognition, and learning (Björklund and Dunnett, 2007). The precursor of DA is L-3,4-dihydroxyphenylalanine (levodopa, L-DOPA), that is synthesized from tyrosine by the rate-limiting enzyme tyrosine hydroxylase (TH). Unlike DA, L-DOPA has a large blood brain barrier (BBB) permeability and is metabolised to DA by DOPA decarboxylase (Nagatsu et al., 1964). Dopaminergic neurons primarily project from the SNc to the dorsal striatum to form the nigrostriatal pathway, or from the VTA to the nucleus accumbens and limbic systems or the PFC to form the mesolimbic and mesocortical pathways, respectively (Smith and Kieval, 2000). Importantly, dopaminergic inputs modulate the striatal processing of cortical and thalamic inputs carried by the SPNs of the direct and indirect pathways differently, because the SPNs of each pathway express different types of DA receptors.

Generally, DA exerts its actions through the activation of five types of G-protein coupled DA receptors (D1-D5), which are classified as either D1-like (D1 and D5) or D2-like (D2-D4) based on their functional properties. These two classes of DA receptors are oppositely coupled to adenylyl cyclase via different G-protein subunits, where D1-like receptors are linked to the stimulatory $G\alpha_{s/olf}$ and D2-like receptors are coupled to the inhibitory $G\alpha_{i/o}$. The binding of DA to D1-like receptors will therefore increase the second messenger cyclic adenosine monophosphate (cAMP) and phosphorylation of protein kinase A (PKA) resulting in an increased intrinsic excitability of the cell, whereas DA interaction with D2-like receptors will reduce cAMP and PKA levels, thus lowering the intrinsic excitability (Gerfen and Surmeier, 2011; Sibley and Monsma, 1992).

Among the five DA receptor types, the D1 and D2 receptors are abundantly expressed in the striatum, being segregated between the dSPNs and iSPNs, respectively. Consequently, DA inputs will activate D1 receptors and increase the excitability of the dSPNs, while the excitability of iSPNs is reduced through the stimulation of D2 receptors (Valjent et al., 2009; Zhai et al., 2018). The subsequent increase and decrease of the direct and indirect pathway, respectively, results in the disinhibition of thalamic and brainstem motor targets of the basal ganglia output nuclei. According to this classical model, dysfunctions of the basal ganglia can result in an overall decreased motor output (hypokinesia) or in excessive uncontrollable movements (dyskinesia), both of which occur in PD. Specifically, when the dopaminergic neurons degenerate, the lack of activation of the D1 and D2 receptors ultimately leads to an increased excitability of the indirect pathway iSPNs, resulting in hypokinesia via disinhibition of the basal ganglia output nuclei. Conversely, overstimulation of the same receptors as a complication of dopaminergic medication, and the following hypoactivity of the indirect pathway and hyperactivity of the direct pathway, would lead to dyskinesia via inhibition of the output nuclei (see Figure 1).

Another important factor that influences the engagement of the D1 and D2 receptors, is their different DA affinities as well as the firing pattern of the dopaminergic SNc neurons. These neurons exhibit rapid bursts of large phasic firing or slower spontaneous tonic firing (Schultz, 2007). Thus, the low-affinity D1 receptors mainly respond to phasic DA release produced during burst firing, while the high-affinity D2 receptors respond to tonic DA release (Floresco et al., 2003; Grace, 2000; Grace et al., 2007). It is also important to mention, that a small subpopulation of SPNs express both D1 and D2 receptors (Meador-Woodruff et al., 1991; Surmeier et al., 1992). Moreover, D1 receptors are expressed exclusively in the SPNs, while D2 receptors are also found postsynaptically in cholinergic interneurons (ChINs) (Maurice et al., 2004) as well as presynaptically in the corticostriatal glutamatergic terminals and midbrain dopaminergic terminals (Bamford et al., 2004; Ford, 2014). These presynaptically expressed D2 receptors function as autoreceptors, providing a negative feedback mechanism to adjust the release of neurotransmitters in response to changes in the extracellular DA levels

(Sibley and Monsma, 1992). The D1 and D2 receptors are also expressed in several other brain regions, including the GPe, SNr, cerebral cortex, as well as in the amygdala and hippocampus, just to mention some (Mishra et al., 2018), while the other DA receptors are more predominant in limbic structures (Defagot et al., 1997; Gurevich and Joyce, 1999; Sibley and Monsma, 1992).

Pharmacological treatments for PD motor symptoms

In the absence of disease-modifying treatments, DA-replacement therapy with L-DOPA is still the most effective strategy for alleviating the motor symptoms of PD (Cenci et al., 2011; Cotzias et al., 1969). Standard L-DOPA pharmacotherapy is administered orally up to eight times per day depending on the individual response and disease stage, due to the short half-life of the drug. L-DOPA is given in combination with peripheral DOPA decarboxylase inhibitors (benserazide or carbidopa) to avoid peripheral biotransformation, and usually reaches peak concentration levels 1-2 h after dosing (Bianchine et al., 1971; Calne et al., 1971; Cedarbaum, 1987). Once in the brain, L-DOPA is taken up by surviving dopaminergic neurons and is converted to DA.

However, the response to L-DOPA changes with the progression of PD, increasing the need for continuously adjusting the drug dosing schedule during long-term treatment with L-DOPA. At this point, the majority of PD patients start to exhibit abnormal involuntary movements (AIMs), termed L-DOPA-induced dyskinesia (LID), or motor fluctuations, that consists in a short-duration motor response to each L-DOPA dose followed by a rapid return to severe parkinsonian immobility ("wearing-off" and "on/off" phenomena) (Cenci et al., 2011; Cenci et al., 2020). Once motor complications have developed, it is common to prolong the therapeutic actions of L-DOPA by using inhibitors of the enzymatic DA breakdown mediated by catechol-O-methyltransferase (COMT) or monoamine oxidase (MAO-B) (Cenci et al., 2022; Cerri and Blandini, 2020). Another 'L-DOPA-sparing' strategy is to reduce and/or delay the use of L-DOPA in favour of DA agonist prescribed as initial treatment to patients in the early phase of PD (Cenci et al., 2011; de Bie et al., 2020; Sy and Fernandez, 2020), or as adjuvant therapy to L-DOPA in more advanced disease stages (Hauser et al., 2014; Jenner, 2015; Nomoto et al., 2014).

DA agonists are compounds that directly stimulate the dopaminergic receptors, and they are commonly classified into ergot derivatives (e.g. bromocriptine, pergolide, lisuride, and cabergoline) and non-ergot derivatives (e.g. pramipexole, ropinirole, rotigotine, and piribedil). All these DA agonists act with high affinity for the D2-like DA receptors, in particular for the D2 and D3 subtypes (Eden et al., 1991; Varga et al., 2009), while ergot DA agonists can also interact with other receptors (e.g. D1-like DA receptors, serotonergic, adrenergic) (Cerri and Blandini, 2020). Importantly, the DA agonists provide a more continuous stimulation of DA receptors and have a much longer duration of action compared to L-DOPA.

Currently, non-ergot DA agonists, specifically ropinirole and pramipexole, are the most commonly used DA agonists for oral treatment of PD (Stocchi et al., 2016), whereas the clinical use of ergot derivatives has markedly declined due to uncommon, but important fibrotic reactions (Antonini and Poewe, 2007; Simonis et al., 2007).

While entailing a lower incidence of motor complications, DA agonists do however have inferior symptomatic efficacy compared to L-DOPA and are associated with the onset of unpleasant side effects. Indeed, the incidence of oedema, constipation, somnolence, dizziness, and psychiatric adverse effects (hallucinations, psychosis, impulsive-compulsive behaviours (ICBs)) is overall higher for these compounds compared to L-DOPA (Stocchi et al., 2020; Stowe et al., 2008). If dyskinesias are the predominant problem, an alternative treatment strategy is to use the effective antidyskinetic N-methyl-d-aspartate (NMDA) antagonist, amantadine, as an adjuvant to L-DOPA (Fox et al., 2018). When therapeutic management using oral medication is no longer sufficient to manage the motor complications, patients are referred to advanced therapies such as continuous subcutaneous (s.c.) infusion of apomorphine, continuous intestinal infusion of L-DOPA, or deep brain stimulation (DBS) (Giugni and Okun, 2014).

Treatment-related complications in PD

Dyskinesia

The cumulative incidence rate of LID is approximately 30% with an onset time of 5-6 years from PD diagnosis (Eusebi et al., 2018), reaching up to 80% of patients treated with L-DOPA (Thanvi et al., 2007). The risk of developing these motor complications is correlated to a young age at PD onset, duration and severity of the parkinsonian motor symptoms, and higher cumulative L-DOPA dosage (Thanvi et al., 2007).

Phenomenologically, dyskinesia consists of involuntary movements with both fast hyperkinetic and slower dystonic features, that affects various parts of the body. In most cases, LID manifests as hyperkinetic, purposeless movements, that flow across body regions in a rapid, irregular sequence (chorea), but other hyperkinetic manifestations such as jerky motions (ballism) and stereotypies are also encountered. In other cases, LID is predominated by sustained twisting movements or abnormal fixed postures (dystonia) (Luquin et al., 1992).

The clinical presentations of LID are classified based on the temporal pattern of involuntary movements relative to the medication intake. Thus, “peak-dose” or “on” dyskinesias occur at the time of the highest brain concentration of L-DOPA, and mainly consists of choreiform movements. When dystonic components occur during peak-dose dyskinesia, they are usually shadowed by the presence of chorea. In contrast, “diphasic” dyskinesias occur less commonly at the beginning and end of each L-DOPA dose and are predominated by ballistic or stereotypic movements

mixed with dystonia (Fahn, 2000). Lastly, isolated dystonia can appear during the "off" state, when L-DOPA concentrations are low. These "off" dystonias can be painful and mainly affect the lower extremities of the body, the most typical form being early-morning dystonia in the feet (Melamed, 1979).

Impulsive-compulsive behaviours

When considering the treatment-related complications in PD, non-motor symptoms are often the most debilitating for the patient. Common non-motor features associated with DA replacement therapy include neuropsychiatric symptoms such as hallucinations, psychosis, and ICBs, of which this thesis will focus on ICBs. In PD patients, ICBs mainly manifest as pathological gambling, binge eating, hypersexuality, and compulsive shopping, although punding, hoarding, and other ICBs have also been reported (Weintraub et al., 2015).

While the incidence of ICBs in newly diagnosed, untreated patients with PD is not different from the general population, an increased risk of ICBs has been reported in patients who receive dopaminergic treatment, in particular DA agonists, with a 5-year cumulative incidence of 46% (Corvol et al., 2018; Weintraub et al., 2010; Weintraub et al., 2013). In addition to dopaminergic medication prescribing practices, additional correlates or potential risk factors have emerged, including young age of onset, sex, depression and anxiety, a familial or personal history of alcoholism or gambling, and pre-existing impulsive or novelty-seeking personality traits (Latella et al., 2019; Marinus et al., 2018).

ICBs are a heterogeneous group of conditions characterized by the inability to exhibit emotional and behavioural self-control, which can lead to impulsive and/or compulsive actions (Berlin and Hollander, 2014). Impulsivity is to act on impulses and urges without foresight or consideration of the negative consequences of these actions (Berlin and Hollander, 2014; Moeller et al., 2001), and has been related to rapid decision-making, lack of mental planning, and risk-taking (Eysenck, 1993). Compulsivity is the repetition of non-goal-oriented behaviours that are performed in order to relieve distress, despite unfavourable consequences (Berlin and Hollander, 2014; Dalley et al., 2011). Thus, a patient suffering from compulsions is often consciously aware of the adverse and perseverative character of the rituals, but feels emotionally compelled to perform them. In contrast, impulsive behaviours generally generate pleasure, although they may lose their pleasurable quality as the behaviour becomes more compulsive and automatic (Berlin and Hollander, 2014).

The higher incidence of ICBs upon treatment with DA agonists do not appear unique to PD patients, as a similar association has been reported in fibromyalgia and restless legs syndrome (Cornelius et al., 2010; Holman, 2009). Since treatment of ICBs continues to be a great challenge, they are often relieved by reducing the DA agonist dose or readjusting the dopaminergic PD medication (Mamikonyan et al., 2008). Alternative treatment strategies include the use of psychiatric medications (i.e. antidepressants) or DBS (Abbes et al., 2018; Weintraub and Mamikonyan, 2019).

Toxin-based rodent models of PD and LID

Parkinsonism refers to motor symptoms similar to the clinical manifestation of PD, although they can result from other conditions than PD, such as specific brain lesions, medications, and toxin exposure. Parkinsonism is commonly modelled preclinically by inducing a severe loss of striatal dopaminergic innervations in rodents using the neurotoxin 6-hydroxydopamine (6-OHDA) (Ungerstedt, 1968). This hydroxylated DA analogue selectively enters catecholamine neurons via the DA or noradrenaline transporter. Once inside the neuron, the toxin undergoes autoxidation, which leads to the production of reactive oxygen species, oxidative damage of cellular components, mitochondrial dysfunction, and ultimately cell death (Rotman and Creveling, 1976). Since 6-OHDA doses not cross the BBB, a direct injection in the nigrostriatal pathway is necessary to induce degeneration of the dopaminergic neurons, and commonly target the striatum, SNr, or the medial forebrain bundle (MFB).

As in patients, parkinsonian motor deficits start to manifest when more than 50% of striatal DA inputs are lost (Boix et al., 2018; Decressac et al., 2012; Fearnley and Lees, 1991). To obtain a model of severe late-stage PD, unilateral injection of 6-OHDA into the MFB is the preferred procedure, which leads to extensive dopaminergic degeneration accounting for 80-90% of the striatal DA depletion (Francardo et al., 2011; Winkler et al., 2002). Advantages of this unilateral model include its stability over time, which is particularly useful for evaluation of long-term pharmacological treatments, as well as the restriction of behavioural impairments to one side of the body, allowing for the intact side to serve as an internal control (Cenci and Björklund, 2020; Cenci et al., 1998). Importantly, rodents with severely denervated striatal motor regions (> 90%) can be used to model the motor complications associated with DA replacement therapy in PD (Cenci and Lundblad, 2007). Indeed, the majority of DA-depleted animals treated chronically with therapeutic-like doses of L-DOPA will develop involuntary movements analogues to LID (Francardo et al., 2011; Winkler et al., 2002). The time course of these dyskinetic behaviours is similar to that of peak-dose dyskinesia in PD patients, coinciding with large increases of extracellular DA levels in the striatum (Lindgren et al., 2010; Meissner et al., 2006). On the other hand, mild early-stage PD is often modelled by bilateral intrastriatal delivery of 6-OHDA (Przedborski et al., 1995). This type of lesion model enables a flexible modulation of the severity and distribution of DA denervation (Francardo et al., 2011; Winkler et al., 2002), and is often used to study the non-motor symptoms of PD due to its bilateral character. Although these toxin-based models do exhibit many PD-relevant pathological features, it is important to mention that they do not mimic several important characteristics, including the progressive time course of the neurodegeneration and the formation of intraneuronal alpha-synuclein inclusions.

Mechanisms of LID

Pre- and postsynaptic alterations in DA transmission

The establishment of LID depends on a series of maladaptive changes induced by the degeneration of dopaminergic neurons in combination with intermittent treatment with L-DOPA, which eventually leads to large fluctuations of DA levels in the brain. This altered response pattern depends on impairments in both the pre- and postsynaptic DA transmission (Cenci, 2014; Cenci and Konradi, 2010). Indeed, the loss of nigrostriatal dopaminergic neurons affects the presynaptic compartment, where L-DOPA is normally converted to DA, stored in synaptic vehicles, and released in a physiological manner. At first, the nigrostriatal DA system can maintain physiological DA transmission thanks to multiple compensatory mechanisms (Leenders et al., 1986; Zigmond et al., 1990). However, a severe loss of dopaminergic terminals will shift the metabolism of L-DOPA to other sites, in particular to serotonergic neurons, which express the enzyme mediating the conversion of L-DOPA to DA (Stansley and Yamamoto, 2013). Nevertheless, the serotonergic neurons release DA in an activity-dependent manner due to the lack of DA autoregulatory mechanisms mediated by presynaptic DA autoreceptors and high-affinity DA reuptake (Tanaka et al., 1999). This gives rise to non-physiological fluctuations in extracellular DA levels upon treatment with L-DOPA (Carta and Bezard, 2011) (see Figure 3).

In addition to these presynaptic adaptations, alterations in the postsynaptic dopaminergic signalling are crucial to the development of LID, particularly the enhanced sensitivity of postsynaptic DA receptors to DA. This supersensitivity depends on an increased coupling of D1 and D2 receptors to their corresponding G-protein, alterations in DA receptor trafficking and internalisation, an increased responsiveness of downstream intracellular canonical signalling molecules, and also an increased activation of non-canonical signalling pathways (Cenci and Konradi, 2010; Klawans et al., 1977; Murer and Moratalla, 2011) (see Figure 3).

While the contribution of D2 receptors has yet to be fully elucidated, the supersensitivity of D1 receptors has long been suggested as a crucial contributor to the development of LID. Indeed, the G-protein coupling efficiency of D1, but not D2 receptors, has been found to be further enhanced in LID (Aubert et al., 2005), and is paralleled by an upregulation of $G\alpha_{s/olf}$ proteins and an overactivity of the adenylyl cyclase signalling cascade downstream of the D1 receptor (Corvol et al., 2004; Hervé et al., 1993; Mishra et al., 1974). This leads to an increase cAMP-PKA-dependent phosphorylation of downstream targets, including the DA- and cAMP-regulated phosphoprotein (DARPP-32) (Santini et al., 2007), the GluA1 subunit of α-amino-3-hydroxy-5-methyl-4-isoxazolepropionic (AMPA) receptors (Snyder et al., 2000), and the extracellular signal-regulated protein kinase 1 and 2 (ERK1/2) (Pavón et al., 2006; Santini et al., 2009; Santini et al., 2007; Westin et al., 2007). It is important to note, that the activation of ERK1/2 is normally associated with the

stimulation of tyrosine-kinase or glutamate receptors during physiological conditions, and not $G\alpha_{s/olf}$-coupled receptors (Gerfen et al., 2002). Thus, the supersensitivity of D1 receptors is attributable to a switch to ERK1/2 activation specifically in dSPNs.

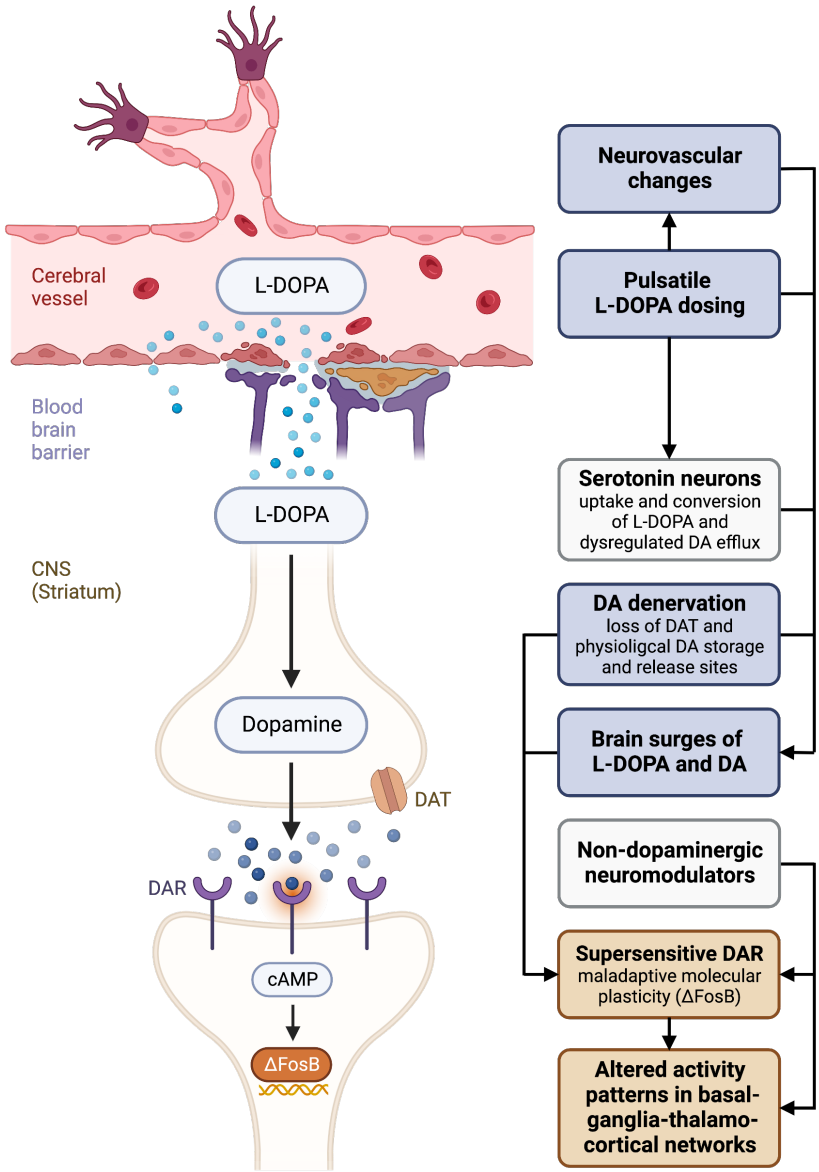

Figure 3. LID depends on pre- and postsynaptic alterations in DA transmission. At the presynaptic level, several factors contribute to the generation of surges of L-DOPA and DA in the brain (blue boxes). These presynaptic alterations, as well as secondary changes in non-dopaminergic neurotransmitter systems (white boxes), contribute to maladaptive changes in the postsynaptic dopaminergic signalling (yellow boxes). *Abbreviations not in text: DAR, DA receptor, CNS, central nervous system.* (Created with BioRender.com)

In turn, this aberrant activation of ERK1/2 in dSPNs triggers the activation of histone 3, leading to chromatin remodelling and maladaptive changes in the transcriptional regulation (Santini et al., 2009). Upon activation, ERK1/2 furthermore mediates a wide array of early response transcription factors that participate in the control of downstream proteins, including c-Fos, c-Jun, and FosB. Among these, the accumulation of the stable isoforms of FosB (ΔFosB) in dSPNs of the DA-denervated striatum is particularly correlated to the severity of dyskinesia upon chronic L-DOPA treatment (Lindgren et al., 2011; Pavón et al., 2006; Westin et al., 2001). Increased D1-dependent ERK1/2 signalling following L-DOPA treatment has moreover been associated with neurovascular changes, including angiogenesis and altered BBB permeability (Cenci, 2014; Lindgren et al., 2009). Importantly, the development of dyskinesia is positively associated with increased endothelial proliferation (nestin, a marker of ongoing angiogenesis) and BBB permeability (parenchymal albumin) in the DA-denervated striatum and basal ganglia output nuclei in an animal model of LID (Lindgren et al., 2009; Westin et al., 2006). This increased BBB permeability associated with angiogenesis has been suggested to contribute to higher extracellular levels of L-DOPA in LID (Cenci, 2014) (see Figure 3).

The contribution of D1 and D2 receptor stimulation to LID

Further implicating the critical role of overactivity of the direct pathway in LID, pharmacological and genetic inactivation of striatal D1 receptors and its downstream targets have been found to attenuate dyskinesia in animal models of LID (Bateup et al., 2010; Darmopil et al., 2009; Engeln et al., 2016; Santini et al., 2012; Santini et al., 2007). In addition, several recent studies have reported that specific optogenetic stimulation of dSPNs can induce dyskinesia in an animal model of PD, even in the absence of L-DOPA treatment (Girasole et al., 2018; Keifman et al., 2019). In line with these findings, the role of selective D1 agonists in inducing dyskinesias, with similar phenotypic components of L-DOPA, is well-established (Carta et al., 2008; Dupre et al., 2007; Grondin et al., 1997; Iderberg et al., 2013; Lindgren et al., 2009; Rascol et al., 2001).

While the pivotal role of the pulsatile stimulation of D1 receptors on dSPNs in LID has long been implicated, a pronounced synaptic remodelling of iSPNs in LID has only recently been described (Fieblinger et al., 2014a; Suarez et al., 2018; Suarez et al., 2016; Suárez et al., 2014). Consistent with a critical role of iSPNs, the chemogenetic stimulation of these neurons improves dyskinesia in a mouse model of LID (Alcacer et al., 2017), while the genetic ablation of D2 receptors specifically in iSPNs reduce the severity of dyskinesias induced by L-DOPA in DA-denervated mice compared to wild type animals (Andreoli, 2021). In another study, the complete loss of D2 receptor signalling, rendered by genetic knockout of D2 receptors in a non-specific manner, did not affect the development of dyskinesia in L-DOPA-treated animals (Darmopil et al., 2009). Thus, the heterogeneous expression of striatal D2 receptors might add to the complexity that has prevented a

full understanding of the implication of D2 receptor stimulation in LID. Further adding to this complexity, some studies have shown that D2/3 agonists can induce dyskinesia when administered de novo to parkinsonian mice and rats (Andreoli et al., 2021; Bagetta et al., 2012), while others report only mild or no effects (Carta et al., 2008; Lundblad et al., 2002). However, D2/3 agonists are known to induce dyskinesia in parkinsonian rats previously primed with L-DOPA (Dupre et al., 2007; Kiessling et al., 2020; Sebastianutto et al., 2020), indicating a role of the D2 receptor in established LID. Interestingly, Andreoli and co-authors recently reported that the D2 receptor is a crucial mediator of the dystonic components of LID in hemiparkinsonian mice (Andreoli et al., 2021).

The serotonergic system in LID

In addition to the maladaptive changes of the dopaminergic system, LID is also associated with secondary changes to several non-dopaminergic systems, including the serotonergic, glutamatergic, and cholinergic system. This has led to an increased interest in improving LID and/or motor fluctuations by targeting non-dopaminergic receptor systems (Cenci et al., 2022) (see Figure 4).

Due to its involvement in the non-physiological release of DA upon L-DOPA treatment, the serotonergic system has attracted great attention as a potential antidyskinetic target. The neurotransmitter release from serotonergic neurons are regulated by several autoreceptors, including the serotonin (5-HT)-1a and 5-HT1b receptors expressed presynaptically at somatodendritic sites and axon terminals, respectively (McDevitt and Neumaier, 2011). Accordingly, agonists of 5-HT1a receptors have been found to reduce the peaks in extracellular DA levels occurring after L-DOPA administration in 6-OHDA-lesioned rats (Iderberg et al., 2015; Lindgren et al., 2010) as well as in PD patients (Politis et al., 2014). Moreover, partial 5-HT1a agonists have been found to improve LID in PD patients, although their utility is complicated by dose-limiting adverse events, in particular a worsening of parkinsonian motor symptoms (Bara-Jimenez et al., 2005; Bonifati et al., 1994; Goetz et al., 2007). Using much more potent and selective 5-HT1a agonists, an alternative approach is thus to combine low doses of 5-HT1a and 5-HT1b receptor agonists to primarily target the presynaptic receptors (Carta et al., 2007; Muñoz et al., 2009). This approach has proven very effective in reducing surges in extracellular DA levels induced by L-DOPA (Lindgren et al., 2010), while ameliorating LID in both rodent and non-human primate models of PD (Bezard et al., 2013; Lindgren et al., 2010; Paolone et al., 2015). It is however important to mention, that the antidyskinetic effects of the 5-HT1a/b agonists may also depend on additional postsynaptic mechanisms, as these drugs can also alleviate dyskinesias induced by DA receptor agonists (Dupre et al., 2008; Jaunarajs et al., 2009). Such postsynaptic effects of 5-HT1a stimulation may rely on a reduced striatal glutamate release (Dupre et al., 2011), possibly mediated by 5-HT1a receptors expressed in the motor cortex (Antonelli et al., 2005; Ostock et al., 2011).

The glutamatergic system in LID

Altered glutamatergic signalling in the cortico-basal ganglia network is strongly associated with LID (Bastide et al., 2015; de Iure et al., 2019; Sgambato-Faure and Cenci, 2012). Indeed, enhanced extracellular levels of glutamate are paralleled by compensatory modifications of the expression and subcellular distribution of both ionotropic and metabotropic glutamate receptors (iGluRs and mGluRs, respectively) in the basal ganglia circuitry in animal models of LID (Mela et al., 2012; Paolone et al., 2015; Robelet et al., 2004; Sgambato-Faure and Cenci, 2012).

Interestingly, an increased activation of striatal iGluRs, namely NMDA receptors, has been demonstrated in PD patients following treatment with L-DOPA (Ahmed et al., 2011). The multitarget drug, amantadine, is currently used for the clinical management of LID, and its antidyskinetic effects are partly attributed to non-competitive antagonism of NMDA receptors (Danysz et al., 1997; Paquette et al., 2012). However, amantadine is also associated with severe side effects, such as

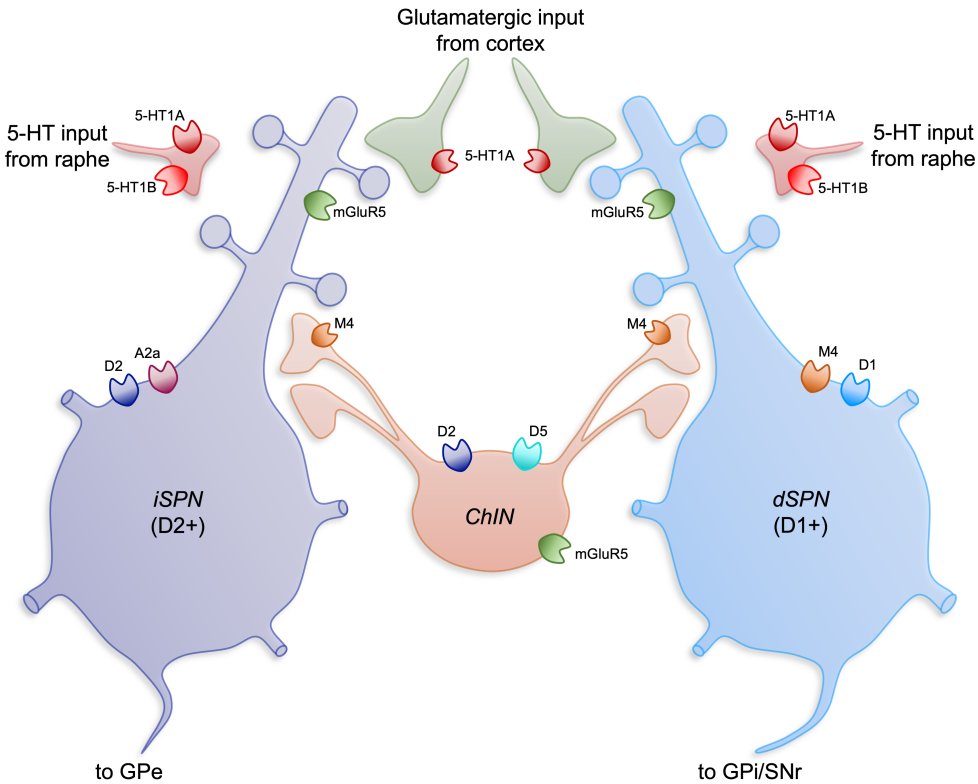

Figure 4. Non-dopaminergic targets within the DA-denervated striatum. The drawing depicts potential receptor targets for the treatment of LID investigated in this thesis. Receptors are shown if ≥ 50% of the indicated cell category is estimated to express it, and larger receptor sizes indicate ~100% expression. Moreover, the larger size of SPNs than ChINs reflects their larger number and perceived importance. Adapted with permission from *Cenci et al. (2022).*

hallucinations, delusion, and constipation (Rascol et al., 2021), that eventually may lead to treatment termination.

On the other hand, the metabotropic receptor type 5 (mGluR5) in particular, has attracted considerable interest as a target in LID. The mGluR5 is expressed postsynaptically in striatal SPNs and interneurons, as well as in the cerebral cortex, hippocampus, and STN (Kerner et al., 1997; Kuwajima et al., 2007; Tallaksen-Greene et al., 1998). It couples to the G-protein subtype $G\alpha_q$, and binding of glutamate will therefore stimulate phosphoinositide hydrolysis and intracellular calcium release resulting in increased neuronal excitability (Pin and Acher, 2002). The striatal expression of mGluR5s has been found to be upregulated in animal models of LID and in PD patients (Konradi et al., 2004; Ouattara et al., 2011; Sanchez-Pernaute et al., 2008). Accordingly, several studies have found that negative allosteric modulators (NAMs) of mGluR5 can improve dyskinesia (Bezard et al., 2014; Mela et al., 2007; Morin et al., 2013; Rylander et al., 2010), an effect that is associated with a partial normalisation of the D1 receptor-mediated accumulation of ΔFosB (Levandis et al., 2008) and overactivation of ERK1/2 in the dSPNs (Fieblinger et al., 2014b; Sebastianutto et al., 2020). In line with these findings, a recent study found that mGluR5s can form heteromeric complexes with D1 receptors, and that such heteromers are upregulated in the striatum in rodent models of PD and LID (Sebastianutto et al., 2020). These functional interactions likely explain the efficacy of mGluR5 NAMs in reducing dyskinesias induced by specific stimulation of D1 receptors (Iderberg et al., 2013; Sebastianutto et al., 2020).

The cholinergic system in LID

In addition to the neurotransmitter systems covered so far, LID expression involves a complex interaction between the dopaminergic and cholinergic system. In fact, 5% of striatal neurons are interneurons forming dense microcircuits within the striatum, of which approximately 1% are cholinergic (Kawaguchi et al., 1995). In the dorsal striatum, the $G\alpha_{i/o}$-coupled M4 receptor is the most abundant muscarinic acetylcholine receptor (mAChR). The M4 receptor is preferentially expressed postsynaptically in dSPNs, but also presynaptically on ChINs functioning as an autoreceptor (Tayebati et al., 2004; Yan et al., 2001). Since the terminals of ChINs overlap with dopaminergic neurons, activation of the M4 receptors can suppress D1 receptor signalling through adenylyl cyclase (Jeon et al., 2010; Sánchez et al., 2009), and has therefore been suggested as a potential antidyskinetic target. Accordingly, treatment with M4 positive allosteric modulators (PAMs) was recently found to ameliorate LID in both rodent and primate models of PD without compromising the symptomatic benefit of L-DOPA (Shen et al., 2015). In line with these findings, a worsening of LID has been found upon treatment with an M4 receptor antagonist, although opposite effects were seen for dyskinesias induced by a D1 receptor agonist (Chambers et al., 2019). In contrast, a recent study reported that LID was

alleviated by both positive allosteric modulation and antagonism of the M4 receptor (Brugnoli et al., 2020), suggesting that both pre- and postsynaptic mechanisms may contribute to the modulatory effects of mAChR on dyskinesia.

In Paper IV, the antidyskinetic properties of ligands targeting these non-dopaminergic systems are evaluated in two distinct preclinical models of dyskinesia.

Mechanisms of drug-induced ICBs

In PD patients, the dopaminergic projections to the ventral striatum are relatively unimpaired (Kish et al., 1988). Nevertheless, the development of ICBs in PD patients has been proposed to depend on sensitised DA transmission in limbic regions, in particular induced by treatment with DA agonists. Specifically, the availability of D2/3 receptors and DA transporters (DAT) plays a key role in the development of ICBs in PD patients. Indeed, molecular neuroimaging studies in PD patients with ICBs have reported decreased D2/3 receptor binding in the ventral striatum compared to non-impulsive PD patients, likely indicating lower D2/3 availability (Payer et al., 2015; Steeves et al., 2009). During a gambling task, Steeves and co-authors furthermore showed an increased release of DA in the ventral striatum in patients with pathological gambling (Steeves et al., 2009). This might be linked to low levels of midbrain D2/3 autoreceptors (Ray et al., 2012), which provide a negative feedback control over striatal DA release. Thus, patients with low midbrain receptor density might have greater dopaminergic responses to reward, and therefore be more impulsive. The DA transmission in the striatum is moreover regulated by presynaptic DATs. Importantly, a reduced striatal DAT availability in medicated PD patients is often associated with an increased risk of ICBs (Cilia et al., 2010; Navalpotro-Gomez et al., 2019; Voon et al., 2014), and may even precede ICB development (Vriend et al., 2014). In the ventral striatum, reduced DAT binding has indeed been found to be inversely correlated with the clinical severity of ICBs (Navalpotro-Gomez et al., 2019). Altogether, these alterations might result in the overstimulation of ventral striatal circuits that contribute to an increased drive towards rewarding stimuli.

The development of ICBs also depend on the ability to inhibit urges and responses controlled by frontocortical regions, such as PFC and cingulate cortex. Thus, altered frontocortical activity may lead to impairments in response inhibition and risk assessment. Indeed, increased D2/3 receptor binding has been reported in the ACC and orbitofrontal cortex (OFC) in PD patients with pathological gambling, indicating a low dopaminergic tone in these regions (Ray et al., 2012). The results from functional imaging studies in PD patients with ICBs are however more complex, reporting both reduced and enhanced activity in the PFC, OFC, and ACC (Cilia et al., 2008; Hammes et al., 2019; Petersen et al., 2018; van Eimeren et al., 2010). In studies of resting-state functional connectivity, treatment-induced ICBs in PD patients are often associated with a disconnection between frontocortical and striatal areas of the limbic circuits (Carriere et al., 2015; Hammes et al., 2019;

Ruitenberg et al., 2018), while an increased connectivity has also been reported (Petersen et al., 2018). Additionally, divergent results have been observed in functional imaging studies using reward-related tasks in PD patients with ICBs (Frosini et al., 2010; Paz-Alonso et al., 2020; Politis et al., 2013; Rao et al., 2010; Voon et al., 2011a). Moreover, it is important to note that several recent studies have reported alterations in brain-wide networks, including the salience, executive, and default-mode network (Imperiale et al., 2018; Mata-Marín et al., 2021; Tessitore et al., 2017). In addition to a disconnection between these networks, another study recently revealed an enhanced functional coupling within the salience network in PD patients with ICBs (Navalpotro-Gomez et al., 2020). This increased within-network connectivity was directly correlated with the clinical severity of impulsivity and novelty-seeking only in patients exhibiting ICBs. Although these studies point towards an important role of dopaminergic therapies in altering the frontocortical-striatal signalling in PD patients with ICBs, the diverging findings highlight the complexity of the underlying mechanisms responsible for the development of ICBs in PD patients.

In addition, other alterations in limbic cortical regions have been described in PD patients with ICBs, including an increased cortical thickness in the ACC, OFC, and frontal pole (Hammes et al., 2019; Pellicano et al., 2015; Tessitore et al., 2016). Importantly, Tessitore et al. (2016) found that these abnormalities in cortical thickness correlated positively with the severity of ICBs. However, other studies have reported a cortical thinning in fronto-striatal circuits in patients with ICBs (Biundo et al., 2015; Imperiale et al., 2018), which encourages further investigations on changes in grey matter volume in relation to ICBs in PD.

Experimental modelling of ICBs in PD

Further implications for an essential role of D2 receptors in ICBs come from rodent studies investigating the rewarding or aversive properties of DA agonists using tests of conditioned place preference/aversion (CPP/CPA). Indeed, stimulation of D2/3 receptors induces CPP, while D1 receptor stimulation mainly induces CPA, suggesting a predominant role of D2 receptors in the reinforcing properties of dopaminergic pharmacotherapies (Zengin-Toktas et al., 2013). The role of striatonigral degeneration in D2 agonist-mediated behavioural reinforcement is however still unclear. While some studies report similar results upon treatment with D2 agonist in parkinsonian and control animals (Engeln et al., 2013; Zengin-Toktas et al., 2013), others observe that lower D2 agonist doses are sufficient to induce CPP in animal models of PD but not intact animals (Loiodice et al., 2017; Riddle et al., 2012).

In rodents, ICBs are typically assessed using a variety of operant tasks that measure response inhibition (motor impulsivity) and decision-making (cognitive impulsivity). These tasks assess the inability to choose advantageous actions over more immediate or risky choices. Utilising such tasks, it has been extensively demonstrated that animals treated with D2/3 agonists display ICB characteristics

like waiting impulsivity (Jiménez-Urbieta et al., 2020; Jiménez-Urbieta et al., 2019), repetitive behaviour (Dardou et al., 2017), probability discounting, and risky decisions (Holtz et al., 2016; Rokosik and Napier, 2012; Tremblay et al., 2017). However, the impact of PD-related pathological dopaminergic signalling on the development of these ICBs is still a matter of debate (Calandrella and Antonini, 2011; Vriend, 2018).

Using Fos protein expression as a biomarker, increased neuronal activation has been reported in the dorsal and ventromedial striatum, as well as in the OFC (Dardou et al., 2017) in 6-OHDA-lesioned rats with pramipexole-induced compulsive-like behaviours. However, a recent study did not find a correlation between striatal Fos/ΔFosB expression and premature responses in the 5-choice serial reaction time task following pramipexole treatment in rats with mild parkinsonism induced by nigral overexpression of alpha-synuclein and controls (Jiménez-Urbieta et al., 2019).

This example illustrates that frequent discrepancies are encountered when reviewing the experimental literature on therapy-induced ICBs. Compared to the literature on motor features and LID, the number of available studies is moreover limited. It is indeed challenging to model the neuropsychiatric complications of PD therapy in animals, given their subjective nature, their yet unclear pathological substrate, and the lack of clearly effective treatments in patients, which could be used to validate the models. Nevertheless, the ICBs induced by PD pharmacotherapy are a very important clinical problem in need of robust experimental models to guide the development of new therapies.

Oscillations in cortico-basal ganglia circuits

There is a vast consensus that the pathophysiological features of PD and LID depend on altered information processing in the cortico-basal ganglia loop, which is reflected in the firing rate of single cells as well as changes in neuronal synchronisation and functional connectivity at the population level (Cenci et al., 2018). Although rhythmic so-called oscillatory activity in the basal ganglia circuitry occurs in physiological conditions (Bevan et al., 2002; Courtemanche et al., 2003), excessive neuronal synchronisation may limit the overall information coding capacity of the circuit (Brittain and Brown, 2014). This is because synchronised neurons are more susceptible to fire together, thereby reducing their independent transmission of different information. Synchronised neuronal activity can be derived from the low-frequency component (< 400 Hz) of the electric potential difference recorded with extracellular intracerebral microelectrodes, and is referred to as local field potentials (LFP). Mechanistically, LFPs are thought to reflect rhythmic synchronisation of dendritic currents induced by excitatory and inhibitory synaptic inputs to a population of cells located in close proximity to the recording electrode (Buzsáki et al., 2012; Lindén et al., 2010). The oscillatory properties of a

neuronal circuit therefore depend on the physiological features of the different cells within the network (Singer, 2018; Wang, 2010). Accordingly, maladaptive changes induced by the dopaminergic denervation in PD and the treatment with L-DOPA, such as alterations in the relative strength of synaptic connectivity (Fieblinger et al., 2014a; Gittis et al., 2011), may contribute to the emergence of oscillatory activity in different parts of the cortico-basal ganglia-thalamic circuits (Cenci et al., 2018; Richter et al., 2013). The further propagation of oscillatory activity within this circuit can be facilitated by alterations in connection properties between distinct brain structures (Belić et al., 2016; Santana et al., 2014).

Oscillations associated with resting tremor and hypokinesia

Because resting tremor is one of the cardinal signs of PD, it was early on of great interest to elucidate the pathophysiological mechanisms underlying parkinsonian tremor. In PD patients, resting tremor is associated with neuronal oscillations at tremor frequencies in the theta range (~4-7 Hz) recorded in several key nodes of the basal ganglia circuitry, including the thalamus (Lenz et al., 1988), STN (Asch et al., 2020; Rodriguez et al., 1998; Rodriguez-Oroz et al., 2001), and GPi (Magnin et al., 2000). In a recent study, this resting tremor moreover showed a tendency to correlate negatively with neuronal activities in the STN in a somewhat higher frequency range (~13-35 Hz), referred to as beta oscillations (Asch et al., 2020).

Indeed, excessive beta oscillatory activities have been recorded during parkinsonian hypokinetic states in various nuclei of the basal-ganglia circuitry in both animal models of PD (Avila et al., 2010; Brazhnik et al., 2012; Sharott et al., 2005; Singh and Papa, 2020), as well as in PD patients (Brown et al., 2001; Kühn et al., 2005; Priori et al., 2004). Beta activity has been found to decrease during both movement preparation and execution (Joundi et al., 2013; Kühn et al., 2004; Lofredi et al., 2018), while a significant rebound is seen after movement termination (Cassidy et al., 2002). In patients, beta oscillations correlate with clinically evaluated parkinsonian motor signs (bradykinesia/rigidity) (Lofredi et al., 2022; Neumann et al., 2016), and are suppressed by dopaminergic treatments or DBS. The suppression of exaggerated beta activity correlates with a clinical improvement in motor performance induced by the respective therapy (Kühn et al., 2008; Kühn et al., 2006; Kühn et al., 2009; Oswal et al., 2016). Similarly, treatment with L-DOPA has been shown to reduce beta activity in 6-OHDA-lesioned rats (Avila et al., 2010; Brazhnik et al., 2012; Dupre et al., 2016). It is however important to mention, that critical differences exist between PD patients and animal models of PD with respect to beta oscillations. For example, akinesia/bradykinesia can be induced in these animal models without a simultaneous increase in beta activity (Ivica et al., 2018; Pan et al., 2016), suggesting that beta activity in rodents is not the direct cause of these motor symptoms. Moreover, beta oscillations are often divided into a low (~13-20 Hz) and high (~21-35 Hz) frequency component. In PD patients, low beta activity is more dominant within the STN, and has been associated with motor impairment and the L-DOPA-induced suppression (Kühn et al., 2009; Tsiokos et

al., 2017). On the contrary, the most robust beta oscillation in awake, behaving rodents is generally found at higher frequencies (Delaville et al., 2014; Delaville et al., 2015), and it remains to be determined if these oscillations are sufficiently comparable to the human beta.

The neural mechanisms specific to the generation of these pathological beta oscillations is still a matter of debate. Various hypotheses have been proposed, placing the origin within the enhanced intrastriatal signalling of ChINs or fast-spiking interneurons (Gittis et al., 2011; McCarthy et al., 2011), the intrinsic oscillatory properties of the GPe-STN network (Cruz et al., 2011; Holgado et al., 2010; Magill et al., 2000), or the cortically emerging beta activity. Importantly, the latter is suggested be either influenced by extrinsic synaptic drive from the basal ganglia or thalamus (Sherman et al., 2016), or to be amplified by feedback inhibition in the GPe-STN network (Baufreton et al., 2005; Litvak et al., 2011; Marreiros et al., 2013). Nevertheless, it is currently unclear whether these mechanisms generate or merely sustain ongoing beta oscillations.

Oscillations associated with LID

While neuronal oscillations in the theta range have generally been linked with resting tremor, a more subtle theta activity was recently reported to display a weak temporal coactivation with beta oscillations in the STN of PD patients, that correlated negatively with tremor (Asch et al., 2020). This might be the same slow oscillation (~4-10 Hz) that has been reported to increase in deep basal ganglia nuclei after DA replacement therapy in both animal models of PD (Brys et al., 2018; Chen et al., 2021; Wang et al., 2019) and in PD patients (Alonso-Frech et al., 2006; Rodriguez-Oroz et al., 2011). In patients, theta activity increases particularly in the presence of dyskinesia (Alonso-Frech et al., 2006), including diphasic dyskinesias that often have a strong dystonic appearance (Alegre et al., 2012), and correlate with its clinical evaluation (Giannicola et al., 2013). In light of these findings, it is interesting to consider that theta oscillations in the deep basal ganglia nuclei are also strongly associated with dystonic symptoms in cervical dystonia (Johnson et al., 2021; Neumann et al., 2017; Piña-Fuentes et al., 2019). Recent studies in 6-OHDA-lesioned animals have confirmed the presence of theta oscillations during periods of LID, in particular in the deeper nuclei of the basal ganglia (Brys et al., 2018; Tamtè et al., 2016; Wang et al., 2019). While these spectral changes have previously been proposed to partly depend on the more active behavioural state, Wang and co-authors recently showed a direct correlation between theta oscillations and dyskinesia in this animal model (Wang et al., 2019).

Besides the increase in theta activity, oscillations in a narrow gamma frequency range (~70-110 Hz, narrowband gamma; NBG) have been reported across cortico-basal ganglia structures in PD patients after L-DOPA treatment (Brown et al., 2001; Cassidy et al., 2002; Litvak et al., 2012; Trottenberg et al., 2006; Williams et al., 2002). Similar NBG activity can be induced by STN-DBS in the absence of L-DOPA (Wiest et al., 2021), and has been shown to correlate with the motor

improvement induced by DBS (Muthuraman et al., 2020). Considering that the power of broadband gamma oscillations increases in conjunction with voluntary movements (Cassidy et al., 2002), increased NBG power, at least in the subcortical structures, has generally been associated with the beneficial prokinetic effects of L-DOPA. In contrast, Halje and colleagues proposed a direct pathological role of cortical NBG oscillations (Halje et al., 2012). They found that persistent NBG oscillations were only present in the DA-denervated motor cortex of the hemiparkinsonian rat specifically during dyskinesia. These oscillations, as well as the dyskinetic symptoms, could be suppressed by topical application of a D1 receptor antagonist on the cortical surface, which points to a strong link between persistent cortical NBG oscillations and dyskinesia. Further supporting these findings, cortical NBG oscillations have been shown to develop with the gradual increase of dyskinetic symptoms induced by daily L-DOPA administration during a priming period of 1 week (Dupre et al., 2016). This study furthermore showed that the independent stimulation of D1 or D2 receptors can induce cortical NBG oscillations in L-DOPA-primed rats. In addition, multi-structure LFP recordings in animal models of LID have demonstrated that NBG oscillations are particularly strong in cortico-striatal circuits, but can also be found in several other structures, including the GPe, thalamus, and STN (Belić et al., 2016; Brys et al., 2018; Tamtè et al., 2016). Importantly, these findings were later confirmed in PD patients, as a result of long-term recordings performed using a combined DBS and electrocorticogram device in dyskinetic subjects (Swann et al., 2016; Swann et al., 2018). Through this experimental design, the authors revealed a strong association between dyskinesia in PD patients and the same type of prominent NBG oscillation as observed in the rat model of LID. Both in the motor cortex and in the STN, the oscillation coincided closely with dyskinesia, while being minimally affected by voluntary movements (Swann et al., 2016), suggesting that this NBG activity is predominantly pathological rather than prokinetic.

In line with what has been reported for oscillations at lower frequencies, the generation of strong NBG oscillations at a network level might depend on neurochemical, physiological, and cellular changes induced by the degeneration of dopaminergic neurons and DA replacement therapy with L-DOPA. The underlying mechanisms responsible for promoting these high frequency oscillations have however attracted much less attention. Nevertheless, several aforementioned studies points towards an important role of the motor cortex (Dupre et al., 2016; Halje et al., 2012; Swann et al., 2016). One hypothesis therefore proposes that NBG oscillations are intrinsically generated in the cortical network from interactions between principal cells and inhibitory interneurons, and then spread to subcortical structures (Cenci et al., 2018). Considering the strong influence of thalamic input on cortical activity, another hypothesis suggests that rhythmic thalamic inputs could drive the cortical NBG oscillations in LID (Petersson et al., 2019). Indeed, preliminary experimental findings suggest that cortical and thalamic nuclei display coherent NBG oscillations during LID, and that a local pharmacological suppression

of these thalamic nuclei eliminates NBG activity in the motor cortex, although a concomitant alleviation of LID was not seen (Dupre, 2015). At present, an in-depth dissection of the underlying mechanisms is necessary to further the understanding of how cellular processes can induced such network dysfunctions and ultimately improve our understanding of LID.

Aims of this thesis

Aims of this thesis

The focus of this thesis has been to develop improved experimental models and biomarkers to advance translational research on the motor and neuropsychiatric complications of PD therapy. To achieve this, we pursued the following aims:

I. To address the relationship between network oscillations and motor activity in rat models of parkinsonism

II. To compare network oscillations induced by selective DA agonists of D1 and D2 receptors in a rat model of LID

III. To examine the impact of adjunct treatment with DA agonists on patterns of LID-related neuroplasticity and drug responses

IV. To develop models of neuropsychiatric complications induced by DA agonist treatment, given alone or combined with L-DOPA

Materials and Methods

Materials and Methods

Animals

Adult, female Sprague-Dawley rats used in the present thesis were purchased from Janvier Labs (Paper I-IV) or the central vivarium of the University of Chile Medical Faculty (Paper I). Animals weighed approximately 225-250 g on arrival. They were housed in standard cages on a 12 h light/dark cycle with *ad libitum* access to food and water.

Surgical procedures

Animal models of PD

In Paper I-III, unilateral nigrostriatal DA denervation was induced by injecting the neurotoxin 6-OHDA (Sigma Aldrich AB) into the MFB according to a well-established method (Cenci and Lundblad, 2007; Francardo et al., 2011). Briefly, the toxin was dissolved at a concentration of 3.5 µg/µl (free base) in 0.2% ice-cold ascorbate-saline and used within 2 h. Two injections of 2.5 and 2 µl toxin solution were performed at a rate of 1 µl/min at the following coordinates (in mm relative to bregma and dural surface): (1) anterior-posterior (AP) = -4.0, medial-lateral (ML) = -1.2, dorsal-ventral (DV) = -7.8, with tooth bar in flat skull position; (2) AP = -4.0, ML = -0.8, DV = -8.0, with tooth bar at +7.9 from flat skull position. Only animals exhibiting ≤ 25% contralateral forelimb use in the cylinder test were included in the study ensuring selection of animals with severe (> 80%) unilateral DA denervation in the striatal motor regions (Francardo et al., 2011; Lundblad et al., 2002). Furthermore, the efficacy of the lesions was verified post-mortem using TH immunohistochemistry. Rats included in the studies had ≥ 90% reduction in the density of striatal DA fiber terminals in the lesioned hemisphere relative to the intact hemisphere.

In Paper I and IV, bilateral striatal DA denervation was performed according to previous studies (Jiménez-Urbieta et al., 2020; Riddle et al., 2012). The toxin 6-OHDA was dissolved at a concentration of 3.3 µg/µl (Paper I) or 3.75 µg/µl (Paper IV) (free base) in 0.2% ascorbate-saline. In Paper I, severe bilateral DA denervation was induced by three injections of 2 µl toxin solution at a rate of 1 µl/min in each side of the striatum at the following coordinates (flat skull position): (1) AP = +1.0, ML = ±3.0, DV = -5.0; (2) AP = -0.1, ML = ±3.7, DV = -5.0; (3) AP = -1.2, ML =

±4.5, DV = -5.0. Sham lesions were carried out injecting the same volume of ascorbate-saline solution. In Paper IV, mild DA denervation (< 50%) was induced by injecting the toxin bilaterally into the DLS at the following coordinates (flat skull position): AP = +0.7, ML = ±3.4, DV = -4.5. A total of 2 µl toxin solution was injected at a rate of 0.5 µl/min. Sham lesions were carried out by placing the needle at the coordinates without injection. The efficacy of the 6-OHDA lesions was evaluated three weeks following surgery using the stepping test (Paper IV) and post-mortem using TH immunohistochemistry (Paper I and IV).

Implantation surgeries

In Paper I-II, electrode implantation surgeries were performed at least two or six weeks after bilateral (Paper I) or unilateral (Paper I-II) 6-OHDA-lesions, respectively. Arrays of tungsten microwire electrodes (33 mm, California Wires) were prepared as previously described (Ivica et al., 2014). Target coordinates and main references are presented in Table 1. All wires from each hemisphere were connected to a custom-designed printed circuit board and secured with UV-curable adhesive (Dymax). A 125 µm silver wire (Advent Research Materials Ltd) on the electrode array was attached to screws in the frontal and occipital skull bone for ground connection, and the implant was anchored to the screws in the skull with dental acrylic cement (Kerr) also covering the ground wires for electrical insulation.

Table 1. Coordinates of brain regions targeted by recording implant.

Target brain region	Center coordinates (mm)	Main references
Rostral forelimb area (RFA)	AP 3.75, ML ± 2.0, DV -1.0	(Neafsey et al., 1986; Neafsey and Sievert, 1982)
Forelimb area of the primary motor cortex (M1FL)	AP 1.76, ML ± 2.71, DV -1.0	(Gioanni and Lamarche, 1985; Neafsey et al., 1986)
Dorsomedial striatum (DMS)	AP 0.11, ML ± 2.65, DV -3.75	(West et al., 1990)
Dorsolateral striatum (DLS)	AP 0.11, ML ± 4.07, DV -4.0	(West et al., 1990)
Trunk area of the primary motor cortex (M1Tr)	AP -0.75, ML ± 1.625, DV -1.0	(Neafsey et al., 1986)
Globus pallidus pars externa (GPe)	AP -1.0, ML ± 3.125, DV -6.125	(Chen et al., 2011)
Substantia nigra pars reticulata (SNr)	AP -5.5, ML ± 2.45, DV -7.8	(Wang et al., 2010)

Center coordinates are given in mm relative to bregma (for AP and ML) and cortical surface (for DV) with tooth bar in flat skull position.

Drugs

An overview of the compounds (and respective vehicle controls) administered *in vivo* is reported in Table 2. For detailed protocols regarding preparation of solutions and study designs, please refer to the method sections of Paper I-IV.

Table 2. Compounds administered *in vivo*

Drug	Receptor target	Principle of action	Dose	Animal model	Supplier	Vehicle	Inj. Route	Paper
L-DOPA	DA	Agonist	6 3/6 6/24	Uni Uni Bi	Sigma Aldrich	Saline + benserazide	s.c.	II III IV
Sumanirole	D2	Agonist	2	Uni	Tocris	Saline	s.c.	II
Ropinirole	D2/3	Agonist	0.5/1.5 0.5/2.5	Uni Bi	HelloBio	Saline	s.c.	III IV
SKF82958	D1/5	Agonist	0.05	Uni	Tocris	Saline	s.c.	II
SKF38393	D1/5	Partial agonist	2	Uni	Sigma Aldrich	Saline	s.c.	III
SCH23390	D1/5	Antagonist	0.05/0.25	Uni	Abcam	Saline	i.p.	III
L741626	D2	Antagonist	1/3	Uni	Tocris	DMSO (10%)	s.c.	III
Amantadine	NMDA	Antagonist	20/40	Uni	Sigma Aldrich	Saline	i.p.	III
MK801	NMDA	Antagonist	0.0175/0.035	Uni	Abcam	Saline	s.c.	III
MTEP	mGluR5	Antagonist	2.5/5	Uni	Abcam	Saline	s.c.	III
8-OH-DPAT	5-HT1a	Agonist	0.035/0.05	Uni	Tocris	Saline	s.c.	III
CP94253	5-HT1b	Agonist	0.75/1	Uni	Tocris	Saline	s.c.	III
VU0467154	M4	PAM	5/10	Uni	VCNDD	Tween80 (10%)	s.c.	III

Behavioural testing

Abnormal involuntary movement (AIM) ratings

In unilateral rat models of PD, dyskinesias are recognised as movements that (i) are induced by L-DOPA or other DA agonist treatments, (ii) affects the side of the body contralateral to the lesion, and (iii) are repetitive, purposeless, and not identifiable within any normal rodent behavioural pattern (Cenci et al., 1998). These AIMs are classified into three subtypes based on their topographic distribution: (i) axial AIMs are contralateral flexion of the neck or torsion of the upper trunk, (ii) limb AIMs are repetitive jerks or dystonic posturing of the contralateral forelimb, and (iii) orolingual AIMs are bursts of empty chewing movements with or without jaw opening or tongue protrusion (Cenci et al., 1998; Cenci and Lundblad, 2007). Each AIM subtype was rated using a frequency scale and an amplitude scale, both having severity grades from 0 to 4. The frequency scale considers the proportion of observation time during which a dyskinetic movement is present (Cenci et al., 1998), whereas the amplitude scale evaluates the deviation of dyskinetic body parts from their natural resting position and the number of muscle groups visibly engaged in the dyskinetic movement (Cenci and Lundblad, 2007; Sebastianutto et al., 2016). Rats were placed individually in transparent cages and were allowed to habituate

for approximately 15 min before each test session. Following drug administration, the three AIM subtypes were rated simultaneously with respect to their frequency and amplitude for monitoring periods of 1 min every 20 min for 3 h (Paper III) or every 5 min for the first 20 min and then every 10 min for the rest of the test session (Paper II). In Paper III, locomotor activity with a contralateral turning bias was evaluated simultaneously using the frequency scale. A composite AIM score was then produced by multiplying the frequency score and amplitude score for each AIM subtype on each monitoring period. Then, all AIM scores were summed to obtain a global measure of dyskinesia for each test session (global AIM score).

Cylinder test

A test of spontaneous limb use during vertical exploratory behaviour (cylinder test) was used to evaluate the efficacy of DA denervation in the striatum induced by the unilateral 6-OHDA lesions in Paper I-III. This test takes advantage of the animals' innate drive to explore a new environment by rearing against the enclosing walls. Briefly, the rats were placed individually in a glass cylinder flanked by mirrors and video recorded for 3-5 min. The total number of supporting wall contacts performed independently with the left and right forepaw was counted. The performance of the forepaw contralateral to the lesion (left paw) was expressed as a percentage of the total number of wall contacts recorded in a session.

Stepping test

The stepping test (also called forelimb paw-adjusting step test) was used to evaluate the efficacy of bilateral DA depletion (Paper IV) and the effects of drug treatments on the lesion-induced forelimb hypokinesia (Paper III-IV). The ability of each rat to perform adjusting steps in response to experimenter-imposed lateral movements was investigated as previously described (Jiménez-Urbieta et al., 2020; Winkler et al., 2002). Briefly, each rat was held firmly with its hindlimbs and one forelimb restrained, letting the unrestrained forelimb contact a table surface. Then, rats were moved 90 cm laterally in the direction towards the rat's midline during a 5 s period while a second experimenter counted the number of adjusting steps. Three weeks post lesion, animals were habituated to the handling associated with this test for 3-5 consecutive days. In bilaterally lesioned animals, this was followed by one day of testing to evaluate the efficacy of the lesion (Paper IV). To evaluate the effects of chronic treatments, the test was applied on 3 consecutive days to reach a stable baseline performance followed by 1 day of testing. The test was carried out at 25 min (Paper IV) or 60 min (Paper III) following drug injection. The results are expressed as the number of forelimb-adjusting steps per session performed with the paw contralateral to the lesion (Paper III) or with both paws in bilaterally lesioned animals (Paper IV).

Ratings of stereotypic behaviours

In Paper III, video recordings obtained during the AIM rating sessions were used to evaluate motor activities with stereotypic features (sniffing, rearing, grooming) (Kelley, 2001). These behaviours were individually rated during monitoring periods of 1 min every 20 min for 60 min following drug administration. A rating scale from 0.0 to 1.0 was used to express the fraction of observation time during which each behavioural item was evident (where 1.0 means, item present during 100% of the monitoring period). Results are expressed as an average of the three types of stereotypic behaviour and the three monitoring periods (20, 40, 60 min).

Open field test

In Paper IV, the open field test was performed to assess motor activity motivated by the exploration of a novel environment (Archer, 1973; Roth and Katz, 1979). Furthermore, when placed in an open field, rodents spontaneously prefer the periphery (outer zone) to the central parts (inner zone) of the arena, a behaviour called thigmotaxis. Increases in the time spent or locomotion in the inner zone can be interpreted as an anxiolytic-like effect of the investigated drug (Prut and Belzung, 2003). The open field test consisted of an open squared box (80 x 80 cm) and a camera suspended above the arena, which tracks the position of the animals' head, body, and tail at selected time points using a video tracking system (ANY-maze, Stoelting Europe). The open field arena was virtually divided in two zones: the outer zone and the inner zone (see Figure 17A). During each session, animals were placed individually in the center of the arena and were allowed to explore the arena freely for 90 min. The test was carried out before initiating treatments as a baseline measure as well as during chronic treatment starting 15 min following injection.

Elevated plus maze (EPM)

In Paper IV, anxiety-related behaviours were assessed in the elevated plus maze (EPM), that relies upon rodents' aversion to open spaces and heights (Handley and Mithani, 1984; Pellow et al., 1985; Walf and Frye, 2007). The EPM (Med-Associates Inc.) consisted of two opposing open arms (length: 50.8 cm, width: 10.16 cm), two opposing wall-enclosed arms (wall height: 40.49 cm), and a center area (10.16 cm per side) as well as a camera suspended above the arena to evaluate the behaviour using a video tracking system (ANY-maze, Stoelting Europe). Animals were placed individually in the centre and was allowed to explore the arena freely for 5 min. The test was carried out during chronic treatment starting 15 min following injection.

Compulsive checking test

In Paper IV, compulsive checking behaviour was assessed using a test previously introduced by Szechtman et al. (1998) for the evaluation of quinpirole-induced

compulsive checking. Briefly, the compulsive checking arena consisted of an open, squared platform (140 x 140 cm) with four plexiglass boxes placed at fixed locations and a camera suspended above the platform to evaluate the behaviour using a video tracking system (ANY-maze, Stoelting Europe). Animals were placed individually in the center of the platform and were allowed to freely explore the platform for 45 min. The test was carried out before initiating treatments as a baseline measure as well as during acute and chronic treatments with different doses starting 15 min following injection. According to Eilam and Golani (1989), rats establish one or two key locations (home base(s)) and organize their behaviour in relation to them. Thus, the platform was virtually divided into 25 zones of 35 x 35 cm of which the outer zone extended 17.5 cm outside the platform. For each rat, the home base(s) were defined as the zone(s) with the highest total duration of stops, where stops refer to periods of no locomotion (Szechtman et al., 1998). Compulsive checking behaviour is present if the rat returns to the home base(s) excessively more frequently than to other zones, excessively rapid, and perform less stops before returning to the home base(s) (Szechtman et al., 1998). Therefore, compulsive checking behaviour parameters were characterised with reference to the home base(s). For detailed descriptions of these criteria measures please refer to the method section of Paper IV.

Rat Iowa Gambling Task (rIGT)

In Paper IV, decision-making processes were investigated in 6-OHDA-lesioned rats using the rat Iowa Gambling Task (rIGT) previously introduced by van den Bos et al. (2006). The rIGT apparatus consisted of a start box, a choice area, and four goal arms. Of the four goal arms, two arms were baited and two arms were empty. The latter were introduced as a control for non-specific exploration and potential spatial learning deficits (de Visser et al., 2011; van den Bos et al., 2014). The two baited arms consisted of a long-term advantageous arm (8 reward pellets and 2 quinine-saturated pellets per 10 choices) and a long-term disadvantageous arm (3 reward pellets and 27 quinine-saturated pellets per 10 choices). Briefly, one week of habituation was followed by two 5-day periods of testing to receive a total of 120 trials, during which the animals were mildly food deprived. Treatments were administered 15 min before initiating each test session. At the beginning of each trial, animals were placed individually in the start box. Once the rat had entered a goal arm with its full body, the chosen arm was closed, preventing the rat from leaving the choice arm before exploring the reward cup. The data were expressed in blocks of 12 trials and scores in the last session were chosen as a measure of final performance. For detailed descriptions of these measures please refer to the method section of Paper IV.

Video tracking analysis

In parallel with electrophysiological recordings in Paper II, animals were recorded with digital video (25 frames/s, Genie HM640 GigE camera; Teledyne DALSA). Animals were filmed from the side and above while freely moving in a circular arena (diameter 55 cm). After 10 min of habituation, the rats were anaesthetised with isoflurane (5%) to connect the implant to the recording headstages. Upon recovery, the animals were recorded for 50 min to establish baseline/vehicle conditions whereafter they received a treatment injection followed by a further 3 h of recording.

The position of each rat was tracked from the top camera videos using the open-source tool DeepLabCut (Mathis et al., 2018). Briefly, a total of 1221 frames picked randomly from 23 videos were used to label different body parts of the rat in order to train a deep learning network over 1030000 iterations. This network was used to track 7 body parts from the top camera videos. Then, x and y coordinates of those body parts were extracted using MATLAB (MathWorks), considering only a detection likelihood of > 0.9. For the analysis of egocentric rotational behaviour, full 360° turns were calculated from the direction of the animal, defined as the direction of the line between the front of the animal and the base of the tail. Next, we examined the motor activity and speed in the open-field arena by tracking the body centroid of each animal.

In Paper I, the instant speed of motions was obtained by deriving the body position in time from sequential video frames (15 frames/s, Flea2 FireWire 1394b camera; Point Gray or 25 frames/s, Genie HM640 GigE camera; Teledyne DALSA) using the open-source software Bonsai (Lopes et al., 2015). Synchronisation between these video frames and accelerometer and electrophysiological signals was performed using a Master-8 pulse generator (A.M.P.I.) or an Arduino system.

Electrophysiological recordings

Signal acquisition

In Paper I-II, wideband neuronal activity was recorded with an RHD2000-Series Amplifier Evaluation System (Intan Technologies) and the software Open Ephys GUI (Siegle et al., 2017). The wideband signals were bandpass filtered between 1 and 7600 Hz and digitized and recorded at 30 kHz. LFPs were extracted offline, low-pass filtered (8th order Butterworth at 500 Hz) and downsampled to 1000 (Paper I) or 2000 Hz (Paper II).

LFP power spectral densities

In Paper I, LFP signals were divided into epochs of 1 s in steps of 0.5 s and the power spectral density (PSD) was estimated for each epoch over the 0.5-80 Hz frequency range in intervals of 1 Hz using the multitaper method. Specifically, the

multiple discrete prolate spheroidal sequences tapers were used with a half-bandwidth window of 2 Hz (three tapers). In Paper II, bipolar LFP time series were computed from all unique pairs of wires within the same structure. For each of these time series, a spectrogram (i.e., time series of PSDs) was estimated over the 0-250 Hz frequency range with Welch's method (8 s Hann window with 50% overlap). Then, power spectra for truly rhythmic activity were separated from arrhythmic "fractal" activity using the irregular-resampling auto-spectral analysis (IRASA; Wen and Liu (2016)) (see Figure 5). Least-square fitting of each spectrum to the function

$$y(f) = Ae^{-\left(\frac{f-B}{C}\right)^2} + Df + E$$

allowed us to define the peak height (A) and peak frequency (B) parametrically and to define criteria for when a peak was detected. This procedure resulted in a possible detection each 4 s. The detection rate was then computed as the average of the binary outcome and if sufficient detections were made (> 5%), further analysis of the power and frequency was performed.

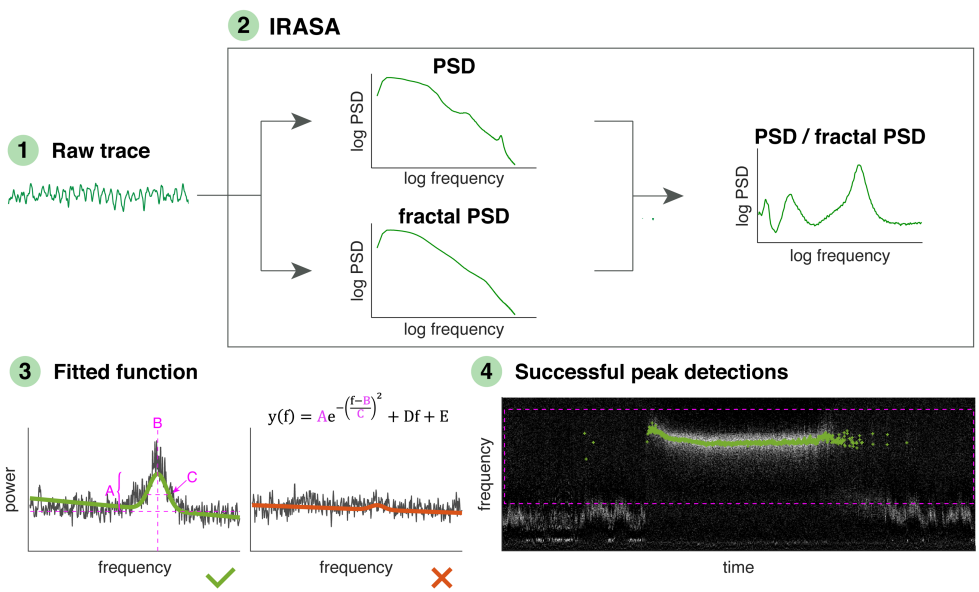

Figure 5. Schematic representation of peak detection analysis. (**1**) Spectrograms (i.e. time series of power spectral densities (PSDs)) were estimated for bipolar LFP time series. (**2**) Power spectra for truly rhythmic *oscillatory* activity were separated from arrhythmic *fractal* activity using the irregular-resampling auto-spectral analysis (IRASA). (**3**) A parametric function y(f) was fitted to each 8 s epoch of the spectral data. If parameters of the function were within defined criteria, a succesful peak detection was declared (green). (**4**) Example spectrogram where each green point marks an 8 s epoch with successful peak detection. Hatched pink square mark the segment of the spectrum fitted. Extracted from *Skovgård et al. (2022)* (Paper II), Figure 2.

Phase synchrony and functional connectivity

To quantify the instantaneous phase of NBG oscillations in Paper II, the analytical signal was calculated (hilbert, MATLAB) from monopolar LFP time series after bandpass filtering $\pm$ 5 Hz around the median frequency of each recording. Mean phase differences and resultant vector lengths were calculated using the CircStat toolbox (Berens, 2022). To obtain a good quality phase estimate, we only included mean phase differences for wire pairs with a mean resultant vector length > 0.5, assuming that a higher magnitude reflects a higher signal to noise ratio of the source of interest and thus a better-quality phase estimate.

Motion Index analysis

In parallel to the electrophysiological recordings in Paper I, accelerometer signals were recorded at a sampling rate of 30 kHz using analogue 3-axis accelerometers (ADXL335), each located in the recording headstages (Intan Technologies) connected to the chronic implant of the rats. Accelerometer data was extracted offline, downsampled to 1000 Hz and divided into epochs similar to the LFP data (1 s in steps of 0.5 s). Then, the average PSD of each axis was estimated over the 1-45 Hz frequency range (see details above). High-pass filtering the data at 1 Hz partially removed the gravity component such that this frequency interval mainly includes the global characteristics of head movements. Next, the PSD was averaged over the three axes to obtain a single value per epoch defined as the motion index. To compensate for variabilities in positions of accelerometers, individual motion index values were normalised to a common space. As a final step, a non-uniform binning procedure was applied and the bin data was interpolated in a uniform grid of 150 points between normalised motion indexes from -5 to 25.

Ex-vivo experiments

Tissue preparation and immunohistochemistry

Animals were anaesthetised with pentobarbital (Apoteksbolaget AB) either 1 or > 24 h after the last treatment injection (for details refer to Paper I-IV). Then, animals were transcardially perfused with 0.9% saline followed by 4% ice-cold buffered paraformaldehyde. In Paper III-IV, brains were then rapidly removed, post-fixed in the paraformaldehyde solution for 2 hours, and transferred to 25% sucrose in 0.1 M phosphate buffer at 4°C for cryoprotection. In Paper I-II, however, heads were kept in paraformaldehyde at 4°C until the computed tomography (CT) scanning of the head had been performed for electrode placement verification, whereafter brains were transferred to 25% sucrose solution. Coronal sections (30 or 40 µm thick in Paper I-II or Paper III-IV, respectively) were cut on a freezing microtome, and then stored in antifreeze solution (0.5 M sodium phosphate buffer,

30% glycerol and 30% ethylene glycol) at -20°C until processed for immunohistochemical analysis.

Immunohistochemical stainings generally followed a series of well-standardized steps. After quenching endogenous peroxidases (3% hydrogen peroxide, 10% methanol in buffer solution), free-floating sections were pre-incubated with blocking serum and then incubated overnight with one of the primary antibodies listed in Table 3. Immunocomplexes were then revealed using one of the biotinylated secondary antibodies listed in Table 4, followed by avidin-biotin peroxidase solution (ABC Elite Kit, Vector Laboratories). The final colour reaction was developed using 3,3'-diaminobenzidine. For a detailed description of each immunostaining, refer to the method section of Paper I-IV.

Table 3. Primary antibodies used in immunohistochemistry

Antibody	Host species	Dilution	Supplier	Paper
Tyrosine hydroxylase (TH)	Rabbit	1:1000	Pel-Freez Merck	I, II, III, IV I
FosB/ΔFosB	Rabbit	1:400	Santa Cruz	III
μ Opioid receptor (MOR)	Rabbit	1:2000	IncStar	III
Nestin	Mouse	1:5000	BD Pharmingen	III
Rat endothelial cell antigen 1 (Reca-1)	Mouse	1:100	BioRad	III
Albumin	Sheep	1:30000	BioRad	III

Table 4. Secondary antibodies used in immunohistochemistry

Antibody	Host species	Dilution	Supplier	Paper
BA 1000 anti rabbit	Goat	1:200	Vector Laboratories	I, II, III, IV
BA 6000 anti sheep	Goat	1:200	Vector Laboratories	III
BA 2001 anti mouse	Horse	1:200	Vector Laboratories	III

Image analysis and quantification

Pictures of slide-mounted brain sections were acquired using a digital camera (Olympus DP72) mounted on a Nikon Eclipse 80i microscope (4x and 20x objective; Paper I-IV) or an Epson L355 scanner (Paper I). Image analysis was performed manually or using the open-source image processing package Fiji (ImageJ, NIH).

In Paper III, immunoreactive cells (ΔFosB) were quantified using an automated particle count function applied after conversion to 8-bit images and setting a threshold value. In Paper I and III, densitometric analysis (TH, albumin extravasation) was performed after conversion to 8-bit images, using calibrated

optical density units. In Paper IV, the extent of the lesions was calculated as the dorsal part of the striatum showing immunoreactivity (TH) as a percentage of the total area. In Paper III, manual quantification (Prussian blue-labeled hemosiderin deposits, FosB/ΔFosB-MOR) was performed on randomly sampled areas picked by the NewCAST software (Visiopharm). Moreover, immunopositive microvessels (nestin) were quantified using an automated image segmentation software VIS (Visiopharm Integrator System; Visiopharm). On randomly sampled areas, the immunopositivity associated with blood vessels was separated from background using a Bayesian algorithm-based pixel classifier.

Computed tomography (CT) scanning of the implanted microwire arrays

In Paper II, the location of wires was identified using CT scanning of the implanted microwire arrays (Mediso Nanoscan PETCT scanner), as previously described (Censoni et al., 2022). Images were reconstructed with the thin-slice Ram-Lak filter to obtain a 30 µm side and 34 µm slice thickness (voxel size). To identify the tip of each wire in the resulting images, bregma and lambda were used as landmarks to align the images to an atlas of the rat brain (Paxinos and Watson, 2007). To visually optimise the alignment between the atlas and the CT scan, this was followed by a manual calibration step. Finally, the coordinates of the wire tips in the atlas were calculated from the voxel coordinates using the resulting affine transformation and each wire was assigned the corresponding anatomical label in the atlas.

Statistical analysis

Statistical analysis was carried out using different versions of Prism (GraphPad software), RStudio (RStudio, PBC), or MATLAB (MathWorks). Comparisons of treatment effects over time and area under the curve were analysed using two-way repeated measures ANOVA or Mixed-effects analysis, as appropriate. Post hoc analyses were carried out using Tukey's or Bonferroni's multiple comparisons test. When compared between groups on single sessions or time points, data was analysed using Kruskal-Wallis test or one-way ANOVA/Mixed-effects analysis, as appropriate. Post hoc analyses were carried out using Dunn's or Tukey's multiple comparisons test, respectively. In Paper II, Scheffe's multiple comparisons test was used as post hoc test for electrophysiological data. Moreover, phase relationships were analysed using Wilcoxon signed-rank test or a MANOVA approach with Scheffe's multiple comparisons test as post hoc. For two-group comparisons unpaired test was used. Relations between variables were examined using the Spearman's rank correlation coefficient (Spearman's Rho). The unimodality test was applied to analyse the shape of distributions.

Data were presented as group mean ± SEM or as box plot and median, with whiskers annotating minimum and maximum values. The level of statistical significance was set at $\alpha = 0.05$. In Paper II, p-values for electrophysiological data

were adjusted to obtain multiplicity-adjusted results and the Bonferroni correction was applied to account for multiple testing in the phase analysis.

Figure 1-3, 10A, 13A, and 16 were created with BioRender.com

Results

Results

Paper I

Cortico-striatal oscillations are correlated to motor activity levels in both physiological and parkinsonian conditions

Oscillatory activities in beta and NBG frequency bands have been suggested as biomarkers for pathophysiological states of PD or dyskinesia, respectively, since they show great similarity across species. These phenomena are currently being investigated to serve as a feedback signal for adaptive or closed-loop controlled delivery of DBS for the treatment of PD (reviewed in Bouthour et al. (2019)). Since changes in beta oscillations are observed during different motor states (Brazhnik et al., 2014; Courtemanche et al., 2003), differentiating the changes related to parkinsonism from those occurring physiologically upon motor state transitions is of great importance for the use of these oscillations as biomarkers of PD. To this end, the aim of this first study was to examine how broad-frequency neuronal oscillations change according to the levels of motor activity in both normal and parkinsonian conditions. The study presented in Paper I is the result of a collaboration between two research groups. For the purpose of this thesis, I will mainly cover the part of the study addressed here in Lund.

Accelerometers provide a sensitive measure of motor activity

Both LFP and accelerometer signals were recorded from primary motor cortex (M1) and DLS (Table 1) in both the intact and the lesioned hemisphere of unilaterally 6-OHDA-lesioned rats. In this study, the motion index refers to the average PSD of accelerometer signals obtained from three head-mounted accelerometers. This accelerometer-derived motion index could accurately detect motor activity even when performed with low or no actual navigation in the open arena. Furthermore, the motion index correlated positively with the speed of the rat. Since the distribution of the motion index was not unimodal, two distinct motor states were defined: *low motion* associated with a state of minimum or no motor activity and *high motion* associated with movement, but not necessarily actual navigation in the arena (see Figure 6).

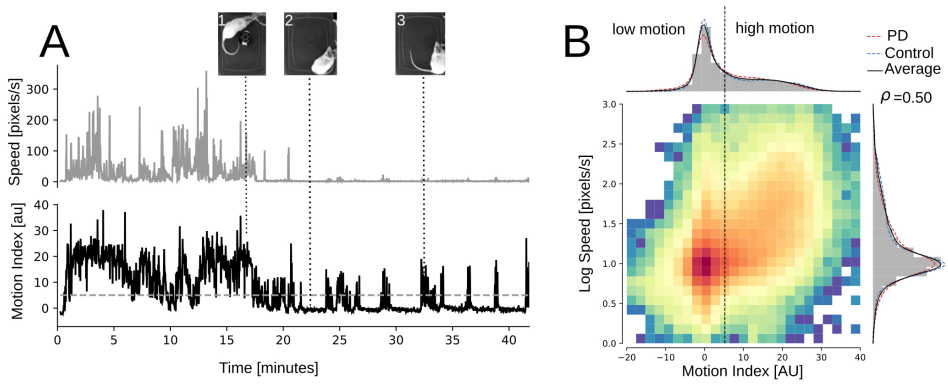

Figure 6. Accelerometer-derived motion-index detects motor activity accurately and is positively correlated to the speed of the rat. A Motor activity from a rat navigating the open arena (0-20 min) is apparent in both the speed (top) and the motion index (bottom) traces. However, head or body movements with no actual navigation in the arena were only detected by the motion index. **B** Normalised distribution of log speed and motion index. Notice the bimodal distribution of the motion index, which can be separated in low and high states, in contrast to the unimodal distribution of speed. Extracted from *Moënne-Loccoz et al. (2020)* (Paper I), Figure 1.

Sorting LFP power spectral density according to motion index results in distinctive oscillatory patterns

To study the relationship between motor activity and neuronal oscillations, we correlated the motion index and the LFP power at different frequencies. Specifically, LFP power bins were sorted in ascending order concerning the concomitantly measured motion index, which revealed a neat relationship between spectral broad-band power changes and motor activity levels (see Figure 7).

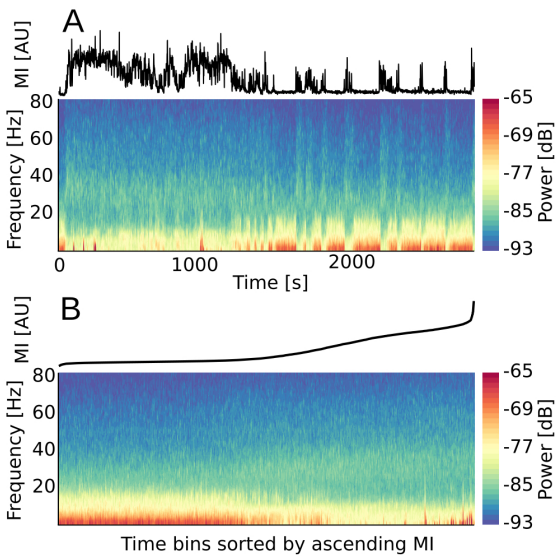

Interestingly, when motion index-frequency charts were represented as z-scores of low-motions, they revealed that low motion index values were associated with an increase in power at frequencies below ~30 Hz, while the power at

Figure 7. Representation of a spectrogram as a function of motion index reveals a tight correlation between motor state and oscillations at specific frequency bands. A Example of a motion index (MI) trace (top) with the corresponding spectrogram from the right motor cortex of a bilaterally 6-OHDA-lesioned rat (bottom). **B** The same spectrogram but sorted according to the ascending motion index. Extracted from *Moënne-Loccoz et al. (2020)* (Paper I), Figure 2.

frequencies above ~40 Hz was increased during high motion index levels. This was seen in the motor cortex (M1) and striatum (DLS) of both the intact and DA-denervated hemispheres. Spearman's correlations furthermore confirmed a negative correlation between the motion index and the power of LFP oscillations at low frequencies (< ~30 Hz) and a positive correlation at high frequencies (> ~35 Hz). While this analysis revealed a common feature between physiological and parkinsonian conditions relative to the motor activity levels and oscillatory activities in broad frequency bands, a difference in a characteristic narrow band (~25–40 Hz) was apparent in both the cortex and striatum of the lesioned hemisphere. This narrowband beta oscillation has previously been described during walking in the DA-denervated SNr, STN, and cortex of hemiparkinsonian rats (Avila et al., 2010; Delaville et al., 2015). Noteworthy, the sorting of the oscillations according to the motion index revealed a novel characteristic of these beta oscillations, that is, the shift from lower (~20 Hz) to higher (~30 Hz) frequencies as the motion index increases (see Figure 8).

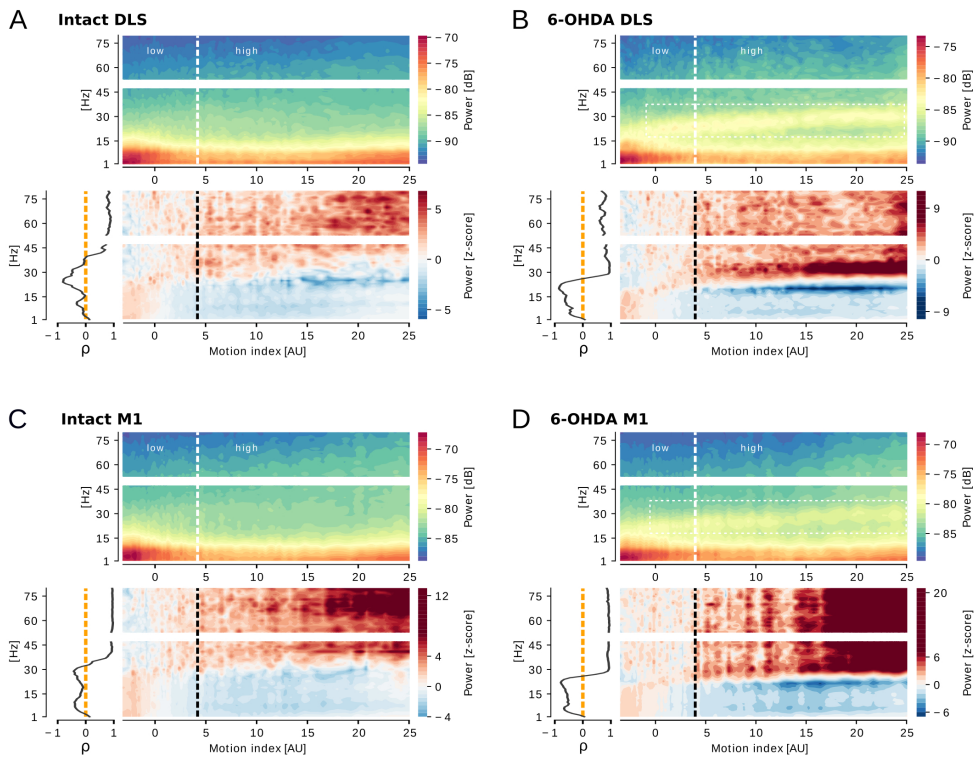

Figure 8. Cortico-striatal oscillations are correlated to motor activity levels. A-D Representative examples of motion index-frequency charts of PSD in decibels (dB; top) or z-score relative to low motion (bottom right), and Spearman's correlation (rho) between power and frequency (bottom left). Low motion index levels were associated with an increase in power below ~30 Hz, while the power above that frequency increased with increasing motion index levels in both the DLS (**A-B**) and M1 (**C-D**) of the intact (**A** and **C**) and lesioned (**B** and **D**) hemisphere of unilaterally 6-OHDA-lesioned rats. Extracted from *Moënne-Loccoz et al. (2020)* (Paper I), Figure 3.

Summary of Paper I

The results of this study revealed that changes in broadband oscillatory activities of the cortex and the striatum are closely correlated to ongoing motor activities independent of parkinsonian conditions. Moreover, we show that the actual frequency of high beta oscillations selective to DA-denervated states is positively modulated when motor activity levels increase.

Paper II

Distinctive effects of D1 and D2 receptor agonists on cortico-basal ganglia oscillations in a rodent model of L-DOPA-induced dyskinesia

In Paper I, we explored broad-frequency oscillatory activities and their association with motor activity. However, the study was limited to normal and parkinsonian conditions, and did not investigate changes in neuronal oscillations induced by dopaminergic PD treatments. Indeed, LID has been found to be strongly associated with oscillatory changes in a narrow gamma frequency band (Halje et al., 2019). To elucidate the contribution of D1 and D2 receptors to the aberrant neuronal activity patterns associated with LID, we set out to compare oscillatory responses in seven critical nodes of the cortico-basal ganglia network induced by selective DA receptor agonists or L-DOPA in unilaterally 6-OHDA-lesioned rats.

D1 and D2 receptors control different features of dyskinesia

Rats with unilateral MFB lesions were primed with L-DOPA (6 mg/kg). Following electrode implantation, animals were treated sequentially with the same dose of L-DOPA, the selective D2 agonist sumanirole (2 mg/kg) and the D1 agonist SKF82958 (0.05 mg/kg). Drug-induced behaviours were rated to dissect the different contributions of D1 and D2 receptor stimulation in the development of LID. Dyskinetic behaviours were induced by all treatments, although with differences in time course and overall severity. Specifically, the D1 agonist induced significantly more dyskinesia than the D2 agonist at peak-drug effect (see coloured bars in Figure 9A) in line with the effects of L-DOPA, although with a significantly shorter time course. Furthermore, the relative expression of orolingual AIMs was lower upon treatment with the D2 agonist compared to L-DOPA, whereas the axial component was higher upon both D1 and D2 receptor stimulation, being significant only for the D1 agonist compared to L-DOPA (see Figure 9).

Distinct patterns of open field motion upon D1 or D2 receptor stimulation

The different treatments resulted in different patterns of motion in the open field arena. When treated with the D2 agonist, animals were able to explore the entire surface of the arena, whereas horizontal locomotion was affected in L-DOPA- and SKF82958-treated animals, as they remained confined to a restricted part of the arena. Moreover, both DA agonists induced more contralateral turns compared to L-DOPA, these turns being faster and narrower upon D1 receptor stimulation compared to the other treatments (see Figure 10).

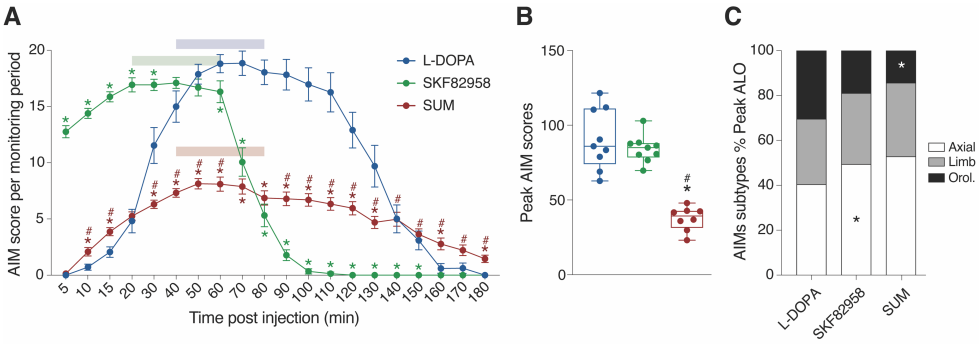

Figure 9. Severity of dyskinetic behaviours induced by selective agonists of D1 or D2 receptors and L-DOPA in unilaterally 6-OHDA-lesioned rats. A The global AIM scores peaked at 20-60 min post injection of SKF82958 and at 40-80 min for both L-DOPA and sumanirole (coloured bars). These periods were chosen for further analyses in order to compare the treatments during functionally analogous time windows. **B** AIM scores calculated as sum of global AIMs during peak drug effect. **C** Axial, limb, and orolingual (ALO) AIM scores represented as a percentage of the global AIMs during peak drug effect. Tukey's post hoc: &p<0.05 vs. veh, *p<0.05 vs. L-DOPA, #p<0.05 vs. SKF82958. Extracted from Figure 3 and Supplemental Figure S4 of *Skovgård et al. (2022)* (Paper II).

Narrowband gamma (NBG) oscillations strongly increased by D1 agonist

In parallel with the behavioural assessment, LFP recordings were performed simultaneously in seven nodes of the cortico-basal ganglia network of both the intact and the lesioned hemisphere (Table 1). When examining oscillatory activity in the NBG frequency range, no activity was detected in the intact hemisphere nor after

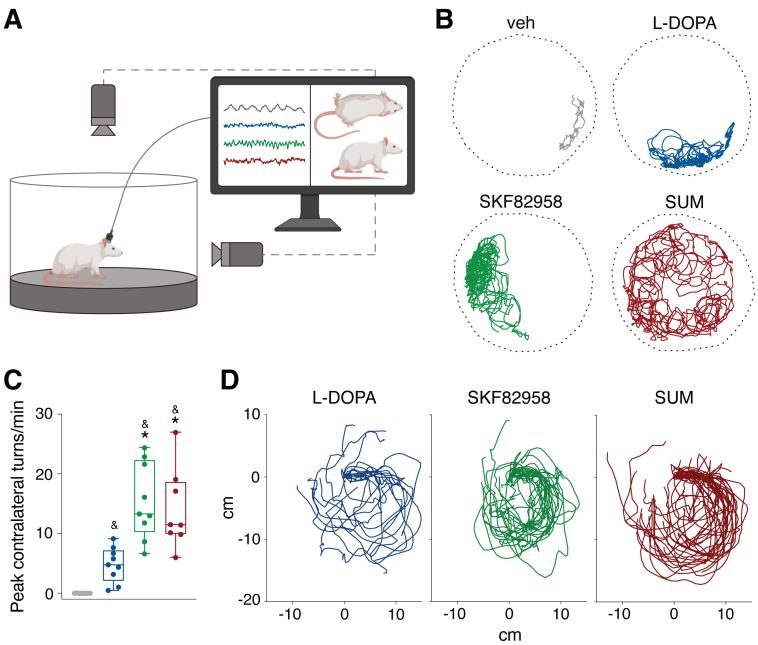

Figure 10. Distinct patterns of open-field motions and rotational behaviour observed upon chronic drug treatments. A Schematic representation of the recording setup. **B** Traces representing the animal movement pattern inside the circular arena within 2 min recording at the peak drug effect. **C** Completed contralateral rotations calculated as mean during peak drug effect. Tukey's post hoc: &p<0.05 vs. veh, *p<0.05 vs. L-DOPA. **D** Aligned traces representative of the turning characteristics within 1 min recording at the peak drug effect. Extracted from Figure 3 and Supplemental Figure S4 of *Skovgård et al. (2022)* (Paper II).

vehicle treatment in either hemisphere. Following treatment with L-DOPA and the DA agonists, however, NBG oscillations appeared in several of the recorded structures of the lesioned hemisphere coinciding temporally with the dyskinetic behaviours. Specifically, the D1 agonist induced strong NBG oscillations in all the recorded structures with the exception of SNr, whereas the D2 agonist only induced NBG oscillations in forelimb motor cortical areas (RFA and M1FL) and DLS, and with significantly inferior power compared to D1 agonist-induced NBG activity. Moreover, the frequency of the elicited NBG oscillations was strongly modulated by the pharmacological treatments, being highest after L-DOPA treatment and lowest after treatment with the D2 agonist (see Figure 11). Importantly, NBG oscillations were strongly correlated with global AIM scores in the majority of structures recorded, being strongest in the forelimb region of the primary motor cortex (M1FL), which further emphasises the close relation between NBG oscillations and dyskinesia.

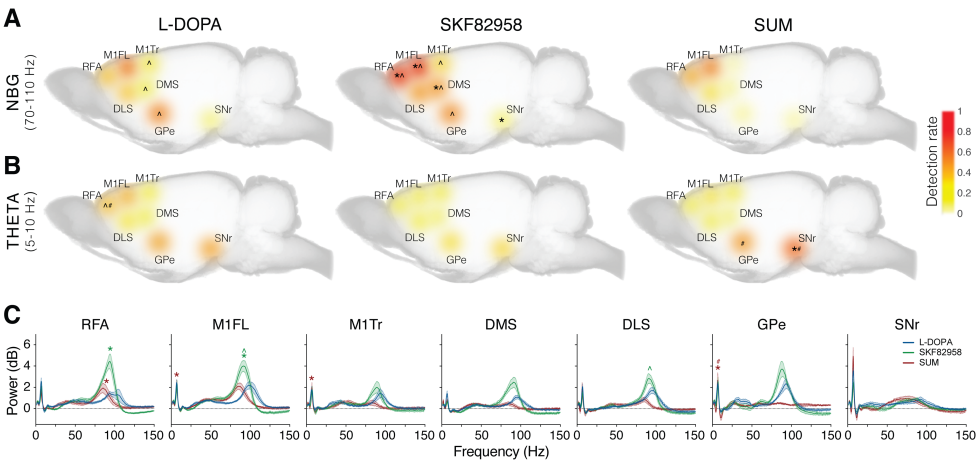

Figure 11. Spectral analysis of multi-structure LFP recordings. A-B Detection rate of NBG (**A**) or theta oscillations (**B**) in the lesioned hemisphere during peak drug effect of L-DOPA (left), the D1 agonist SKF82958 (middle), or the D2 agonist SUM (right). **C** Averaged LFP power spectra (0-150 Hz) in cortico-basal ganglia structures of the lesioned hemisphere during peak drug effect. Scheffe's post hoc: *p<0.05 vs. L-DOPA, #p<0.05 vs. SKF82958, ^p<0.05 vs. SUM. Extracted from Figure 4 and Figure 8 of *Skovgård et al. (2022)* (Paper II).

D2 receptor stimulation increases theta oscillations in the deep basal ganglia nuclei

Theta oscillations were present in all recorded structures in both hemispheres, and the detection rate of theta activity was constant during the time course of the dyskinetic behaviour with only minor changes in the early and late phase of dyskinesia. In the GPe of the lesioned hemisphere, theta oscillations became more prevalent upon treatment with the D2 agonist compared to the D1 agonist, and showed significantly higher power compared to all other treatments during peak dyskinesia. Moreover, the detection rate of theta oscillations in the SNr was

increased bilaterally by D2 receptor stimulation compared to the other treatments (see Figure 11). Noteworthy, a robust correlation between dyskinesia severity and theta power was found in the GPe of the lesioned hemisphere, which is in contrast to the weak correlations found for all other structures. Moreover, correlations between theta power and an index of overall motions indicated that theta power measured in the DA-denervated GPe upon D2 receptor stimulation was specifically correlated with the expression of dyskinesia, whereas the bilateral theta-increases in the SNr seemed to reflect an overall increase in horizontal motions.

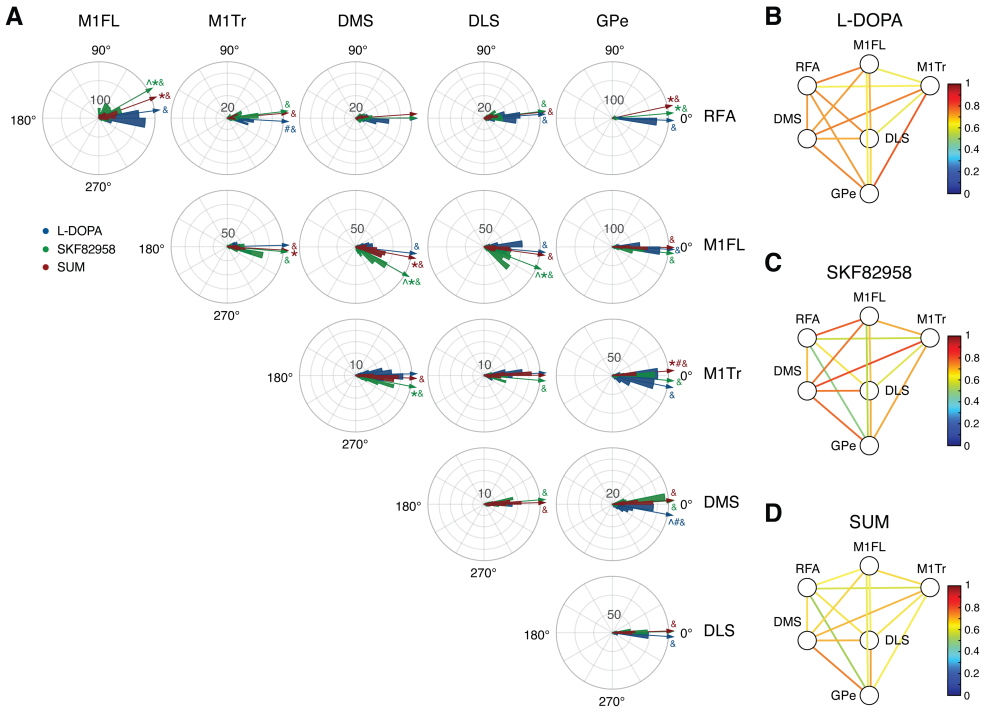

Figure 12. Phase synchrony and functional connectivity in the NBG frequency band. A Phase plots showing the distribution of instantaneous phase differences between pairs of structures for NBG oscillations. Arrows reflect the mean angular direction of the distribution of the mean phase differences. Scheffe's post hoc: *p<0.05 vs. L-DOPA, #p<0.05 vs. SKF82958, ^p<0.05 vs. SUM. Bonferroni correction: &p<0.05 vs. 0°. **B-D** Diagrams of NBG functional connectivity for L-DOPA (**B**), SKF82958 (**C**), and SUM (**D**), as represented by the magnitude of the resultant vector of the phase distributions (see colour scale). Extracted from Figure 7 of *Skovgård et al. (2022)* (Paper II).

NBG phase synchrony reveals a stronger effect of D1 receptor stimulation on cortico-subcortical coupling

To identify potential drivers of NBG oscillations in the cortico-basal ganglia network, we examined phase relationships between different structures during peak dyskinesia severity. This revealed that NBG oscillations in the M1FL were leading motor cortical and striatal structures, with a stronger effect following treatment with

the D1 agonist, which suggests that this region might be a key driver of these oscillations. In line with the consistent phase differences, primary motor cortical areas (M1FL and M1Tr) showed strong functional connectivity within the cortex and in the cortico-striatal circuit upon D1 receptor stimulation. Interestingly, RFA and M1Tr showed functional connectivity to GPe, with a more pronounced role of the D1 receptor (see Figure 12).

Summary of Paper II

This study represents a comprehensive investigation of dyskinetic behaviours and associated neuronal changes in cortico-basal ganglia networks induced by D1 or D2 agonists in a unilateral rat model of PD. First, we show how pharmacological stimulation of either D1 or D2 receptors mediates different aspects of dyskinetic behaviours. Then, we characterise the LFP oscillatory patterns in the cortico-basal ganglia network induced by D1 or D2 agonists. In conclusion, the main finding of this study is that drugs acting on D1 receptors induce strong network-wide NBG oscillations, whereas D2 receptor stimulation induces weaker and topographically more restricted NBG activity, while increasing theta oscillations in the deep basal ganglia nuclei.

Paper III

Dopamine agonist cotreatment alters neuroplasticity and pharmacology of L-DOPA-induced dyskinesia

In Paper I and II we investigated the neuronal oscillatory patterns related to pathophysiological states of PD and dyskinesia to elucidate the potential of these oscillations as biomarkers. In the second part of this thesis, we were interested in exploring how dyskinesia as well as non-motor complications related to dopaminergic treatments in PD are best modelled preclinically. Current models of LID are obtained by treating DA-depleted animals with L-DOPA. However, patients with LID receive combination therapies that often include DA agonists. Thus, in this third paper, we aimed to establish whether adjunct treatment with the D2/3 agonist ropinirole impacts on patterns of LID-related neuroplasticity and drug responses in unilaterally 6-OHDA-lesioned rats.

Behavioural characterization of dyskinesia induced by L-DOPA and the D2/3 agonist ropinirole

In the first experiment, we compared the motor effects of chronic treatment with the D2/3 agonist ropinirole and L-DOPA. Rats with unilateral MFB lesions were divided into four groups to receive chronic treatment with either L-DOPA (3 or 6 mg/kg; LD3 or LD6) or ropinirole (0.5 or 1.5 mg/kg; R0.5 or R1.5). While all treatments had a motor stimulant effect, only animals treated with LD6 developed AIM scores meeting the criteria of moderate-severe dyskinesia as defined in Ohlin et al. (2012). In contrast, treatment with LD3, R0.5, and R1.5 induced subthreshold levels of AIMs in all test sessions. In the second treatment phase, animals from the previous LD3, R0.5, and R1.5 groups were given daily injections of LD3+R0.5, while animals previously treated with LD6 either continued on LD6 or were switched to R0.5. Interestingly, LD3+R0.5-cotreatment induced a gradual development of AIMs, which reached the same severity as LD6 treatment independent of the initial treatment allocation. In addition, treatment with LD3+R0.5 induced AIM scores with similar subtype compositions as LD6, and improved forelimb hypokinesia to a similar extent. However, switching from initial LD6 to R0.5 dramatically reduced the AIM scores to levels below the criteria of moderate-severe dyskinesia (see Figure 13).

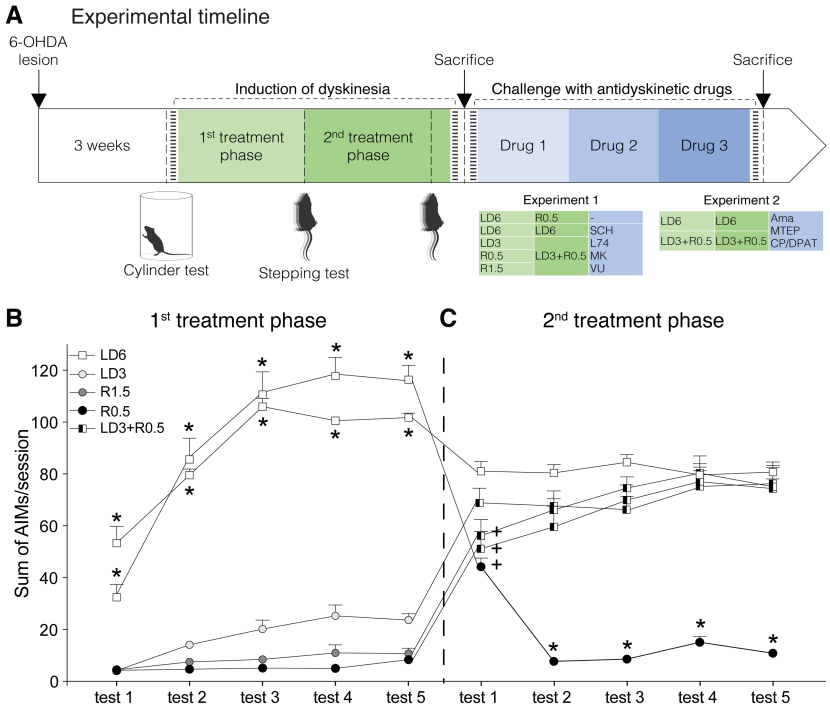

Figure 13. Study design and development of dyskinesia during the chronic drug treatments. A In experiment 1, hemiparkinsonian rats were randomised to four treatment groups during the first treatment phase (LD3 n=14, LD6 n=23, R0.5 n=10, and R1.5 = 10) and were then allocated to three treatment groups in the second treatment phase (LD6 n=9, R0.5 n=14, and LD3+R0.5 n=34). Some animals continued to receive challenges with different antidyskinetic treatment principles. In experiment 2, additional hemiparkinsonian rats were allocated to two treatment groups (LD6 n=10 or LD3+R0.5 n=12) followed by drug challenges. **B-C** Time course of summed ALO AIM scores during the first (**B**) or the second (**C**) treatment phase of experiment 1. Bonferroni's post hoc: *p<0.05 vs. all other groups, +p<0.05 vs. LD6. Extracted from Figure 2 of *Espa et al., accepted manuscript* (Paper III).

Different involvement of D1 and D2 receptors in dyskinesias induced by LD6 vs. LD3+R0.5

We assessed whether dyskinesias induced by LD6 or the combined treatment with LD3+R0.5 differentially relied on D1 and D2 receptors by using selective antagonists of the two receptor classes. The D2 antagonist, L741,626, produced similar reductions of AIMs in both LD6- and LD3+R0.5-treated animals, mainly affecting the end phase of the dyskinesia time curve. Interestingly, the D1 antagonist, SCH23390, markedly reduced LD6-induced AIMs throughout the test session at both doses tested, whereas the effects in the combined treatment group were moderate (see Figure 14). This suggests that LD6-induced dyskinesia relies more on D1 than D2 receptor stimulation, whereas dyskinesias induced by combined treatment with LD3+R0.5 are less dependent on D1 receptor stimulation, relying to a similar extent on the two receptor classes.

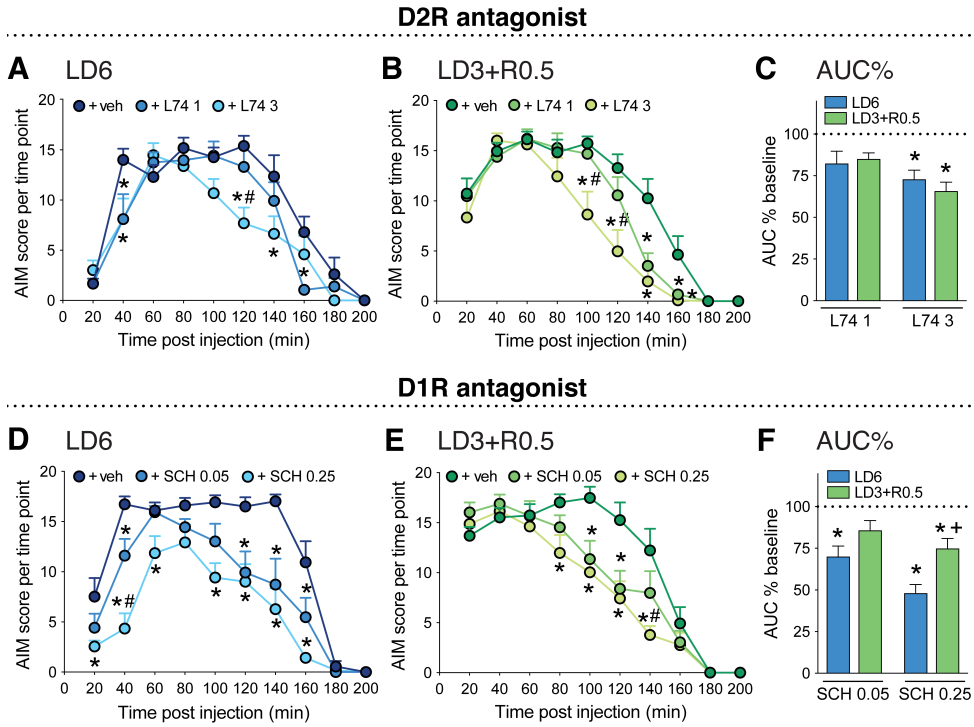

Figure 14. Pharmacological indicators of D1 and D2 receptor engagement in dyskinesias induced by LD6 or LD3+R0.5. A-B Effects of the D2 antagonist L-741626 (L74; 1 and 3 mg/kg) on the time course of ALO AIM scores induced by LD6 (n=9) (**A**) or LD3+R0.5 (n=12) (**B**). Bonferroni's post hoc: *p<0.05 vs. +veh, #p<0.05 vs. +L74 1. **C** Area under the curve of AIMs per test session, expressed as percent of baseline (dashed line). Tukey's post hoc: *p<0.05 vs. baseline. **D-E** Effects of the D1 antagonist SCH23390 (SCH; 0.05 and 0.25 mg/kg) on the time course of ALO AIM scores induced by LD6 (**D**) or LD3+R0.5 (**E**). Bonferroni's post hoc: *p<0.05 vs. +veh, #p<0.05 vs. +SCH 0.05. **F** Area under the curve of AIMs per test session, expressed as percent of baseline (dashed line). Tukey's post hoc: *p<0.05 vs. baseline, +p<0.05 vs. LD6+SCH 0.25. Extracted from Figure 3 of *Espa et al., accepted manuscript* (Paper III).

ΔFosB is differentially modulated in the two dyskinesia models

The development of LID is associated with an upregulation of striatal ΔFosB, a response mediated by D1 receptors (Darmopil et al., 2009; Westin et al., 2007). At the end of the second chronic treatment phase, the number of ΔFosB-positive neurons was markedly increased in LD6-treated animals, whereas the increase in LD3+R0.5-treated animals was less pronounced. Negligible levels of ΔFosB were detected in rats treated with vehicle or R0.5 monotreatment. Since the relative stimulation of D1 vs. D2 receptors affects the compartmental arrangement of Fos protein expression (Paul et al., 1992; Wirtshafter and Asin, 2001; Wirtshafter et al., 1997), we examined the distribution of ΔFosB-containing neurons in striosomes vs. matrix. This analysis revealed a distinctively high striosome/matrix expression ratio in LD3-R0.5-treated animals (see Figure 15).

Expression of LID-related neuroplasticity markers

LID has been associated with neurovascular changes (Cenci, 2014), which correlate with dyskinesia severity (Lerner et al., 2017; Westin et al., 2007) and depend on D1 receptor stimulation (Lindgren et al., 2009). We therefore examined markers of angiogenesis and BBB hyperpermeability in the DLS and SNr, two regions expressing prominent neurovascular plasticity in LID (Lindgren et al., 2009; Ohlin et al., 2011; Ohlin et al., 2012). In both these regions, LD6-treated animals exhibited an increase in nestin-immunoreactive microvessels (a marker of ongoing angiogenesis) and parenchymal albumin immunoreactivity (a marker of BBB leakage), as expected. Moreover, the number of perivascular hemosiderin deposits (a marker of extravasated erythrocytes) in the SNr was increased upon treatment with LD6. In contrast, the expression of these neuroplasticity markers in LD3+R0.5-treated animals was not different from saline-treated controls.

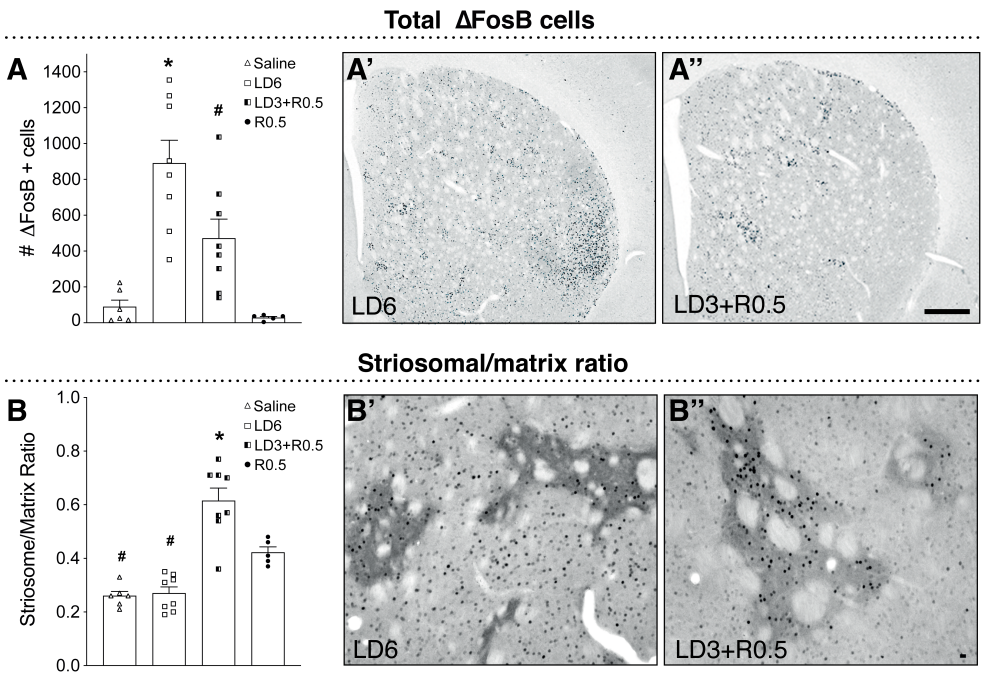

Figure 15. Molecular indicators of D1 and D2 receptor engagement during chronic drug treatments. A Automated cell counts of ΔFosB immunoreactive cells across the striatum. **A'-A''** Low-magnification photomicrographs showing the distribution pattern of ΔFosB-positive cells in animals treated with LD6 (**A'**) and LD3+R0.5 (**A''**). **B** Striosomal/matrix expression ratio of ΔFosB-positive cells. **B'-B''** Photomicrographs of double ΔFosB-MOR immunostained sections from animals treated with LD6 (**B'**) and LD3+R0.5 (**B''**). Tukey's post hoc: *p<0.05 vs. all other groups, #p<0.05 vs. R0.5 (Saline n=6, LD6 n=8, LD3+R0.5 n=8, R0.5 n=5). Scale bar: 50μm. Extracted from Figure 3 of *Espa et al., accepted manuscript* (Paper III).

Effects of different antidyskinetic treatment principles

In the last part of the study, we compared the responsiveness of the two dyskinesia models to pharmacological principles currently used or considered for the treatment of LID. Amantadine, a non-competitive antagonist of NMDA receptors, strongly reduced LD3+R0.5-induced dyskinesia in all phases of the dyskinesia curve, whereas the effects on LD6-induced dyskinesia were less pronounced. A similar pattern of group differences was found using MK801, a selective uncompetitive antagonist of NMDA receptors. This indicates that dyskinesias induced by LD3+R0.5 cotreatment rely on NMDA receptor activity to a larger extent than LD6-induced dyskinesias, which might be related to a stronger relative dependence of LD3+R0.5-induced dyskinesias on D2 vs. D1 receptors.

Next, we investigated the antidyskinetic effects of drugs proven to modulate D1 receptor-mediated striatal signalling in LID (Cenci et al., 2022). MTEP, a selective allosteric antagonist of mGluR5, produced a marked reduction of peak dyskinesia severity of LD6-induced dyskinesia, with modest effects on dyskinesia induced by the combined treatment with LD3+R0.5. Similar patterns were seen following treatment with the M4 PAM VU0467154, although the overall antidyskinetic effect was quite modest in both the LD6 and LD3+R0.5 groups.

Lastly, we evaluated low-dose combinations of 5-HT1a and 5-HT1b receptor agonists, that has been found to blunt peaks of striatal and nigral DA release that accompany the expression of LID (Lindgren et al., 2010). The antidyskinetic effect of the 5HT1a/b agonists, CP94253 and 8-OH-DPAT, was overall similar in the two dyskinesia models.

Summary of Paper III

This study introduces and validates a new animal model of dyskinesia induced by combined treatment with L-DOPA and the D2/3 agonist ropinirole. This combination therapy produces dyskinesias that are phenotypically similar to the classical LID model, although they significantly depart regarding neuronal and microvascular plasticity patterns. Importantly, the combined treatment model is less reliant on D1 receptors and likely to engage D2 receptors to a larger degree than classical LID. Moreover, the two dyskinesia models exhibit partially different responses to antidyskinetic treatment principles.

Paper IV

Dopamine agonist drives impulsive-compulsive behaviours in rats independent of L-DOPA cotreatment and early parkinsonism

The results of Paper III revealed a remarkable impact of DA agonist cotreatment on LID-related neuroplasticity and pharmacological response profiles. Since the use of DA agonists in PD has been associated with an increased risk of developing ICBs, we set out to investigate if L-DOPA cotreatment would affect measures of ICB-like behaviours induced by the D2/3 agonist ropinirole, and whether a possible effect of L-DOPA would be contingent on the presence of DA denervation in motor striatal regions.

Increased motor activity and anxiety-like behaviour upon treatment with the D2/3 agonist

To investigate motor and non-motor features of dopaminergic treatments, bilaterally 6-OHDA-lesioned rats and sham-lesioned controls were each divided into three treatment groups to receive chronic administrations of L-DOPA (24 mg/kg, LD24), the D2 agonist ropinirole (2.5 mg/kg, R2.5), or their combination (LD24+R2.5), in line with the treatment paradigms of Paper III (see Figure 16). Three weeks post lesion, 6-OHDA-lesioned animals showed persistent forelimb akinesia in the stepping test, which was improved by all the dopaminergic treatments tested.

In the open field test, animals treated with R2.5 and LD24+R2.5 exhibited a large increase in distance travelled and speed compared to vehicle and L-DOPA. Moreover, R2.5-treated animals showed a marked increase in the time spent in the inner zone and in the number of entries to the inner zone, indicating an anxiolytic-like effect of the R2.5 monotreatment (see Figure 17). To investigate this effect

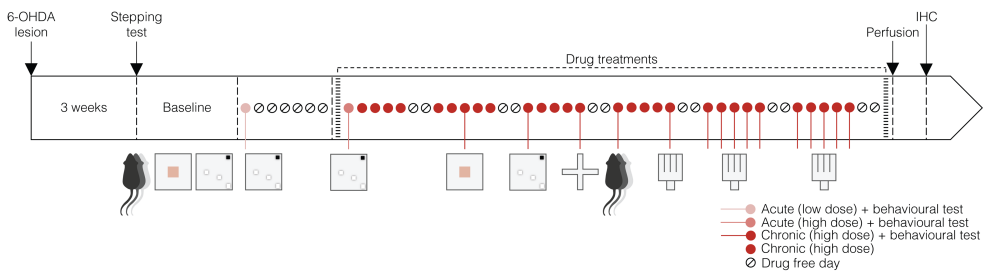

Figure 16. Schematic representation of the study design. Bilaterally sham- and 6-OHDA-lesioned rats were divided into three treatment groups (n=9 and n=10, respectively, in each treatment group) to receive treatment with LD6/LD24, R0.5/R2.5, or the combined treatment of LD6+R0.5/LD24+R2.5. A separate group of 6-OHDA-lesioned rats received 0.9% saline (n=6). During the 6 weeks of treatment, animals were assessed in the open field, the EPM, the compulsive checking test, and the rIGT. Extracted from Figure 1 of *Skovgård et al., unpublished manuscript* (Paper IV).

further, rats were evaluated in the EPM test. In line with the results of the open field test, the D2/3 agonist strongly increased the number of entries to the open arms of the maze in both lesioned and sham-lesioned animals. Moreover, lesioned rats treated with LD24+R2.5 tended to spend more time in the open arms when compared with LD24. This shows that L-DOPA did not modify the natural tendency for open-arm avoidance, whereas ropinirole had an anxiolytic-like effect when given alone or in combination with L-DOPA.

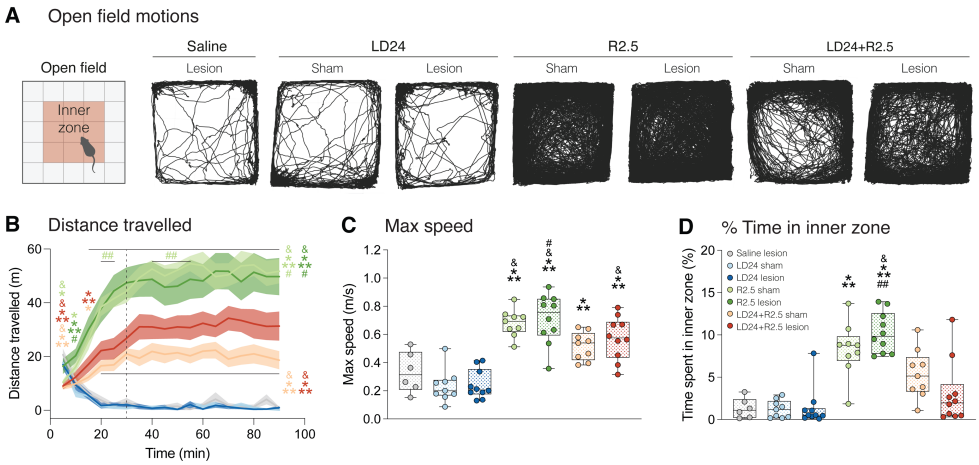

Figure 17. Motor activity and anxiety-like behaviour in an open field arena in 6-OHDA- or sham-lesioned rats upon chronic treatment with a D2 agonist, L-DOPA, or their combination. A Representative examples of track plots of motions within the arena during the 90 min session. **B** Time course of distance travelled in the open field arena. **C** Maximum speed of motor activity. **D** Time spent in inner zone (%) of the arena. Post hoc: &p<0.05 vs. Saline, *p<0.05 vs. LD24 Sham, **p<0.05 vs. LD24 Lesion, #p<0.05 vs. LD24+R2.5 Sham, ##p<0.05 vs. LD24+R2.5 Lesion. Extracted from Figure 2 of *Skovgård et al., unpublished manuscript.*

Compulsive checking behaviour is induced by the D2/3 agonist regardless of L-DOPA cotreatment

The ability of the chronic drug treatments to induce compulsive behaviours was assessed using a test originally introduced as a model of obsessive compulsive disorder (Szechtman et al., 1998). Animals treated with ropinirole travelled repeatedly between two zones of the arena. Specifically, R2.5- and LD24+R2.5-treated rats returned to these home bases excessively often and rapidly compared to saline and L-DOPA-treated animals. In line with these findings, there was a clear trend for ropinirole-treated animals to visit fewer places before returning to the home bases, reaching significance only for sham-lesioned animals compared to LD24. Furthermore, animals treated with ropinirole showed a higher ratio of observed to expected checks compared to L-DOPA and vehicle, which is a measure of compulsive checking that considers the increased motor activity induced by ropinirole (see Figure 18). Altogether, these findings suggest a clear trend of

ropinirole to induce compulsive checking behaviour when administered chronically alone or combined with L-DOPA.

We furthermore investigated the development of compulsive checking behaviour by comparing the chronic effects already obtained to acute effects induced by either low (LD6, R0.5, and LD6+R0.5) or high doses (LD24, R2.5, and LD24+R2.5) of each treatment. Interestingly, repeated treatment with ropinirole induced different patterns of change in the compulsive checking measures. While most criteria measures tended to develop along repeated injections of ropinirole, a difference in the length of checks was already seen upon acute treatment with low doses of ropinirole and further sensitised with repeated injections. In addition, the effects on the ratio of observed to expected checks were induced already at the acute low dose, but did not develop consistently with repeated injections of ropinirole.

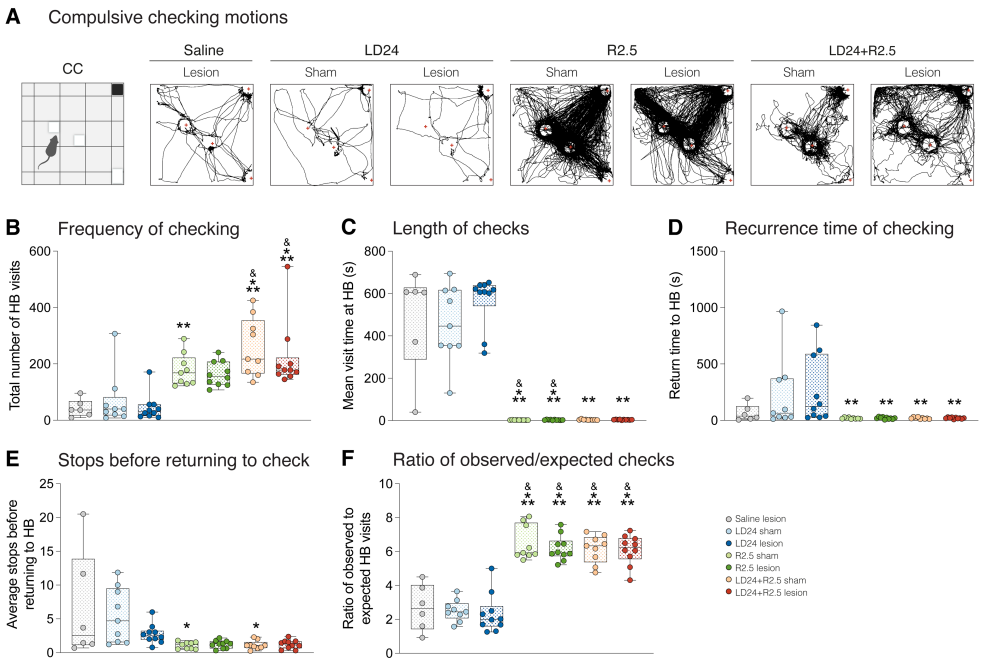

Figure 18. Criteria measures of compulsive checking behaviour upon chronic drug treatments in bilaterally 6-OHDA- or sham-lesioned rats. A Representative examples of track plots of motions within the arena during a 45 min session. **B-F** Criteria measures of compulsive checking behaviour are presented during the last 30 min for hyperlocomotive rats (R2.5 and LD24+R2.5) and during the total 45 min session for control and LD24-treated rats, and includes frequency of checking (**B**), length of checks (**C**), recurrence time of checking (**D**), stops before returning to checking (**E**), and the ratio of observed to expected checks (**F**). Post hoc: &p<0.05 vs. Saline, *p<0.05 vs. LD24 Sham, **p<0.05 vs. LD24 Lesion. Extracted from Figure 4 of *Skovgård et al., unpublished manuscript* (Paper IV).

D2/3 agonist alters affective decision-making in 6-OHDA-lesioned rats

Following the first three weeks of chronic treatment, decision-making processes were investigated in 6-OHDA-lesioned animals using the rIGT (van den Bos et al., 2006). Animals treated with LD24 learned to discriminate between empty and baited arm faster and to a higher degree than ropinirole-treated animals. Moreover, the number of switches between different arms was consistently higher in ropinirole-treated animals, which indicates a higher level of exploratory behaviour induced by the D2 agonist. When investigating if the animals learned to discriminate the advantageous arm from all other arms, we found a clear trend for animals in all treatment groups to perform more advantageous arm choices at the last trial block. Importantly, the fraction of advantageous arm choices upon treatment with LD24 was consistently and significantly higher than ropinirole-treated animals already from trial block 73-84 onwards. Thus, LD24-treated animals learned to discriminate the advantageous arms faster than ropinirole-treated animals (see Figure 19).

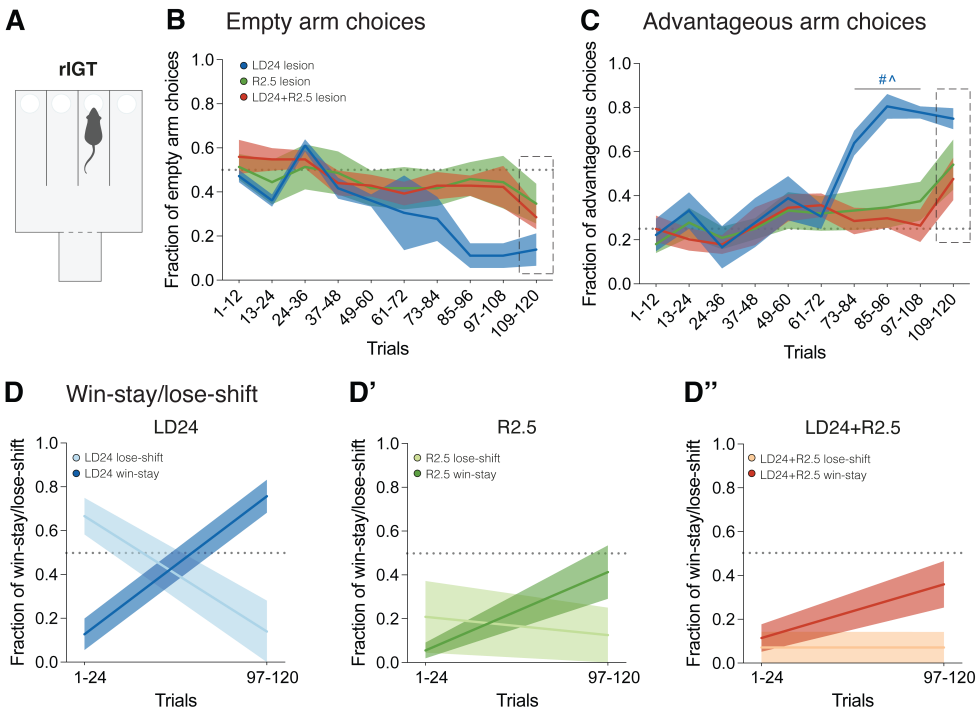

Figure 19. Performance in the rat Iowa Gambling Task (rIGT) upon chronic drug treatments in 6-OHDA-lesioned rats. A Scheme of the rIGT arena. **B** Fraction of empty arm choices to the total arm choices per 12 trials. **C** Fraction of advantageous arm choices to the total arm choices per 12 trials. **D-D''** Win-stay/lose-shift choices in the advantageous arms at the first and last 24 trials following chronic treatment with LD24 (**D**), R2.5 (**D'**), or LD24+R2.5 (**D''**). Dotted lines mark the chance level for each analysis and hatched squares mark the last trial block. Post hoc: ^p<0.05 vs. R2.5, #p<0.05 vs. LD24+R2.5. Extracted from Figure 5 of *Skovgård et al., unpublished manuscript* (Paper IV).

For the advantageous arm choices, we further investigated the fraction of win-stay or lose-shift for each treatment. Animals treated with LD24 tended to increase the fraction of win-stay and decrease the fraction of lose-shift during the test. This is in contrast to the trends seen in ropinirole-treated animals, where the fraction of lose-shift tended to be stable along all trials with a minor increase in the fraction of win-stay (see Figure 19). Altogether, this suggests that treatment with ropinirole, alone or combined with L-DOPA, induces impairments in the ability to establish an advantageous strategy along the task when compared to L-DOPA as monotherapy.

Measures of anxiety correlated with compulsive behaviour and overall performance in the rIGT

Since ICBs are often accompanied by anxiety as a comorbidity (Schapira et al., 2017; Voon et al., 2011b), we investigated the impact of anxiety-like behaviour on measures of compulsivity and decision-making. Interestingly, we found that high anxiety levels, as defined by the time spent on the open arms of the EPM, were associated with low levels of compulsive-like behaviour as assessed in the compulsive checking paradigm, while no significant correlation was found with the fraction of advantageous arm choices in the rIGT. However, high anxiety levels were associated with a lower overall task performance in the rIGT, as measured by the total number of reward pellets collected.

Summary of Paper IV

The results obtained from Paper IV reveal that enhanced compulsivity and impulsive decision-making are equally induced by a D2/3 agonist when administered alone or combined with L-DOPA. Furthermore, our results show that partial DA depletion of the striatum does not confer a greater risk of developing compulsive behaviours, indicating that D2/3 receptor stimulation is sufficient to induce these behaviours if sufficiently potent.

Discussion

Discussion

Preclinical models of LID have greatly improved our understanding of the underlying pathology and guided clinical proof-of-principle trials across multiple therapeutic targets (Fox and Brotchie, 2019). Nevertheless, it has proven difficult to translate promising antidyskinetic principles to the clinic, which calls for an improvement of both clinical trial methodology and preclinical models in this translational area (Cenci et al., 2022; Fox and Brotchie, 2019). Currently, animal models of LID are produced by administering L-DOPA monotherapy to severely DA-denervated animals (Cenci and Crossman, 2018), which, however, does not reflect L-DOPA-sparing practices used in the clinic. Indeed, in patients with advanced PD and motor complications, L-DOPA is often combined with a DA agonist to achieve longer-lasting therapeutic effects and reduce the daily L-DOPA dose (Cenci et al., 2022). Although less prone to induce dyskinesia, the DA agonists have a high liability to induce neuropsychiatric side effects, in particular ICBs (Stocchi et al., 2020).

In this context, this thesis aims at developing improved experimental models to advance translational research on the motor and neuropsychiatric complications of PD therapy. Both well-established and new experimental models are used to define correlations and causal links between regimens of dopaminergic treatment, behavioural changes, and biomarkers of network and cellular dysfunction in the cortico-basal ganglia circuitry. Importantly, the biomarkers examined in these studies reflect neurophysiological or histomolecular alterations that are known to also occur in human PD.

Biomarkers of network dysfunctions in the cortico-basal ganglia circuitry

The motor symptoms of PD as well as the motor complications of L-DOPA therapy are associated with synchronised oscillatory activities in the cortico-basal ganglia network. Specifically, motor symptoms of PD have been linked to beta oscillations in deep basal ganglia nuclei (Brown et al., 2001), whereas dyskinesia has been linked to NBG oscillations, in particular in the motor cortex (Swann et al., 2016). Because these aberrant oscillations share great similarity across species, they have been suggested as physiological biomarkers to guide pharmacological and electrical neuromodulatory interventions (Petersson et al., 2019).

Indeed, both beta and NBG oscillations have been proposed as promising control signals for adaptive DBS in PD patients (Little et al., 2013; Swann et al.,

2018). While L-DOPA-induced NBG oscillations are minimally affected by voluntary movements (Swann et al., 2016), changes in beta oscillations are observed during different motor states (Brazhnik et al., 2014; Lofredi et al., 2018). When using beta oscillations as a biomarker for PD, it is therefore important to account for movement artefacts that may otherwise affect the detection of beta activity.

In Paper I we therefore address how neuronal oscillations in the cortico-striatal structures change according to the levels of motor activity in normal or parkinsonian conditions. LFP recordings were obtained from the motor cortex and the striatum in both intact and severely DA-denervated rats with bilateral or unilateral lesions. In both brain regions, the power of broad-band LFP oscillations in the beta (12-30 Hz) or gamma range (35-110 Hz) showed a significant correlation (negative or positive, respectively) with an accelerometer-based index of overall motor activity. Similar correlations were observed in both normal and parkinsonian conditions. These findings suggest that changes in broad-band oscillatory activities of cortico-basal ganglia networks are correlated to ongoing motions and do not reflect disease-specific states.

Importantly, we also identified the characteristic narrowband beta oscillations (~25–40 Hz), that has previously been described in the DA-denervated cortex, STN, and SNr in hemiparkinsonian rats (Avila et al., 2010; Brazhnik et al., 2012; Delaville et al., 2015). These studies found that beta power varies with the behavioural state, being significantly enhanced during treadmill walking relative to inattentive rest. Although exaggerated beta oscillations have so far been described to occur in a fixed frequency range in hemiparkinsonian rats, the sorting of the oscillations according to motion index in our study revealed a gradual shift from lower to higher frequencies as the motor activity increased. This new observation might rely on the use of the accelerometer-based index of motor activity allowing us to include all types of activities, ranging from subtle head movements to actual locomotion, while the original studies divided the recordings into specific motor epochs (e.g. rest, grooming, treadmill walking). Interestingly, the use of accelerometers and other inertial sensors are currently being investigated for precise assessment of movement kinematics in PD patients (Habets et al., 2021). It is also important to mention that exaggerated beta activity as measured by conventional methods is currently being questioned to be limited in showing causality with motor symptoms of PD (Brazhnik et al., 2021). As a result, several analytical methods have recently been proposed to quantify oscillatory synchrony in the beta frequency range using more nuanced features (Karekal et al., 2022). In this context, our findings highlight the relevance of developing more sophisticated algorithms to differentiate physiological from pathological oscillations in different motor states.

The role of D1 and D2 receptors in network dysfunctions in LID

While it is well known that exaggerated beta oscillations are suppressed by dopaminergic treatments as they improve parkinsonian motor symptoms (Kühn et al., 2006), preclinical studies have only recently confirmed that NBG oscillations

are modulated by pharmacological interventions affecting the dyskinetic state of the animals (Brys et al., 2018; Tamtè et al., 2016). Thus, NBG oscillations are not only considered a promising feedback signal for closed-loop neuromodulation, but are also proposed as a reliable and directly translatable biomarker of the action of candidate antidyskinetic treatments.

Previous preclinical studies have established an association between the expression of dyskinesia and NBG oscillations across the cortico-basal ganglia circuitry upon L-DOPA treatment (Belić et al., 2016; Brys et al., 2018; Dupre et al., 2016; Halje et al., 2012; Tamtè et al., 2016). Importantly, LID-related NBG oscillations have also been observed in the motor cortex and STN of dyskinetic PD patients (Swann et al., 2016). However, the role of D1 and D2 receptors in the expression of NBG oscillations has so far only been investigated in specific motor cortical areas and only upon acute administration of DA receptor agonists in hemiparkinsonian rats (Dupre et al., 2016; Halje et al., 2012). In Paper II, we therefore set out to investigate the oscillatory responses to chronic treatment with selective D1 and D2 receptor agonists in unilaterally 6-OHDA-lesioned rats primed with L-DOPA. Utilizing a technology that enables large-scale recordings in freely moving animals (Ivica et al., 2014), LFPs oscillations in both NBG and theta frequency bands were recorded simultaneously from seven critical nodes of the cortico-basal ganglia circuitry.

We show that D1 receptor stimulation induced strong NBG oscillations across the cortico-basal ganglia circuitry with the exception of SNr, being most prominent in the motor cortical areas involved in forelimb movements. Following treatment with the D2 agonist, NBG oscillations were detected only in the forelimb motor cortex and DLS, being less pronounced compared to D1-induced NBG activity. After discovering that cortical NBG oscillations in conjunction with LID can be suppressed by locally applying a D1 receptor antagonist, Halje and co-authors previously proposed that supersensitive DA receptors make the cortical circuits prone to network resonance in the NBG frequency range (Halje et al., 2012). Contributing to this theory, our findings demonstrate a particularly prominent role of the D1 receptor in inducing cortical and pallidal NBG oscillations as compared to the D2 receptor, which is in line with the crucial role of D1 receptor sensitivity in LID (Fabbrini and Guerra, 2021). In addition, our phase analysis revealed that NBG oscillations in the primary forelimb motor region were leading cortico-striatal structures, with a stronger effect upon D1 receptor stimulation. This suggests that this cortical region might be a key driver of NBG oscillations, at least for the circuits recorded in this study. In line with the consistent phase differences, D1 receptor stimulation resulted in a stronger functional connectivity intracortically as well as in the cortico-striatal and cortico-pallidal systems, indicating that these high-frequency oscillations are intrinsically generated in the cortical network, from which they spread to subcortical structures.

Interestingly, another oscillatory phenomenon seemed to be more specific to D2 receptor stimulation, that is, the induction of prominent theta oscillations in the DA-

denervated GPe and SNr. Several studies have previously reported increased theta activity in deep basal ganglia nuclei after treatment with L-DOPA in both patients (Alonso-Frech et al., 2006) and animal models of PD (Brys et al., 2018; Chen et al., 2021; Wang et al., 2019). In patients, this theta rhythm was found to increase specifically in the presence of dyskinesia (Alegre et al., 2012; Alonso-Frech et al., 2006; Giannicola et al., 2013), while a direct association between theta oscillations and dyskinesia was only recently described in animal models of LID (Wang et al., 2019). Importantly, our results revealed a profound role of D2 receptor stimulation in the induction of these LID-related theta rhythms in deep basal ganglia nuclei. However, it still remains to be established which form of dyskinesia is mimicked by the D2 agonist in our animal model. In a recent study, D2 receptors were found to selectively mediate dystonic features of dyskinesia in hemiparkinsonian mice, in the absence of D1 receptor stimulation (Andreoli et al., 2021). In line with these findings, we found that dyskinesias induced by the D2 agonist were predominated by dystonic components (axial AIMs) relative to hyperkinetic components (limb and orolingual AIMs), with a slower turning speed compared to D1 agonist-induced dyskinesia. Interestingly, enhanced theta activity has been reported in PD patients experiencing diphasic dyskinesias (Alegre et al., 2012), with a strong dystonic appearance, as well as in patients experiencing cervical dystonia (Neumann et al., 2017). In this light, the stronger increase in theta oscillations in GPe and SNr induced by D2 receptor stimulation in our study may underlie the slower pattern of dyskinetic behaviours induced by D2 compared to D1 receptor agonists. Keeping in mind that D2/3 agonists are associated with a higher risk of developing ICBs, another interesting consideration is that theta activity in the STN of PD patients has not only been associated with dyskinesia, but also with ICBs (Rodriguez-Oroz et al., 2011).

Results from Paper II demonstrate that the dyskinetic effects of D1 and D2 receptor agonists are associated with distinct patterns of cortico-basal ganglia oscillations, suggesting a recruitment of partially distinct networks. Another important implication of this study is that LFP spectral contents in the globus pallidus may be used to parse the relative contribution of D1 vs D2 receptors in mediating different forms of dyskinesia in PD. Thus, the composition of the dopaminergic therapies prescribed to each individual PD patients might affect these neurophysiological biomarkers and should be considered in future investigations.

Modelling of dyskinesias induced by L-DOPA and DA agonist cotreatment

Animal models of LID are widely used to test candidate antidyskinetic treatments, although it has proven difficult to translate promising pharmacological principles into clinical practice. The question however remains, how these preclinical models can be improved to obtain better translatability?

One consideration is the role of D2 receptor stimulation in LID. While some studies have shown that de novo administration of D2 agonists can induce dyskinesia in animal models of PD (Andreoli et al., 2021; Bagetta et al., 2012),

others report only mild or no effects (Carta et al., 2008; Lundblad et al., 2002). However, D2/3 agonists are known to induce dyskinesia in parkinsonian rats previously primed with L-DOPA (Dupre et al., 2007; Kiessling et al., 2020; Sebastianutto et al., 2020). The results of Paper III demonstrate that the D2/3 agonist ropinirole could not induce dyskinesia when administered de novo to hemiparkinsonian rats, nor could subthreshold doses of L-DOPA monotherapy. In L-DOPA-primed animals, however, both D1 and D2 receptor agonists elicited dyskinesia as shown in Paper II and III, supporting a role of D2 receptor stimulation in established LID. Considering that D2/3 agonists are frequently used in the clinical management of motor complications in PD, alone or combined with L-DOPA, it is important to understand whether adjunct treatment with such DA agonists impacts the patterns of LID-related neuroplasticity and drug responses. Currently, preclinical models of dyskinesia are based on L-DOPA monotherapy (Cenci and Crossman, 2018), and do not mimic the combination therapies with DA agonists that many patients are prescribed. Prompted by these considerations, Paper III therefore presents a new animal model of dyskinesia induced by combined treatment with a low dose of L-DOPA and the D2/3 agonist ropinirole in unilaterally lesioned rats.

This combined L-DOPA-ropinirole therapy induced dyskinesias that were phenotypically similar to the classical LID model with regard to severity and subtype composition. Despite similar dyskinetic behaviours, the combined treatment resulted in lower ΔFosB expression levels and an increased striosomal/matrix ΔFosB expression ratio in the striatum compared to L-DOPA alone. The latter is in line with previous studies showing that D2 agonists alter the compartmental distribution of D1 agonist-induced Fos expression with a concomitant striosomal augmentation and matrix suppression of Fos induction (Wirtshafter and Asin, 2001; Wirtshafter et al., 1997). In addition, the combined treatment group did not exhibit any upregulation of angiogenesis markers and BBB hyperpermeability previously shown to depend on D1 receptor stimulation (Lindgren et al., 2009; Westin et al., 2007). Collectively, these findings indicate that dyskinesias induced by the combined treatment regimen are less reliant on D1 receptors while engaging D2 receptors to a larger degree than the classical LID model, which was also confirmed by pharmacologically antagonising either D1 or D2 receptors in each dyskinesia model.

When examining the antidyskinetic efficacy of different pharmacological principles, we found that compounds modulating D1 receptor signalling had a stronger effect in animals treated with L-DOPA alone, whereas both amantadine and the highly selective NMDA receptor antagonist MK801 produced a markedly larger antidyskinetic effect in L-DOPA-ropinirole cotreated animals. This highlights the importance of considering the regimen of DA replacement therapy in future clinical and preclinical evaluations of potential antidyskinetic treatments. In preclinical studies, using pharmacologically distinct animal models of LID may

moreover improve the chances of identifying robust antidyskinetic candidates for clinical translation.

Characterisation of ICBs induced by different dopaminergic treatments

Although DA agonists monotherapy might reduce or delay dyskinetic behaviours in PD patients, they increase the risk of developing ICBs (Corvol et al., 2018; Erga et al., 2017; Weintraub et al., 2010). However, the association between ICBs and pharmacotherapies combining L-DOPA and DA agonists remains a matter of debate. While some clinical studies have observed a higher incidence of ICBs following co-treatment with L-DOPA and DA agonists in PD patients (Sharma et al., 2015; Weintraub et al., 2010), other studies have reported similar (Bastiaens et al., 2013; Corvol et al., 2018) or even lower (Erga et al., 2017) incidences of ICBs as compared to DA agonist monotherapy. To the best of our knowledge, the impact of combining DA agonists with L-DOPA has never been investigated preclinically. Thus, in Paper IV, our first goal was to investigate the effects of the D2/3 agonist ropinirole, administered alone or combined with L-DOPA, on different measures of ICBs in both intact and DA-depleted animals.

The results of Paper IV demonstrate that treatment with ropinirole induces both compulsive behaviours in a test of compulsive checking and an impairment in developing an advantageous decision-making strategy in the rIGT, regardless of L-DOPA coadministration. In the latter test paradigm, the reduced capacity to adopt an advantageous decision-making strategy may reflect an impaired ability to learn from negative feedback (a reduced sensitivity to punishment), resulting in higher risk taking. In contrast, this study does not demonstrate a role of L-DOPA treatment in the induction of ICBs, neither when given alone nor as cotreatment to ropinirole. These findings are in line with previous studies showing that D2/3 agonist monotherapy can induce compulsive behaviours in rodent models of gambling (Cocker et al., 2017; Winstanley et al., 2011), hoarding (Decourt et al., 2022), as well as another test of compulsive checking (Eagle et al., 2014). Moreover, D2/3 agonists have been found to potentiate the choice of uncertain outcomes in the rodent betting task (Tremblay et al., 2017) and in tasks of probability discounting (Floris et al., 2022; Holtz et al., 2016; Pes et al., 2017; Rokosik and Napier, 2012). When taken together, our results demonstrate that therapy-dependent ICBs can be attributed to the direct stimulation of D2/3 receptors by ropinirole, and that L-DOPA cotreatment is unlikely to increase the liability for this type of neuropsychiatric complications.

Since DA agonists have been linked to the emergence of ICBs in several conditions not associated with a loss of endogenous DA function (Cornelius et al., 2010; Holman, 2009), we also set out to investigate the impact of striatal DA depletion on compulsive-like effects induced by ropinirole, alone or combined with L-DOPA. We used an animal model with mild bilateral striatal DA denervation, because animals with large dopaminergic lesions would develop dyskinesia when treated with L-DOPA, resulting in technical and interpretational difficulties in the

assessment of neuropsychiatric functions. Importantly, the effects on compulsive behaviour induced by ropinirole were replicated in this 6-OHDA rat model mimicking early-stage PD. This indicates that ICBs arise directly as a result of treatment with DA agonists, regardless of the pathophysiological changes associated with PD. These findings are in agreement with previous investigations utilising 6-OHDA lesions, which have found no alterations in the response of lesioned animals to DA agonists in tests of compulsive-like gambling behaviour (Cocker et al., 2019) and preference for uncertainty (Rokosik and Napier, 2012; Tremblay et al., 2017). However, it is important to mention that studies using rats with nigrostriatal lesions induced by viral-mediated human-mutated alpha-synuclein or 6-OHDA injections in SNc and VTA have found increased compulsive behaviour in an operant post-training signal attenuation task upon treatment with the D2/3 agonist pramipexole (Dardou et al., 2017; Decourt et al., 2022). These discrepancies might be explained by differences in the extent of the dopaminergic lesions, that may underlie different compensatory mechanisms in the striatum, as well as differences in the pharmacological regimens. Indeed, the DA-depletion induced by our intrastriatal 6-OHDA lesion procedure was somewhat less robust than reported by previous studies using this model (Baunez et al., 2007; Rokosik and Napier, 2012). Moreover, we use a relatively high dose of ropinirole in this animal model, mimicking a human dose higher than the standard therapeutic daily dose, while the dose of L-DOPA corresponds to a low daily maintenance dose as given in combination with DA agonists. Therefore, it is possible that the use of a high bolus injection of ropinirole might obscure any potentiating effects of the mild DA-depletions. This calls for additional investigations of the relationship between the severity of dopaminergic lesions and incremental doses of DA agonists.

Notwithstanding these limitations, our results demonstrate that partial DA-depletion does not confer a greater risk of developing ICB-like traits, indicating that D2/3 receptor stimulation is sufficient to induce these behaviours if sufficiently potent. These results encourage further investigations of the expression and cellular distribution of molecular biomarkers of neuronal activity to elucidate the underlying mechanisms of treatment-induced ICBs in PD.

Concluding remarks

The development of novel therapeutic approaches for the motor complications of PD is dependent on our understanding of the pathophysiological phenomena at both cellular and systems levels. Elucidating such phenomena requires studying valid animal models that mimic central aspects of the disease of interest. Indeed, well-characterised animal models of LID have shaped current pathophysiological notions and guided clinical investigations of multiple therapeutic targets. However, these models are not considering the relative balance between D1 and D2 receptor stimulation induced by different regimens of dopaminergic replacement therapies. Moreover, when investigating motor and non-motor complications with regard to drug development, there is a great potential in complementing data from

neurochemical, histological, and behavioural approaches with electrophysiological biomarkers for a more precise targeting of circuit dysfunctions in PD.

This thesis work presents a vast set of findings obtained from different rodent models of parkinsonism, treated with different dopaminergic regimens, and investigated with complementary techniques. Importantly, we show that treatment with L-DOPA vs. DA receptor-specific medications induce quite different profiles of behavioural alterations and pathophysiological changes at the network- and cellular level. Our results shed new light on the pathophysiological implications of dopaminergic pharmacotherapy for PD and reveal the importance of including realistic models of combined therapies in future translational research on LID.

It is our hope that the fundamental contributions of this thesis will encourage future efforts towards development of personalised treatments for PD. Specifically, we imagine a future scenario where the choice of antidyskinetic pharmacotherapy or electrical neuromodulation will be personalised based on the regimen of dopaminergic replacement therapy in the affected patient. This thesis work moreover encourages further investigations on the relationship between specific dyskinetic and dystonic manifestations induced by the relative engagement of D1 and D2 receptors in different phases of the L-DOPA dosing cycle, their oscillatory fingerprints, and the underlying circuit dysfunctions in PD. Moreover, the demonstration that D1 and D2 receptor stimulation induces distinct network dysfunctions may raise an interest in identifying a neurophysiological readout of the non-motor complications induced by D2/3 agonist in PD, which would offer a unique opportunity to evaluate new neuropsychiatric drug candidates in animals.

Acknowledgements

Acknowledgements

I am truly grateful having had the opportunity to pursue a PhD degree amongst some of the most beautiful minds within neuroscience. As if that was not enough, I was lucky to share this journey with so many wonderful people. These last pages are dedicated to everyone who has given me encouragement, guidance, kindness and smiles during these past five years.

First of all, I own my greatest appreciation and gratitude to my supervisor, *Angela*. Thank you for always believing in me and for your guidance that helped me to develop as an independent scientist. As a mentor, you have always challenged me to go the extra mile and encouraged me when I needed it the most, and your excellent scientific mind and enthusiasms for science has been a great inspiration. Thank you!

I would like to extend my sincere thanks to my co-supervisors. *Pär*, thank you for being my go-to expert on anything computational, for your patience when teaching me MATLAB, and for being an endless source of inspiration on what to do next. *Per*, thank you for welcoming me in your lab and for giving me the opportunity to work with ground-breaking electrophysiological techniques - it was a great joy! I have really appreciated your guidance over the years and your always invaluable inputs putting things into perspective.

Irene, Sebastian, and *Elena*, my three wise "postdocs", and above all, friends! I am so grateful for your caring support on this journey and for everything that we have shared, professionally and personally. Without you, this thesis would not be.

To my dear colleagues at the BGP lab, *Anki, Silvia, Laura, Mirjam, Melina, Chang, Ana-Elena, Camilla, Valentina, Veronica, Tim, Erik, Lindsay, Apostolos, Oksana, Morteza, Abderahim,* and *Osama*. You have been the backbone of my Swedish adventure and I could not have asked for a better collection of people to work with! Thank you for brightening the days with good conversations, for the many walks around Lund, for the great memories that we have shared, and all the small gestures that made me smile. I am really going to miss you!

I am especially grateful to my students, *Marcus, Elisabeth*, and *Guy*. I learned so much from you!

One thing that I have really appreciated during my PhD, is the collaborations that I have been part of. A special thanks to everyone in the ADAPT-PD for your invaluable knowledge and for bringing a clinical perspective to my preclinical work.

I would like to thank *Romulo Fuentes* and all the people in his lab that contributed to the first paper of this thesis. I also owe a great thanks to all former and present collaborators and colleagues in the Petersson labs, *Joel, Luciano, Evgenya, Ivani, Tiberiu, Emilio, Aziz,* and *Sebastian*. Thank you for your always skilled inputs and for welcoming my contributions to your projects over the years.

Doing a collaborative PhD has given me the opportunity to cross paths with so many excellent people over the years. Thanks to present and former F11 and A13 colleagues for your daily smiles and kindness, to everyone at the MV for all the lunch talks and fika breaks during the first years, and to everybody at the BMC who has supported me in one way or the other. Thank you!

I would never have pursued a PhD within neuroscience, if it wasn't for some very special people at Lundbeck and the University of Copenhagen, who showed me the wonders of the brain during my time as a Master's student, and I was so lucky that one followed me to Lund. *Michael*, jeg er så taknemmelig for at din dør altid er åben for en god snak og for din altid positive tilgang til livet. Jeg håber at vores veje mødes igen i fremtidige jobs, og om ikke andet, er jeg sikker på at vi nok skal få set hinanden på anden vis!

Jeg var aldrig kommet hel igennem denne PhD, hvis ikke det var for mine skønne veninder. At have jer som sparringspartnere igennem livet, er noget jeg er helt utroligt taknemmelig for. Tak fordi I hepper på mig når det går godt, men mest af alt fordi I også er her, når det ikke gør. I betyder alverden!

Tusind tak til min søde familie for jeres fantastiske støtte og for at være et fast holdepunkt i udfordrende tider. Uden jeres forbilledlighed og jeres ukuelige tro på mig igennem livet, var det her aldrig lykkedes. Og så skal jeg nok tage en ekstra tørn med julegaverne næste år, for jeg skylder vidst lidt … TAK for jer!

En helt særlig tak til dig, *Mads*. Tak fordi du altid er her for mig og får det hele til at lykkes. Jeg er dig evigt taknemmelig for alt det, du har gjort og tilsidesat for, at jeg kunne opnå min drøm om at skrive en PhD. På dage hvor jeg mister troen på det hele, hjælper det altid at se mig selv igennem dine øjne, og jeg kunne ikke have gjort det her uden dig. Tak for dig og for vores Sveriges-eventyr – nu glæder jeg mig til at se, hvad det næste bringer!

Til sidst tak til dig, *Uma*! Tak for al den glæde du bringer, for dine kreative påfund, og for at skabe balance i mit liv. Det er det største privilegie at se dig udfolde dig som menneske, og jeg er så uendelig stolt af dig!

. .. .

References

References

Abbes, M., et al., 2018. Subthalamic stimulation and neuropsychiatric symptoms in Parkinson's disease: results from a long-term follow-up cohort study. J Neurol Neurosurg Psychiatry 89, 836-843.

Ahmed, I., et al., 2011. Glutamate NMDA receptor dysregulation in Parkinson's disease with dyskinesias. Brain 134, 979-986.

Albin, R. L., et al., 1989. The functional anatomy of basal ganglia disorders. Trends Neurosci 12, 366-375.

Alcacer, C., et al., 2017. Chemogenetic stimulation of striatal projection neurons modulates responses to Parkinson's disease therapy. J Clin Invest 127, 720-734.

Alegre, M., et al., 2012. Subthalamic activity during diphasic dyskinesias in Parkinson's disease. Movement Disorders 27, 1178-1181.

Alexander, G. E., Crutcher, M. D., 1990. Functional architecture of basal ganglia circuits: neural substrates of parallel processing. Trends Neurosci 13, 266-271.

Alexander, G. E., et al., 1986. Parallel organization of functionally segregated circuits linking basal ganglia and cortex. Annu Rev Neurosci 9, 357-381.

Alonso-Frech, F., et al., 2006. Slow oscillatory activity and levodopa-induced dyskinesias in Parkinson's disease. Brain 129, 1748-1757.

Andreoli, L., 2021. Striatal pathways in dyskinesia and dystonia. Faculty of Medicine. Lund University, Lund University, Faculty of Medicine Doctoral Dissertation.

Andreoli, L., et al., 2021. Distinct patterns of dyskinetic and dystonic features following D1 or D2 receptor stimulation in a mouse model of parkinsonism. Neurobiology of Disease 157, 105429.

Antonelli, T., et al., 2005. Effects of sarizotan on the corticostriatal glutamate pathways. Synapse 58, 193-199.

Antonini, A., Poewe, W., 2007. Fibrotic heart-valve reactions to dopamine-agonist treatment in Parkinson's disease. Lancet Neurol 6, 826-829.

Aoki, S., et al., 2019. An open cortico-basal ganglia loop allows limbic control over motor output via the nigrothalamic pathway. eLife 8, e49995.

Archer, J., 1973. Tests for emotionality in rats and mice: A review. Animal Behaviour 21, 205-235.

Asch, N., et al., 2020. Independently together: subthalamic theta and beta opposite roles in predicting Parkinson's tremor. Brain Commun 2, fcaa074.

Aubert, I., et al., 2005. Increased D1 dopamine receptor signaling in levodopa-induced dyskinesia. Annals of Neurology 57, 17-26.

Avila, I., et al., 2010. Beta frequency synchronization in basal ganglia output during rest and walk in a hemiparkinsonian rat. Exp Neurol 221, 307-319.

Bagetta, V., et al., 2012. Rebalance of striatal NMDA/AMPA receptor ratio underlies the reduced emergence of dyskinesia during D2-like dopamine agonist treatment in experimental Parkinson's disease. J Neurosci 32, 17921-17931.

Bamford, N. S., et al., 2004. Dopamine modulates release from corticostriatal terminals. J Neurosci 24, 9541-9552.

Bara-Jimenez, W., et al., 2005. Effects of serotonin 5-HT1A agonist in advanced Parkinson's disease. Mov Disord 20, 932-936.

Bastiaens, J., et al., 2013. Prospective cohort study of impulse control disorders in Parkinson's disease. Movement Disorders 28, 327-333.

Bastide, M. F., et al., 2015. Pathophysiology of L-dopa-induced motor and non-motor complications in Parkinson's disease. Prog Neurobiol 132, 96-168.

Bateup, H. S., et al., 2010. Distinct subclasses of medium spiny neurons differentially regulate striatal motor behaviors. Proc Natl Acad Sci U S A 107, 14845-14850.

Baufreton, J., et al., 2005. Enhancement of excitatory synaptic integration by GABAergic inhibition in the subthalamic nucleus. J Neurosci 25, 8505-8517.

Baunez, C., et al., 2007. Bilateral high-frequency stimulation of the subthalamic nucleus on attentional performance: transient deleterious effects and enhanced motivation in both intact and parkinsonian rats. Eur J Neurosci 25, 1187-1194.

Belić, J. J., et al., 2016. Untangling Cortico-Striatal Connectivity and Cross-Frequency Coupling in L-DOPA-Induced Dyskinesia. Front Syst Neurosci 10, 26.

Berens, P., 2022. Circular Statistics Toolbox (Directional Statistics). MATLAB Central File Exchange.

Berlin, G. S., Hollander, E., 2014. Compulsivity, impulsivity, and the DSM-5 process. CNS Spectrums 19, 62-68.

Bevan, M. D., et al., 2002. Move to the rhythm: oscillations in the subthalamic nucleus-external globus pallidus network. Trends Neurosci 25, 525-531.

Bezard, E., et al., 2014. The mGluR5 negative allosteric modulator dipraglurant reduces dyskinesia in the MPTP macaque model. Mov Disord 29, 1074-1079.

Bezard, E., et al., 2013. Study of the antidyskinetic effect of eltoprazine in animal models of levodopa-induced dyskinesia. Mov Disord 28, 1088-1096.

Bianchine, J. R., et al., 1971. Metabolism and absorption of L-3,4 dihydroxyphenylalanine in patients with Parkinson's disease. Ann N Y Acad Sci 179, 126-140.

Biundo, R., et al., 2015. Patterns of cortical thickness associated with impulse control disorders in Parkinson's disease. Mov Disord 30, 688-695.

Björklund, A., Dunnett, S. B., 2007. Fifty years of dopamine research. Trends in Neurosciences 30, 185-187.

Boix, J., et al., 2018. Gait Analysis for Early Detection of Motor Symptoms in the 6-OHDA Rat Model of Parkinson's Disease. Front Behav Neurosci 12, 39.

Bonifati, V., et al., 1994. Buspirone in levodopa-induced dyskinesias. Clinical neuropharmacology 17, 73-82.

Bouthour, W., et al., 2019. Biomarkers for closed-loop deep brain stimulation in Parkinson disease and beyond. Nat Rev Neurol 15, 343-352.

Brazhnik, E., et al., 2012. State-dependent spike and local field synchronization between motor cortex and substantia nigra in hemiparkinsonian rats. J Neurosci 32, 7869-7880.

Brazhnik, E., et al., 2014. Functional correlates of exaggerated oscillatory activity in basal ganglia output in hemiparkinsonian rats. Exp Neurol 261, 563-577.

Brazhnik, E., et al., 2021. Early decreases in cortical mid-gamma peaks coincide with the onset of motor deficits and precede exaggerated beta build-up in rat models for Parkinson's disease. Neurobiology of Disease, 105393.

Brittain, J. S., Brown, P., 2014. Oscillations and the basal ganglia: motor control and beyond. Neuroimage 85 Pt 2, 637-647.

Brown, P., et al., 2001. Dopamine Dependency of Oscillations between Subthalamic Nucleus and Pallidum in Parkinson's Disease. The Journal of Neuroscience 21, 1033-1038.

Brugnoli, A., et al., 2020. Striatal and nigral muscarinic type 1 and type 4 receptors modulate levodopa-induced dyskinesia and striato-nigral pathway activation in 6-hydroxydopamine hemilesioned rats. Neurobiology of Disease 144, 105044.

Brys, I., et al., 2018. Neurophysiological effects in cortico-basal ganglia-thalamic circuits of antidyskinetic treatment with 5-HT(1A) receptor biased agonists. Exp Neurol 302, 155-168.

Buzsáki, G., et al., 2012. The origin of extracellular fields and currents--EEG, ECoG, LFP and spikes. Nat Rev Neurosci 13, 407-420.

Calandrella, D., Antonini, A., 2011. Pathological gambling in Parkinson's disease: disease related or drug related? Expert review of neurotherapeutics 11, 809-814.

Calne, D. B., et al., 1971. Idiopathic Parkinsonism treated with an extracerebral decarboxylase inhibitor in combination with levodopa. Br Med J 3, 729-732.

Carriere, N., et al., 2015. Impaired corticostriatal connectivity in impulse control disorders in Parkinson disease. Neurology 84, 2116-2123.

Carta, A. R., et al., 2008. Behavioral and biochemical correlates of the dyskinetic potential of dopaminergic agonists in the 6-OHDA lesioned rat. Synapse 62, 524-533.

Carta, M., Bezard, E., 2011. Contribution of pre-synaptic mechanisms to L-DOPA-induced dyskinesia. Neuroscience 198, 245-251.

Carta, M., et al., 2007. Dopamine released from 5-HT terminals is the cause of l-DOPA-induced dyskinesia in parkinsonian rats. Brain 130, 1819-1833.

Cassidy, M., et al., 2002. Movement-related changes in synchronization in the human basal ganglia. Brain 125, 1235-1246.

Cedarbaum, J. M., 1987. Clinical pharmacokinetics of anti-parkinsonian drugs. Clin Pharmacokinet 13, 141-178.

Cenci, M. A., 2014. Presynaptic Mechanisms of l-DOPA-Induced Dyskinesia: The Findings, the Debate, and the Therapeutic Implications. Front Neurol 5, 242.

Cenci, M. A., Björklund, A., 2020. Animal models for preclinical Parkinson's research: An update and critical appraisal. Prog Brain Res 252, 27-59.

Cenci, M. A., Crossman, A. R., 2018. Animal models of l-dopa-induced dyskinesia in Parkinson's disease. Mov Disord 33, 889-899.

Cenci, M. A., et al., 2018. On the neuronal circuitry mediating L-DOPA-induced dyskinesia. J Neural Transm (Vienna) 125, 1157-1169.

Cenci, M. A., Konradi, C., 2010. Maladaptive striatal plasticity in L-DOPA-induced dyskinesia. Prog Brain Res 183, 209-233.

Cenci, M. A., et al., 1998. L-DOPA-induced dyskinesia in the rat is associated with striatal overexpression of prodynorphin- and glutamic acid decarboxylase mRNA. Eur J Neurosci 10, 2694-2706.

Cenci, M. A., Lundblad, M., 2007. Ratings of L-DOPA-induced dyskinesia in the unilateral 6-OHDA lesion model of Parkinson's disease in rats and mice. Curr Protoc Neurosci Chapter 9, Unit 9.25.

Cenci, M. A., et al., 2011. Current options and future possibilities for the treatment of dyskinesia and motor fluctuations in Parkinson's disease. CNS Neurol Disord Drug Targets 10, 670-684.

Cenci, M. A., et al., 2020. Dyskinesia matters. Mov Disord 35, 392-396.

Cenci, M. A., et al., 2022. Non-dopaminergic approaches to the treatment of motor complications in Parkinson's disease. Neuropharmacology 210, 109027.

Censoni, L., et al., 2022. Verification of multi-structure targeting in chronic microelectrode brain recordings from CT scans. J Neurosci Methods 382, 109719.

Cerri, S., Blandini, F., 2020. An update on the use of non-ergot dopamine agonists for the treatment of Parkinson's disease. Expert Opinion on Pharmacotherapy 21, 2279-2291.

Chambers, N. E., et al., 2019. Effects of Muscarinic Acetylcholine m1 and m4 Receptor Blockade on Dyskinesia in the Hemi-Parkinsonian Rat. Neuroscience 409, 180-194.

Chaudhuri, K. R., et al., 2006. Non-motor symptoms of Parkinson's disease: diagnosis and management. Lancet Neurol 5, 235-245.

Chaudhuri, K. R., Naidu, Y., 2008. Early Parkinson's disease and non-motor issues. J Neurol 255 Suppl 5, 33-38.

Chen, J., et al., 2021. Dyskinesia is Closely Associated with Synchronization of Theta Oscillatory Activity Between the Substantia Nigra Pars Reticulata and Motor Cortex in the Off L-dopa State in Rats. Neurosci Bull 37, 323-338.

Chen, L., et al., 2011. Modulation of the activity of globus pallidus by dopamine D1-like receptors in parkinsonian rats. Neuroscience 194, 181-188.

Cilia, R., et al., 2010. Reduced dopamine transporter density in the ventral striatum of patients with Parkinson's disease and pathological gambling. Neurobiol Dis 39, 98-104.

Cilia, R., et al., 2008. Functional abnormalities underlying pathological gambling in Parkinson disease. Arch Neurol 65, 1604-1611.

Cocker, P. J., et al., 2019. The β-adrenoceptor blocker propranolol ameliorates compulsive-like gambling behaviour in a rodent slot machine task: implications for iatrogenic gambling disorder. European Journal of Neuroscience 50, 2401-2414.

Cocker, P. J., et al., 2017. Chronic administration of the dopamine D(2/3) agonist ropinirole invigorates performance of a rodent slot machine task, potentially indicative of less distractible or compulsive-like gambling behaviour. Psychopharmacology (Berl) 234, 137-153.

Cornelius, J. R., et al., 2010. Impulse control disorders with the use of dopaminergic agents in restless legs syndrome: a case-control study. Sleep 33, 81-87.

Corvol, J. C., et al., 2018. Longitudinal analysis of impulse control disorders in Parkinson disease. Neurology 91, e189-e201.

Corvol, J. C., et al., 2004. Persistent increase in olfactory type G-protein alpha subunit levels may underlie D1 receptor functional hypersensitivity in Parkinson disease. J Neurosci 24, 7007-7014.

Cotzias, G. C., et al., 1969. Modification of Parkinsonism--chronic treatment with L-dopa. N Engl J Med 280, 337-345.

Courtemanche, R., et al., 2003. Synchronous, focally modulated beta-band oscillations characterize local field potential activity in the striatum of awake behaving monkeys. J Neurosci 23, 11741-11752.

Cruz, A. V., et al., 2011. Effects of dopamine depletion on information flow between the subthalamic nucleus and external globus pallidus. J Neurophysiol 106, 2012-2023.

Cui, G., et al., 2013. Concurrent activation of striatal direct and indirect pathways during action initiation. Nature 494, 238-242.

Dalley, Jeffrey W., et al., 2011. Impulsivity, Compulsivity, and Top-Down Cognitive Control. Neuron 69, 680-694.

Danysz, W., et al., 1997. Aminoadamantanes as NMDA receptor antagonists and antiparkinsonian agents--preclinical studies. Neurosci Biobehav Rev 21, 455-468.

Dardou, D., et al., 2017. Chronic pramipexole treatment induces compulsive behavior in rats with 6-OHDA lesions of the substantia nigra and ventral tegmental area. Behavioural Brain Research 332, 327-336.

Darmopil, S., et al., 2009. Genetic inactivation of dopamine D1 but not D2 receptors inhibits L-DOPA-induced dyskinesia and histone activation. Biol Psychiatry 66, 603-613.

de Bie, R. M. A., et al., 2020. Initiation of pharmacological therapy in Parkinson's disease: when, why, and how. Lancet Neurol 19, 452-461.

de Iure, A., et al., 2019. Striatal spreading depolarization: Possible implication in levodopa-induced dyskinetic-like behavior. Mov Disord 34, 832-844.

de Visser, L., et al., 2011. Rodent versions of the iowa gambling task: opportunities and challenges for the understanding of decision-making. Front Neurosci 5, 109.

Decourt, M., et al., 2022. Assessment of Repetitive and Compulsive Behaviors Induced by Pramipexole in Rats: Effect of Alpha-Synuclein-Induced Nigrostriatal Degeneration. Biomedicines 10.

Decressac, M., et al., 2012. Comparison of the behavioural and histological characteristics of the 6-OHDA and α-synuclein rat models of Parkinson's disease. Exp Neurol 235, 306-315.

Defagot, M. C., et al., 1997. Distribution of D4 dopamine receptor in rat brain with sequence-specific antibodies. Brain Res Mol Brain Res 45, 1-12.

Delaville, C., et al., 2014. Oscillatory Activity in Basal Ganglia and Motor Cortex in an Awake Behaving Rodent Model of Parkinson's Disease. Basal Ganglia 3, 221-227.

Delaville, C., et al., 2015. Subthalamic Nucleus Activity in the Awake Hemiparkinsonian Rat: Relationships with Motor and Cognitive Networks. The Journal of Neuroscience 35, 6918-6930.

Dobbs, L. K., et al., 2016. Dopamine Regulation of Lateral Inhibition between Striatal Neurons Gates the Stimulant Actions of Cocaine. Neuron 90, 1100-1113.

Dupre, K. B., et al., 2016. Effects of L-dopa priming on cortical high beta and high gamma oscillatory activity in a rodent model of Parkinson's disease. Neurobiol Dis 86, 1-15.

Dupre, K. B., Dodge C, Delaville C, Brazhnik E, Novikov J, Walters JR, 2015. Ventromedial thalamis is critical for expression of cortical narrowband high gamma oscillations but not l-DOPA-induced dyskinesia in hemiparkinsonian rats. Paper presented at the SFN Annual Meeting.

Dupre, K. B., et al., 2008. Striatal 5-HT1A receptor stimulation reduces D1 receptor-induced dyskinesia and improves movement in the hemiparkinsonian rat. Neuropharmacology 55, 1321-1328.

Dupre, K. B., et al., 2007. The differential effects of 5-HT(1A) receptor stimulation on dopamine receptor-mediated abnormal involuntary movements and rotations in the primed hemiparkinsonian rat. Brain Res 1158, 135-143.

Dupre, K. B., et al., 2011. Local modulation of striatal glutamate efflux by serotonin 1A receptor stimulation in dyskinetic, hemiparkinsonian rats. Exp Neurol 229, 288-299.

Eagle, D. M., et al., 2014. The dopamine D2/D3 receptor agonist quinpirole increases checking-like behaviour in an operant observing response task with uncertain reinforcement: a novel possible model of OCD. Behav Brain Res 264, 207-229.

Eden, R. J., et al., 1991. Preclinical pharmacology of ropinirole (SK&F 101468-A) a novel dopamine D2 agonist. Pharmacol Biochem Behav 38, 147-154.

Eilam, D., Golani, I., 1989. Home base behavior of rats (Rattus norvegicus) exploring a novel environment. Behav Brain Res 34, 199-211.

Engeln, M., et al., 2013. Reinforcing properties of Pramipexole in normal and parkinsonian rats. Neurobiol Dis 49, 79-86.

Engeln, M., et al., 2016. Selective Inactivation of Striatal FosB/ΔFosB-Expressing Neurons Alleviates L-DOPA-Induced Dyskinesia. Biol Psychiatry 79, 354-361.

Erga, A. H., et al., 2017. Impulsive and Compulsive Behaviors in Parkinson's Disease: The Norwegian ParkWest Study. J Parkinsons Dis 7, 183-191.

Eusebi, P., et al., 2018. Risk factors of levodopa-induced dyskinesia in Parkinson's disease: results from the PPMI cohort. npj Parkinson's Disease 4, 33.

Eysenck, H. J., 1993. The nature of impulsivity. The impulsive client: Theory, research, and treatment. American Psychological Association, Washington, DC, US, pp. 57-69.

Fabbrini, A., Guerra, A., 2021. Pathophysiological Mechanisms and Experimental Pharmacotherapy for L-Dopa-Induced Dyskinesia. J Exp Pharmacol 13, 469-485.

Fahn, S., 2000. The spectrum of levodopa-induced dyskinesias. Ann Neurol 47, S2-9; discussion S9-11.

Fearnley, J. M., Lees, A. J., 1991. Ageing and Parkinson's disease: substantia nigra regional selectivity. Brain 114 (Pt 5), 2283-2301.

Fieblinger, T., et al., 2014a. Cell type-specific plasticity of striatal projection neurons in parkinsonism and L-DOPA-induced dyskinesia. Nat Commun 5, 5316.

Fieblinger, T., et al., 2014b. Mechanisms of dopamine D1 receptor-mediated ERK1/2 activation in the parkinsonian striatum and their modulation by metabotropic glutamate receptor type 5. J Neurosci 34, 4728-4740.

Floresco, S. B., et al., 2003. Afferent modulation of dopamine neuron firing differentially regulates tonic and phasic dopamine transmission. Nature Neuroscience 6, 968-973.

Floris, G., et al., 2022. The steroidogenic inhibitor finasteride reverses pramipexole-induced alterations in probability discounting. Brain Res Bull 181, 157-166.

Ford, C. P., 2014. The role of D2-autoreceptors in regulating dopamine neuron activity and transmission. Neuroscience 282, 13-22.

Foster, N. N., et al., 2021. The mouse cortico-basal ganglia-thalamic network. Nature 598, 188-194.

Fox, S. H., Brotchie, J. M., 2019. Viewpoint: Developing drugs for levodopa-induced dyskinesia in PD: Lessons learnt, what does the future hold? Eur J Neurosci 49, 399-409.

Fox, S. H., et al., 2008. Non-dopaminergic treatments in development for Parkinson's disease. The Lancet Neurology 7, 927-938.

Fox, S. H., et al., 2018. International Parkinson and movement disorder society evidence-based medicine review: Update on treatments for the motor symptoms of Parkinson's disease. Mov Disord 33, 1248-1266.

Francardo, V., et al., 2011. Impact of the lesion procedure on the profiles of motor impairment and molecular responsiveness to L-DOPA in the 6-hydroxydopamine mouse model of Parkinson's disease. Neurobiol Dis 42, 327-340.

Frosini, D., et al., 2010. Parkinson's disease and pathological gambling: results from a functional MRI study. Mov Disord 25, 2449-2453.

Gerfen, C. R., 1984. The neostriatal mosaic: compartmentalization of corticostriatal input and striatonigral output systems. Nature 311, 461-464.

Gerfen, C. R., 1985. The neostriatal mosaic. I. Compartmental organization of projections from the striatum to the substantia nigra in the rat. J Comp Neurol 236, 454-476.

Gerfen, C. R., et al., 2002. D1 dopamine receptor supersensitivity in the dopamine-depleted striatum results from a switch in the regulation of ERK1/2/MAP kinase. J Neurosci 22, 5042-5054.

Gerfen, C. R., Surmeier, D. J., 2011. Modulation of striatal projection systems by dopamine. Annu Rev Neurosci 34, 441-466.

Giannicola, G., et al., 2013. The effects of levodopa and deep brain stimulation on subthalamic local field low-frequency oscillations in Parkinson's disease. Neurosignals 21, 89-98.

Gioanni, Y., Lamarche, M., 1985. A reappraisal of rat motor cortex organization by intracortical microstimulation. Brain Res 344, 49-61.

Girasole, A. E., et al., 2018. A Subpopulation of Striatal Neurons Mediates Levodopa-Induced Dyskinesia. Neuron 97, 787-795.e786.

Gittis, A. H., et al., 2011. Rapid target-specific remodeling of fast-spiking inhibitory circuits after loss of dopamine. Neuron 71, 858-868.

Giugni, J. C., Okun, M. S., 2014. Treatment of advanced Parkinson's disease. Curr Opin Neurol 27, 450-460.

Goetz, C. G., et al., 2007. Sarizotan as a treatment for dyskinesias in Parkinson's disease: a double-blind placebo-controlled trial. Mov Disord 22, 179-186.

Grace, A. A., 2000. The tonic/phasic model of dopamine system regulation and its implications for understanding alcohol and psychostimulant craving. Addiction 95 Suppl 2, S119-128.

Grace, A. A., et al., 2007. Regulation of firing of dopaminergic neurons and control of goal-directed behaviors. Trends Neurosci 30, 220-227.

Grillner, S., et al., 2020. Basal Ganglia-A Motion Perspective. Compr Physiol 10, 1241-1275.

Grondin, R., et al., 1997. Potential therapeutic use of the selective dopamine D1 receptor agonist, A-86929: an acute study in parkinsonian levodopa-primed monkeys. Neurology 49, 421-426.

Gurevich, E. V., Joyce, J. N., 1999. Distribution of dopamine D3 receptor expressing neurons in the human forebrain: comparison with D2 receptor expressing neurons. Neuropsychopharmacology 20, 60-80.

Haber, S. N., 2003. The primate basal ganglia: parallel and integrative networks. J Chem Neuroanat 26, 317-330.

Habets, J. G. V., et al., 2021. Rapid Dynamic Naturalistic Monitoring of Bradykinesia in Parkinson's Disease Using a Wrist-Worn Accelerometer. Sensors (Basel) 21.

Halje, P., et al., 2019. Oscillations in cortico-basal ganglia circuits: implications for Parkinson's disease and other neurologic and psychiatric conditions. J Neurophysiol 122, 203-231.

Halje, P., et al., 2012. Levodopa-induced dyskinesia is strongly associated with resonant cortical oscillations. J Neurosci 32, 16541-16551.

Hammes, J., et al., 2019. Dopamine metabolism of the nucleus accumbens and fronto-striatal connectivity modulate impulse control. Brain 142, 733-743.

Handley, S. L., Mithani, S., 1984. Effects of alpha-adrenoceptor agonists and antagonists in a maze-exploration model of ‘fear’-motivated behaviour. Naunyn-Schmiedeberg's Archives of Pharmacology 327, 1-5.

Hauser, R. A., et al., 2014. Long-term safety and sustained efficacy of extended-release pramipexole in early and advanced Parkinson's disease. Eur J Neurol 21, 736-743.

Hervé, D., et al., 1993. G(olf) and Gs in rat basal ganglia: possible involvement of G(olf) in the coupling of dopamine D1 receptor with adenylyl cyclase. J Neurosci 13, 2237-2248.

Hikosaka, O., et al., 2000. Role of the Basal Ganglia in the Control of Purposive Saccadic Eye Movements. Physiological Reviews 80, 953-978.

Holgado, A. J., et al., 2010. Conditions for the generation of beta oscillations in the subthalamic nucleus-globus pallidus network. J Neurosci 30, 12340-12352.

Holman, A. J., 2009. Impulse control disorder behaviors associated with pramipexole used to treat fibromyalgia. J Gambl Stud 25, 425-431.

Holtz, N. A., et al., 2016. Pharmacologically distinct pramipexole-mediated akinesia vs. risk-taking in a rat model of Parkinson's disease. Prog Neuropsychopharmacol Biol Psychiatry 70, 77-84.

Iderberg, H., et al., 2015. NLX-112, a novel 5-HT1A receptor agonist for the treatment of L-DOPA-induced dyskinesia: Behavioral and neurochemical profile in rat. Exp Neurol 271, 335-350.

Iderberg, H., et al., 2013. Modulating mGluR5 and 5-HT1A/1B receptors to treat l-DOPA-induced dyskinesia: effects of combined treatment and possible mechanisms of action. Exp Neurol 250, 116-124.

Imperiale, F., et al., 2018. Brain structural and functional signatures of impulsive–compulsive behaviours in Parkinson's disease. Molecular Psychiatry 23, 459-466.

Ivica, N., et al., 2018. Changes in neuronal activity of cortico-basal ganglia-thalamic networks induced by acute dopaminergic manipulations in rats. Eur J Neurosci 47, 236-250.

Ivica, N., et al., 2014. Design of a high-density multi-channel electrode for multi-structure parallel recordings in rodents. Annu Int Conf IEEE Eng Med Biol Soc 2014, 393-396.

Jacobs, B. L., Fornal, C. A., 1997. Serotonin and motor activity. Curr Opin Neurobiol 7, 820-825.

Jaunarajs, K. L., et al., 2009. Serotonin 1B receptor stimulation reduces D1 receptor agonist-induced dyskinesia. Neuroreport 20, 1265-1269.

Jenner, P., 2015. Treatment of the later stages of Parkinson's disease - pharmacological approaches now and in the future. Transl Neurodegener 4, 3.

Jeon, J., et al., 2010. A subpopulation of neuronal M4 muscarinic acetylcholine receptors plays a critical role in modulating dopamine-dependent behaviors. J Neurosci 30, 2396-2405.

Jiménez-Urbieta, H., et al., 2020. Motor impulsivity and delay intolerance are elicited in a dose-dependent manner with a dopaminergic agonist in parkinsonian rats. Psychopharmacology (Berl) 237, 2419-2431.

Jiménez-Urbieta, H., et al., 2019. Pramipexole-induced impulsivity in mildparkinsonian rats: a model of impulse control disorders in Parkinson's disease. Neurobiol Aging 75, 126-135.

Johnson, V., et al., 2021. Embedded adaptive deep brain stimulation for cervical dystonia controlled by motor cortex theta oscillations. Experimental Neurology 345, 113825.

Joundi, R. A., et al., 2013. Persistent suppression of subthalamic beta-band activity during rhythmic finger tapping in Parkinson's disease. Clin Neurophysiol 124, 565-573.

Karekal, A., et al., 2022. Novel approaches for quantifying beta synchrony in Parkinson's disease. Experimental Brain Research.

Kawaguchi, Y., et al., 1995. Striatal interneurones: chemical, physiological and morphological characterization. Trends Neurosci 18, 527-535.

Keifman, E., et al., 2019. Optostimulation of striatonigral terminals in substantia nigra induces dyskinesia that increases after L-DOPA in a mouse model of Parkinson's disease. Br J Pharmacol 176, 2146-2161.

Kelley, A. E., 2001. Measurement of rodent stereotyped behavior. Curr Protoc Neurosci Chapter 8, Unit 8.8.

Kelley, A. E., et al., 1982. The amygdalostriatal projection in the rat--an anatomical study by anterograde and retrograde tracing methods. Neuroscience 7, 615-630.

Kerner, J. A., et al., 1997. Expression of group one metabotropic glutamate receptor subunit mRNAs in neurochemically identified neurons in the rat neostriatum, neocortex, and hippocampus. Brain Res Mol Brain Res 48, 259-269.

Kiessling, C. Y., et al., 2020. Dopamine receptor cooperativity synergistically drives dyskinesia, motor behavior, and striatal GABA neurotransmission in hemiparkinsonian rats. Neuropharmacology 174, 108138.

Kish, S. J., et al., 1988. Uneven pattern of dopamine loss in the striatum of patients with idiopathic Parkinson's disease. Pathophysiologic and clinical implications. N Engl J Med 318, 876-880.

Klaus, A., et al., 2017. The Spatiotemporal Organization of the Striatum Encodes Action Space. Neuron 95, 1171-1180.e1177.

Klawans, H. L., et al., 1977. Levodopa-induced dopamine receptor hypersensitivity. Trans Am Neurol Assoc 102, 80-83.

Konradi, C., et al., 2004. Transcriptome analysis in a rat model of L-DOPA-induced dyskinesia. Neurobiol Dis 17, 219-236.

Kordower, J. H., et al., 2013. Disease duration and the integrity of the nigrostriatal system in Parkinson's disease. Brain 136, 2419-2431.

Kouli, A., et al., 2018. Parkinson’s Disease: Etiology, Neuropathology, and Pathogenesis. In: Stoker, T. B., Greenland, J. C., (Eds), Parkinson’s Disease: Pathogenesis and Clinical Aspects. Codon Publications.

Kravitz, A. V., et al., 2010. Regulation of parkinsonian motor behaviours by optogenetic control of basal ganglia circuitry. Nature 466, 622-626.

Kühn, A. A., et al., 2008. High-frequency stimulation of the subthalamic nucleus suppresses oscillatory beta activity in patients with Parkinson's disease in parallel with improvement in motor performance. J Neurosci 28, 6165-6173.

Kühn, A. A., et al., 2006. Reduction in subthalamic 8-35 Hz oscillatory activity correlates with clinical improvement in Parkinson's disease. Eur J Neurosci 23, 1956-1960.

Kühn, A. A., et al., 2005. The relationship between local field potential and neuronal discharge in the subthalamic nucleus of patients with Parkinson's disease. Exp Neurol 194, 212-220.

Kühn, A. A., et al., 2009. Pathological synchronisation in the subthalamic nucleus of patients with Parkinson's disease relates to both bradykinesia and rigidity. Exp Neurol 215, 380-387.

Kühn, A. A., et al., 2004. Event-related beta desynchronization in human subthalamic nucleus correlates with motor performance. Brain 127, 735-746.

Kuwajima, M., et al., 2007. Localization and expression of group I metabotropic glutamate receptors in the mouse striatum, globus pallidus, and subthalamic nucleus: regulatory effects of MPTP treatment and constitutive Homer deletion. J Neurosci 27, 6249-6260.

Latella, D., et al., 2019. Impulse control disorders in Parkinson's disease: A systematic review on risk factors and pathophysiology. J Neurol Sci 398, 101-106.

Leenders, K. L., et al., 1986. Brain dopamine metabolism in patients with Parkinson's disease measured with positron emission tomography. J Neurol Neurosurg Psychiatry 49, 853-860.

Lenz, F. A., et al., 1988. Single unit analysis of the human ventral thalamic nuclear group: correlation of thalamic "tremor cells" with the 3-6 Hz component of parkinsonian tremor. J Neurosci 8, 754-764.

Lerner, R. P., et al., 2017. Levodopa-induced abnormal involuntary movements correlate with altered permeability of the blood-brain-barrier in the basal ganglia. Sci Rep 7, 16005.

Levandis, G., et al., 2008. Systemic administration of an mGluR5 antagonist, but not unilateral subthalamic lesion, counteracts l-DOPA-induced dyskinesias in a rodent model of Parkinson's disease. Neurobiol Dis 29, 161-168.

Lindén, H., et al., 2010. Intrinsic dendritic filtering gives low-pass power spectra of local field potentials. J Comput Neurosci 29, 423-444.

Lindgren, H. S., et al., 2010. L-DOPA-induced dopamine efflux in the striatum and the substantia nigra in a rat model of Parkinson's disease: temporal and quantitative relationship to the expression of dyskinesia. J Neurochem 112, 1465-1476.

Lindgren, H. S., et al., 2009. Differential involvement of D1 and D2 dopamine receptors in L-DOPA-induced angiogenic activity in a rat model of Parkinson's disease. Neuropsychopharmacology 34, 2477-2488.

Lindgren, H. S., et al., 2011. Putaminal upregulation of FosB/DeltaFosB-like immunoreactivity in Parkinson's disease patients with dyskinesia. J Parkinsons Dis 1, 347-357.

Little, S., et al., 2013. Adaptive deep brain stimulation in advanced Parkinson disease. Ann Neurol 74, 449-457.

Litvak, V., et al., 2012. Movement-related changes in local and long-range synchronization in Parkinson's disease revealed by simultaneous magnetoencephalography and intracranial recordings. J Neurosci 32, 10541-10553.

Litvak, V., et al., 2011. Resting oscillatory cortico-subthalamic connectivity in patients with Parkinson's disease. Brain 134, 359-374.

Lofredi, R., et al., 2018. Dopamine-dependent scaling of subthalamic gamma bursts with movement velocity in patients with Parkinson's disease. Elife 7.

Lofredi, R., et al., 2022. Subthalamic beta bursts correlate with dopamine-dependent motor symptoms in 106 Parkinson’s patients. bioRxiv, 2022.2005.2006.490913.

Loiodice, S., et al., 2017. Pramipexole induced place preference after L-dopa therapy and nigral dopaminergic loss: linking behavior to transcriptional modifications. Psychopharmacology 234, 15-27.

Lopes, G., et al., 2015. Bonsai: an event-based framework for processing and controlling data streams. Frontiers in Neuroinformatics 9.

Lundblad, M., et al., 2002. Pharmacological validation of behavioural measures of akinesia and dyskinesia in a rat model of Parkinson's disease. Eur J Neurosci 15, 120-132.

Luquin, M. R., et al., 1992. Levodopa-induced dyskinesias in Parkinson's disease: clinical and pharmacological classification. Mov Disord 7, 117-124.

Ma, S. Y., et al., 1997. Correlation between neuromorphometry in the substantia nigra and clinical features in Parkinson's disease using disector counts. J Neurol Sci 151, 83-87.

Macpherson, T., Hikida, T., 2019. Role of basal ganglia neurocircuitry in the pathology of psychiatric disorders. Psychiatry Clin Neurosci 73, 289-301.

Magill, P. J., et al., 2000. Relationship of activity in the subthalamic nucleus-globus pallidus network to cortical electroencephalogram. J Neurosci 20, 820-833.

Magnin, M., et al., 2000. Single-unit analysis of the pallidum, thalamus and subthalamic nucleus in parkinsonian patients. Neuroscience 96, 549-564.

Mallet, N., et al., 2012. Dichotomous organization of the external globus pallidus. Neuron 74, 1075-1086.

Mallet, N., et al., 2016. Arkypallidal Cells Send a Stop Signal to Striatum. Neuron 89, 308-316.

Mamikonyan, E., et al., 2008. Long-term follow-up of impulse control disorders in Parkinson's disease. Mov Disord 23, 75-80.

Marinus, J., et al., 2018. Risk factors for non-motor symptoms in Parkinson's disease. Lancet Neurol 17, 559-568.

Markowitz, J. E., et al., 2018. The Striatum Organizes 3D Behavior via Moment-to-Moment Action Selection. Cell 174, 44-58.e17.

Marreiros, A. C., et al., 2013. Basal ganglia-cortical interactions in Parkinsonian patients. Neuroimage 66, 301-310.

Mata-Marín, D., et al., 2021. Aberrant Salient and Corticolimbic Connectivity in Hypersexual Parkinson's Disease. Brain Connect 11, 639-650.

Mathis, A., et al., 2018. DeepLabCut: markerless pose estimation of user-defined body parts with deep learning. Nature Neuroscience 21, 1281-1289.

Maurice, N., et al., 2004. D2 dopamine receptor-mediated modulation of voltage-dependent Na+ channels reduces autonomous activity in striatal cholinergic interneurons. J Neurosci 24, 10289-10301.

McCarthy, M. M., et al., 2011. Striatal origin of the pathologic beta oscillations in Parkinson's disease. Proceedings of the National Academy of Sciences 108, 11620-11625.

McDevitt, R. A., Neumaier, J. F., 2011. Regulation of dorsal raphe nucleus function by serotonin autoreceptors: a behavioral perspective. J Chem Neuroanat 41, 234-246.

Meador-Woodruff, J. H., et al., 1991. Comparison of the distributions of D1 and D2 dopamine receptor mRNAs in rat brain. Neuropsychopharmacology 5, 231-242.

Meissner, W., et al., 2006. Increased slow oscillatory activity in substantia nigra pars reticulata triggers abnormal involuntary movements in the 6-OHDA-lesioned rat in the presence of excessive extracelullar striatal dopamine. Neurobiology of Disease 22, 586-598.

Mela, F., et al., 2012. In vivo evidence for a differential contribution of striatal and nigral D1 and D2 receptors to L-DOPA induced dyskinesia and the accompanying surge of nigral amino acid levels. Neurobiol Dis 45, 573-582.

Mela, F., et al., 2007. Antagonism of metabotropic glutamate receptor type 5 attenuates l-DOPA-induced dyskinesia and its molecular and neurochemical correlates in a rat model of Parkinson's disease. J Neurochem 101, 483-497.

Melamed, E., 1979. Early-morning dystonia. A late side effect of long-term levodopa therapy in Parkinson's disease. Arch Neurol 36, 308-310.

Mishra, A., et al., 2018. Physiological and Functional Basis of Dopamine Receptors and Their Role in Neurogenesis: Possible Implication for Parkinson's disease. J Exp Neurosci 12, 1179069518779829.

Mishra, R. K., et al., 1974. Enhancement of dopamine-stimulated adenylate cyclase activity in rat caudate after lesions in substantia nigra: evidence for denervation supersensitivity. Proc Natl Acad Sci U S A 71, 3883-3887.

Moeller, F. G., et al., 2001. Psychiatric aspects of impulsivity. Am J Psychiatry 158, 1783-1793.

Moënne-Loccoz, C., et al., 2020. Cortico-Striatal Oscillations Are Correlated to Motor Activity Levels in Both Physiological and Parkinsonian Conditions. Frontiers in Systems Neuroscience 14.

Morin, N., et al., 2013. MPEP, an mGlu5 receptor antagonist, reduces the development of L-DOPA-induced motor complications in de novo parkinsonian monkeys: biochemical correlates. Neuropharmacology 66, 355-364.

Muñoz, A., et al., 2009. Serotonin neuron-dependent and -independent reduction of dyskinesia by 5-HT1A and 5-HT1B receptor agonists in the rat Parkinson model. Exp Neurol 219, 298-307.

Murer, M. G., Moratalla, R., 2011. Striatal Signaling in L-DOPA-Induced Dyskinesia: Common Mechanisms with Drug Abuse and Long Term Memory Involving D1 Dopamine Receptor Stimulation. Front Neuroanat 5, 51.

Muthuraman, M., et al., 2020. Cross-frequency coupling between gamma oscillations and deep brain stimulation frequency in Parkinson's disease. Brain 143, 3393-3407.

Nagatsu, T., et al., 1964. TYROSINE HYDROXYLASE. THE INITIAL STEP IN NOREPINEPHRINE BIOSYNTHESIS. J Biol Chem 239, 2910-2917.

Navalpotro-Gomez, I., et al., 2019. Nigrostriatal dopamine transporter availability, and its metabolic and clinical correlates in Parkinson's disease patients with impulse control disorders. Eur J Nucl Med Mol Imaging 46, 2065-2076.

Navalpotro-Gomez, I., et al., 2020. Disrupted salience network dynamics in Parkinson's disease patients with impulse control disorders. Parkinsonism & related disorders 70, 74-81.

Neafsey, E. J., et al., 1986. The organization of the rat motor cortex: a microstimulation mapping study. Brain Res 396, 77-96.

Neafsey, E. J., Sievert, C., 1982. A second forelimb motor area exists in rat frontal cortex. Brain Res 232, 151-156.

Neumann, W.-J., et al., 2017. A localized pallidal physiomarker in cervical dystonia. Annals of Neurology 82, 912-924.

Neumann, W. J., et al., 2016. Subthalamic synchronized oscillatory activity correlates with motor impairment in patients with Parkinson's disease. Mov Disord 31, 1748-1751.

Nomoto, M., et al., 2014. Transdermal rotigotine in advanced Parkinson's disease: a randomized, double-blind, placebo-controlled trial. J Neurol 261, 1887-1893.

Ohlin, K. E., et al., 2011. Vascular endothelial growth factor is upregulated by L-dopa in the parkinsonian brain: implications for the development of dyskinesia. Brain 134, 2339-2357.

Ohlin, K. E., et al., 2012. Impact of L-DOPA treatment on regional cerebral blood flow and metabolism in the basal ganglia in a rat model of Parkinson's disease. NeuroImage 61, 228-239.

Ostock, C. Y., et al., 2011. Role of the primary motor cortex in L-Dopa-induced dyskinesia and its modulation by 5-HT1A receptor stimulation. Neuropharmacology 61, 753-760.

Oswal, A., et al., 2016. Deep brain stimulation modulates synchrony within spatially and spectrally distinct resting state networks in Parkinson's disease. Brain 139, 1482-1496.

Ouattara, B., et al., 2011. Metabotropic glutamate receptor type 5 in levodopa-induced motor complications. Neurobiol Aging 32, 1286-1295.

Pan, M. K., et al., 2016. Neuronal firing patterns outweigh circuitry oscillations in parkinsonian motor control. J Clin Invest 126, 4516-4526.

Paolone, G., et al., 2015. Eltoprazine prevents levodopa-induced dyskinesias by reducing striatal glutamate and direct pathway activity. Mov Disord 30, 1728-1738.

Paquette, M. A., et al., 2012. Anti-dyskinetic mechanisms of amantadine and dextromethorphan in the 6-OHDA rat model of Parkinson's disease: role of NMDA vs. 5-HT1A receptors. Eur J Neurosci 36, 3224-3234.

Parker, J. G., et al., 2018. Diametric neural ensemble dynamics in parkinsonian and dyskinetic states. Nature 557, 177-182.

Parkinson, J., 2002. An essay on the shaking palsy. 1817. J Neuropsychiatry Clin Neurosci 14, 223-236; discussion 222.

Paul, M. L., et al., 1992. D1-like and D2-like dopamine receptors synergistically activate rotation and c-fos expression in the dopamine-depleted striatum in a rat model of Parkinson's disease. J Neurosci 12, 3729-3742.

Pavón, N., et al., 2006. ERK phosphorylation and FosB expression are associated with L-DOPA-induced dyskinesia in hemiparkinsonian mice. Biol Psychiatry 59, 64-74.

Paxinos, G., Watson, C., 2007. The rat brain in stereotaxic coordinates.

Payer, D. E., et al., 2015. [^{11}C]-(+)-PHNO PET imaging of dopamine D(2/3) receptors in Parkinson's disease with impulse control disorders. Mov Disord 30, 160-166.

Paz-Alonso, P. M., et al., 2020. Functional inhibitory control dynamics in impulse control disorders in Parkinson's disease. Mov Disord 35, 316-325.

Pellicano, C., et al., 2015. Morphometric changes in the reward system of Parkinson's disease patients with impulse control disorders. Journal of Neurology 262, 2653-2661.

Pellow, S., et al., 1985. Validation of open : closed arm entries in an elevated plus-maze as a measure of anxiety in the rat. Journal of Neuroscience Methods 14, 149-167.

Pes, R., et al., 2017. Pramipexole enhances disadvantageous decision-making: Lack of relation to changes in phasic dopamine release. Neuropharmacology 114, 77-87.

Petersen, K., et al., 2018. Ventral striatal network connectivity reflects reward learning and behavior in patients with Parkinson's disease. Hum Brain Mapp 39, 509-521.

Petersson, P., et al., 2019. Significance and Translational Value of High-Frequency Cortico-Basal Ganglia Oscillations in Parkinson's Disease. J Parkinsons Dis 9, 183-196.

Pin, J. P., Acher, F., 2002. The metabotropic glutamate receptors: structure, activation mechanism and pharmacology. Curr Drug Targets CNS Neurol Disord 1, 297-317.

Piña-Fuentes, D., et al., 2019. The characteristics of pallidal low-frequency and beta bursts could help implementing adaptive brain stimulation in the parkinsonian and dystonic internal globus pallidus. Neurobiol Dis 121, 47-57.

Politis, M., et al., 2013. Neural response to visual sexual cues in dopamine treatment-linked hypersexuality in Parkinson's disease. Brain 136, 400-411.

Politis, M., et al., 2014. Serotonergic mechanisms responsible for levodopa-induced dyskinesias in Parkinson's disease patients. J Clin Invest 124, 1340-1349.

Postuma, R. B., et al., 2015. MDS clinical diagnostic criteria for Parkinson's disease. Mov Disord 30, 1591-1601.

Priori, A., et al., 2004. Rhythm-specific pharmacological modulation of subthalamic activity in Parkinson's disease. Exp Neurol 189, 369-379.

Prut, L., Belzung, C., 2003. The open field as a paradigm to measure the effects of drugs on anxiety-like behaviors: a review. European Journal of Pharmacology 463, 3-33.

Przedborski, S., et al., 1995. Dose-dependent lesions of the dopaminergic nigrostriatal pathway induced by intrastriatal injection of 6-hydroxydopamine. Neuroscience 67, 631-647.

Rao, H., et al., 2010. Decreased ventral striatal activity with impulse control disorders in Parkinson's disease. Mov Disord 25, 1660-1669.

Rascol, O., et al., 2021. Amantadine in the treatment of Parkinson's disease and other movement disorders. The Lancet Neurology 20, 1048-1056.

Rascol, O., et al., 2001. Induction by dopamine D1 receptor agonist ABT-431 of dyskinesia similar to levodopa in patients with Parkinson disease. Arch Neurol 58, 249-254.

Ray, N. J., et al., 2012. Extrastriatal dopaminergic abnormalities of DA homeostasis in Parkinson's patients with medication-induced pathological gambling: A [11C] FLB-457 and PET study. Neurobiology of Disease 48, 519-525.

Redgrave, P., et al., 2010. Goal-directed and habitual control in the basal ganglia: implications for Parkinson's disease. Nat Rev Neurosci 11, 760-772.

Richter, U., et al., 2013. Mechanisms underlying cortical resonant states: implications for levodopa-induced dyskinesia. Rev Neurosci 24, 415-429.

Riddle, J. L., et al., 2012. Pramipexole- and methamphetamine-induced reward-mediated behavior in a rodent model of Parkinson's disease and controls. Behavioural Brain Research 233, 15-23.

Robelet, S., et al., 2004. Chronic L-DOPA treatment increases extracellular glutamate levels and GLT1 expression in the basal ganglia in a rat model of Parkinson's disease. Eur J Neurosci 20, 1255-1266.

Rodriguez, M. C., et al., 1998. The subthalamic nucleus and tremor in Parkinson's disease. Mov Disord 13 Suppl 3, 111-118.

Rodriguez-Oroz, M. C., et al., 2011. Involvement of the subthalamic nucleus in impulse control disorders associated with Parkinson's disease. Brain 134, 36-49.

Rodriguez-Oroz, M. C., et al., 2001. The subthalamic nucleus in Parkinson's disease: somatotopic organization and physiological characteristics. Brain 124, 1777-1790.

Rokosik, S. L., Napier, T. C., 2012. Pramipexole-induced increased probabilistic discounting: comparison between a rodent model of Parkinson's disease and controls. Neuropsychopharmacology 37, 1397-1408.

Roth, K. A., Katz, R. J., 1979. Stress, behavioral arousal, and open field activity—A reexamination of emotionality in the rat. Neuroscience & Biobehavioral Reviews 3, 247-263.

Rotman, A., Creveling, C. R., 1976. A rationale for the design of cell-specific toxic agents: the mechanism of action of 6-hydroxydopamine. FEBS Lett 72, 227-230.

Rudow, G., et al., 2008. Morphometry of the human substantia nigra in ageing and Parkinson's disease. Acta Neuropathol 115, 461-470.

Ruitenberg, M. F. L., et al., 2018. Impulsivity in Parkinson's Disease Is Associated With Alterations in Affective and Sensorimotor Striatal Networks. Front Neurol 9, 279.

Rylander, D., et al., 2010. A mGluR5 antagonist under clinical development improves L-DOPA-induced dyskinesia in parkinsonian rats and monkeys. Neurobiol Dis 39, 352-361.

Sánchez, G., et al., 2009. Muscarinic inhibition of hippocampal and striatal adenylyl cyclase is mainly due to the M(4) receptor. Neurochem Res 34, 1363-1371.

Sanchez-Pernaute, R., et al., 2008. Enhanced binding of metabotropic glutamate receptor type 5 (mGluR5) PET tracers in the brain of parkinsonian primates. Neuroimage 42, 248-251.

Santana, M. B., et al., 2014. Spinal cord stimulation alleviates motor deficits in a primate model of Parkinson disease. Neuron 84, 716-722.

Santini, E., et al., 2009. L-DOPA activates ERK signaling and phosphorylates histone H3 in the striatonigral medium spiny neurons of hemiparkinsonian mice. J Neurochem 108, 621-633.

Santini, E., et al., 2012. Dopamine- and cAMP-regulated phosphoprotein of 32-kDa (DARPP-32)-dependent activation of extracellular signal-regulated kinase (ERK) and mammalian target of rapamycin complex 1 (mTORC1) signaling in experimental parkinsonism. J Biol Chem 287, 27806-27812.

Santini, E., et al., 2007. Critical involvement of cAMP/DARPP-32 and extracellular signal-regulated protein kinase signaling in L-DOPA-induced dyskinesia. J Neurosci 27, 6995-7005.

Saunders, A., et al., 2015. A direct GABAergic output from the basal ganglia to frontal cortex. Nature 521, 85-89.

Schapira, A. H. V., et al., 2017. Non-motor features of Parkinson disease. Nat Rev Neurosci 18, 435-450.

Schultz, W., 2007. Multiple dopamine functions at different time courses. Annu Rev Neurosci 30, 259-288.

Sebastianutto, I., et al., 2020. D1-mGlu5 heteromers mediate noncanonical dopamine signaling in Parkinson's disease. J Clin Invest 130, 1168-1184.

Sebastianutto, I., et al., 2016. Validation of an improved scale for rating l-DOPA-induced dyskinesia in the mouse and effects of specific dopamine receptor antagonists. Neurobiol Dis 96, 156-170.

Sgambato-Faure, V., Cenci, M. A., 2012. Glutamatergic mechanisms in the dyskinesias induced by pharmacological dopamine replacement and deep brain stimulation for the treatment of Parkinson's disease. Prog Neurobiol 96, 69-86.

Sharma, A., et al., 2015. Impulse control disorders and related behaviours (ICD-RBs) in Parkinson's disease patients: Assessment using "Questionnaire for impulsive-compulsive disorders in Parkinson's disease" (QUIP). Ann Indian Acad Neurol 18, 49-59.

Sharott, A., et al., 2005. Dopamine depletion increases the power and coherence of beta-oscillations in the cerebral cortex and subthalamic nucleus of the awake rat. Eur J Neurosci 21, 1413-1422.

Shen, W., et al., 2015. M4 Muscarinic Receptor Signaling Ameliorates Striatal Plasticity Deficits in Models of L-DOPA-Induced Dyskinesia. Neuron 88, 762-773.

Sherman, M. A., et al., 2016. Neural mechanisms of transient neocortical beta rhythms: Converging evidence from humans, computational modeling, monkeys, and mice. Proceedings of the National Academy of Sciences 113, E4885-E4894.

Sibley, D. R., Monsma, F. J., Jr., 1992. Molecular biology of dopamine receptors. Trends Pharmacol Sci 13, 61-69.

Siegle, J. H., et al., 2017. Open Ephys: an open-source, plugin-based platform for multichannel electrophysiology. J Neural Eng 14, 045003.

Simonis, G., et al., 2007. Meta-analysis of heart valve abnormalities in Parkinson's disease patients treated with dopamine agonists. Mov Disord 22, 1936-1942.

Singer, W., 2018. Neuronal oscillations: unavoidable and useful? Eur J Neurosci 48, 2389-2398.

Singh, A., Papa, S. M., 2020. Striatal Oscillations in Parkinsonian Non-Human Primates. Neuroscience 449, 116-122.

Skovgård, K., et al., 2022. Distinctive Effects of D1 and D2 Receptor Agonists on Cortico-Basal Ganglia Oscillations in a Rodent Model of L-DOPA-Induced Dyskinesia. Neurotherapeutics.

Smith, Y., Kieval, J. Z., 2000. Anatomy of the dopamine system in the basal ganglia. Trends in Neurosciences 23, S28-S33.

Smith, Y., et al., 2004. The thalamostriatal system: a highly specific network of the basal ganglia circuitry. Trends Neurosci 27, 520-527.

Snyder, G. L., et al., 2000. Regulation of phosphorylation of the GluR1 AMPA receptor in the neostriatum by dopamine and psychostimulants in vivo. J Neurosci 20, 4480-4488.

Stansley, B. J., Yamamoto, B. K., 2013. L-dopa-induced dopamine synthesis and oxidative stress in serotonergic cells. Neuropharmacology 67, 243-251.

Steeves, T. D., et al., 2009. Increased striatal dopamine release in Parkinsonian patients with pathological gambling: a [11C] raclopride PET study. Brain 132, 1376-1385.

Stocchi, F., et al., 2020. Safety considerations when using non-ergot dopamine agonists to treat Parkinson's disease. Expert Opinion on Drug Safety 19, 1155-1172.

Stocchi, F., et al., 2016. Advances in dopamine receptor agonists for the treatment of Parkinson's disease. Expert Opin Pharmacother 17, 1889-1902.

Stowe, R. L., et al., 2008. Dopamine agonist therapy in early Parkinson's disease. Cochrane Database Syst Rev, Cd006564.

Suarez, L. M., et al., 2018. Differential Synaptic Remodeling by Dopamine in Direct and Indirect Striatal Projection Neurons in Pitx3(-/-) Mice, a Genetic Model of Parkinson's Disease. J Neurosci 38, 3619-3630.

Suarez, L. M., et al., 2016. L-DOPA Oppositely Regulates Synaptic Strength and Spine Morphology in D1 and D2 Striatal Projection Neurons in Dyskinesia. Cereb Cortex 26, 4253-4264.

Suárez, L. M., et al., 2014. L-DOPA treatment selectively restores spine density in dopamine receptor D2-expressing projection neurons in dyskinetic mice. Biol Psychiatry 75, 711-722.

Surmeier, D. J., et al., 1992. Dopamine receptor subtypes colocalize in rat striatonigral neurons. Proc Natl Acad Sci U S A 89, 10178-10182.

Swann, N. C., et al., 2016. Gamma Oscillations in the Hyperkinetic State Detected with Chronic Human Brain Recordings in Parkinson's Disease. J Neurosci 36, 6445-6458.

Swann, N. C., et al., 2018. Adaptive deep brain stimulation for Parkinson's disease using motor cortex sensing. J Neural Eng 15, 046006.

Sy, M. A. C., Fernandez, H. H., 2020. Pharmacological Treatment of Early Motor Manifestations of Parkinson Disease (PD). Neurotherapeutics 17, 1331-1338.

Szechtman, H., et al., 1998. Quinpirole induces compulsive checking behavior in rats: a potential animal model of obsessive-compulsive disorder (OCD). Behav Neurosci 112, 1475-1485.

Tallaksen-Greene, S. J., et al., 1998. Localization of mGluR1a-like immunoreactivity and mGluR5-like immunoreactivity in identified populations of striatal neurons. Brain Res 780, 210-217.

Tamtè, M., et al., 2016. Systems-level neurophysiological state characteristics for drug evaluation in an animal model of levodopa-induced dyskinesia. J Neurophysiol 115, 1713-1729.

Tanaka, H., et al., 1999. Role of serotonergic neurons in L-DOPA-derived extracellular dopamine in the striatum of 6-OHDA-lesioned rats. Neuroreport 10, 631-634.

Tayebati, S. K., et al., 2004. Age-related changes of muscarinic cholinergic receptor subtypes in the striatum of Fisher 344 rats. Exp Gerontol 39, 217-223.

Tecuapetla, F., et al., 2016. Complementary Contributions of Striatal Projection Pathways to Action Initiation and Execution. Cell 166, 703-715.

Tessitore, A., et al., 2017. Intrinsic brain connectivity predicts impulse control disorders in patients with Parkinson's disease. Mov Disord 32, 1710-1719.

Tessitore, A., et al., 2016. Cortical thickness changes in patients with Parkinson's disease and impulse control disorders. Parkinsonism Relat Disord 24, 119-125.

Thanvi, B., et al., 2007. Levodopa-induced dyskinesia in Parkinson's disease: clinical features, pathogenesis, prevention and treatment. Postgrad Med J 83, 384-388.

Tremblay, M., et al., 2017. Chronic D2/3 agonist ropinirole treatment increases preference for uncertainty in rats regardless of baseline choice patterns. European Journal of Neuroscience 45, 159-166.

Trottenberg, T., et al., 2006. Subthalamic gamma activity in patients with Parkinson's disease. Exp Neurol 200, 56-65.

Tsiokos, C., et al., 2017. Pallidal low β-low γ phase-amplitude coupling inversely correlates with Parkinson disease symptoms. Clin Neurophysiol 128, 2165-2178.

Ungerstedt, U., 1968. 6-Hydroxy-dopamine induced degeneration of central monoamine neurons. Eur J Pharmacol 5, 107-110.

Valjent, E., et al., 2009. Looking BAC at striatal signaling: cell-specific analysis in new transgenic mice. Trends Neurosci 32, 538-547.

van den Bos, R., et al., 2014. A rodent version of the Iowa Gambling Task: 7 years of progress. Front Psychol 5, 203.

van den Bos, R., et al., 2006. Toward a rodent model of the Iowa gambling task. Behavior Research Methods 38, 470-478.

van Eimeren, T., et al., 2010. Drug-induced deactivation of inhibitory networks predicts pathological gambling in PD. Neurology 75, 1711-1716.

Varga, L. I., et al., 2009. Critical review of ropinirole and pramipexole - putative dopamine D(3)-receptor selective agonists - for the treatment of RLS. J Clin Pharm Ther 34, 493-505.

Voon, V., et al., 2011a. Dopamine agonists and risk: impulse control disorders in Parkinson's disease. Brain 134, 1438-1446.

Voon, V., et al., 2014. Impulse control disorders in Parkinson's disease: decreased striatal dopamine transporter levels. J Neurol Neurosurg Psychiatry 85, 148-152.

Voon, V., et al., 2011b. Impulse control disorders in Parkinson disease: a multicenter case--control study. Ann Neurol 69, 986-996.

Vriend, C., 2018. The neurobiology of impulse control disorders in Parkinson's disease: from neurotransmitters to neural networks. Cell and tissue research 373, 327-336.

Vriend, C., et al., 2014. Reduced dopamine transporter binding predates impulse control disorders in Parkinson's disease. Mov Disord 29, 904-911.

Walf, A. A., Frye, C. A., 2007. The use of the elevated plus maze as an assay of anxiety-related behavior in rodents. Nature Protocols 2, 322-328.

Wang, Q., et al., 2019. Eltoprazine prevents levodopa-induced dyskinesias by reducing causal interactions for theta oscillations in the dorsolateral striatum and substantia nigra pars reticulate. Neuropharmacology 148, 1-10.

Wang, X. J., 2010. Neurophysiological and computational principles of cortical rhythms in cognition. Physiol Rev 90, 1195-1268.

Wang, Y., et al., 2010. Noradrenergic lesion of the locus coeruleus increases apomorphine-induced circling behavior and the firing activity of substantia nigra pars reticulata neurons in a rat model of Parkinson's disease. Brain Res 1310, 189-199.

Weintraub, D., et al., 2015. Clinical spectrum of impulse control disorders in Parkinson's disease. Mov Disord 30, 121-127.

Weintraub, D., et al., 2010. Impulse control disorders in Parkinson disease: a cross-sectional study of 3090 patients. Arch Neurol 67, 589-595.

Weintraub, D., Mamikonyan, E., 2019. The Neuropsychiatry of Parkinson Disease: A Perfect Storm. Am J Geriatr Psychiatry 27, 998-1018.

Weintraub, D., et al., 2013. Screening for impulse control symptoms in patients with de novo Parkinson disease: a case-control study. Neurology 80, 176-180.

Wen, H., Liu, Z., 2016. Separating Fractal and Oscillatory Components in the Power Spectrum of Neurophysiological Signal. Brain Topography 29, 13-26.

West, M. O., et al., 1990. A region in the dorsolateral striatum of the rat exhibiting single-unit correlations with specific locomotor limb movements. J Neurophysiol 64, 1233-1246.

Westin, J. E., et al., 2001. Persistent changes in striatal gene expression induced by long-term L-DOPA treatment in a rat model of Parkinson's disease. Eur J Neurosci 14, 1171-1176.

Westin, J. E., et al., 2006. Endothelial proliferation and increased blood-brain barrier permeability in the basal ganglia in a rat model of 3,4-dihydroxyphenyl-L-alanine-induced dyskinesia. J Neurosci 26, 9448-9461.

Westin, J. E., et al., 2007. Spatiotemporal pattern of striatal ERK1/2 phosphorylation in a rat model of L-DOPA-induced dyskinesia and the role of dopamine D1 receptors. Biol Psychiatry 62, 800-810.

Wiest, C., et al., 2021. Subthalamic deep brain stimulation induces finely-tuned gamma oscillations in the absence of levodopa. Neurobiol Dis 152, 105287.

Williams, D., et al., 2002. Dopamine-dependent changes in the functional connectivity between basal ganglia and cerebral cortex in humans. Brain 125, 1558-1569.

Winkler, C., et al., 2002. L-DOPA-induced dyskinesia in the intrastriatal 6-hydroxydopamine model of parkinson's disease: relation to motor and cellular parameters of nigrostriatal function. Neurobiol Dis 10, 165-186.

Winstanley, C. A., et al., 2011. Dopamine Modulates Reward Expectancy During Performance of a Slot Machine Task in Rats: Evidence for a 'Near-miss' Effect. Neuropsychopharmacology 36, 913-925.

Wirtshafter, D., Asin, K. E., 2001. Comparative effects of scopolamine and quinpirole on the striatal fos expression induced by stimulation of D(1) dopamine receptors in the rat. Brain Res 893, 202-214.

Wirtshafter, D., et al., 1997. Compartmentally specific effects of quinpirole on the striatal Fos expression induced by stimulation of D1-dopamine receptors in intact rats. Brain Res 771, 271-277.

Wu, Y., et al., 2000. The organization of the striatal output system: a single-cell juxtacellular labeling study in the rat. Neurosci Res 38, 49-62.

Yan, Z., et al., 2001. Coordinated expression of muscarinic receptor messenger RNAs in striatal medium spiny neurons. Neuroscience 103, 1017-1024.

Zengin-Toktas, Y., et al., 2013. Motivational properties of D2 and D3 dopamine receptors agonists and cocaine, but not with D1 dopamine receptors agonist and L-dopa, in bilateral 6-OHDA-lesioned rat. Neuropharmacology 70, 74-82.

Zhai, S., et al., 2018. Striatal synapses, circuits, and Parkinson's disease. Curr Opin Neurobiol 48, 9-16.

Zigmond, M. J., et al., 1990. Compensations after lesions of central dopaminergic neurons: some clinical and basic implications. Trends Neurosci 13, 290-296.

About the author

Katrine Skovgård started her doctoral studies at Lund University in 2018 after completing her Master's thesis at Lundbeck A/S. She holds a BSc in Pharmacy and MSc in Pharmaceutical Sciences from the University of Copenhagen, and has a strong interest in pharmacology and project management. Her doctoral studies were centred on developing and characterising improved experimental models and biomarkers to advance translational research on the motor and neuropsychiatric complications of Parkinson's disease therapy.

Printed by Media-Tryck, Lund 2023 NORDIC SWAN ECOLABEL 3041 0903

LUND UNIVERSITY

FACULTY OF MEDICINE

Department of Experimental Medical Science

Lund University, Faculty of Medicine
Doctoral Dissertation Series 2023:3
ISBN 978-91-8021-342-4
ISSN 1652-8220